

ABSTRACT

Design and Synthesis of Dihydronaphthalene Vascular Disrupting Agents and Indolequinone-Based Bioreductives

Abhishek Dogra

Mentor: Kevin G. Pinney, Ph.D.

Cancer remains a deadly affliction for millions across the United States, and the number of new cases is only expected to rise in the years to come. In the field of anticancer research, vascular disrupting agents (VDAs) that preferentially target the tumor vasculature show great promise. The naturally occurring combretastatins, especially combretastatin A-4 (CA4) and combretastatin A-1 (CA1), in suitable prodrug form, have proven to be highly effective VDAs. In this study, efforts were directed towards the synthesis of two combretastatin analogs bearing key features of CA4 on a dihydronaphthalene framework: Oxi 6196 and a β -dihydronaphthalene analog.

In addition to VDAs, another class of exciting anticancer drugs is bioreductive agents that are selectively targeted towards the hypoxic region of tumors. These compounds are chemically reduced selectively and intracellularly to form active cytotoxic compounds. This study also presents the design and synthesis of two analogs of indolequinone-based prodrugs, which can be triggered to release an attached VDA upon bioreductive activation from the 3- or the 2-position, as well as the attempted synthesis of a CA4-tirapazamine bioconjugate drug.

Design and Synthesis of Dihydronaphthalene Vascular Disrupting Agents and
Indolequinone-Based Bioreductives

by

Abhishek Dogra

A Thesis

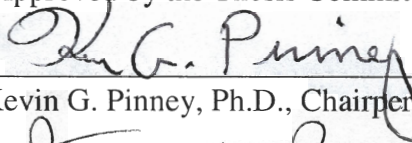
Approved by the Department of Chemistry and Biochemistry



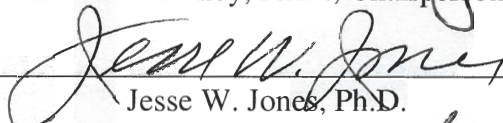
David E. Pennington, Ph.D., Interim Chairperson

Submitted to the Graduate Faculty of
Baylor University in Partial Fulfillment of the
Requirements for the Degree
of
Master of Science

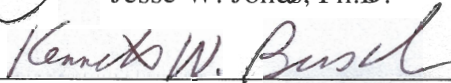
Approved by the Thesis Committee



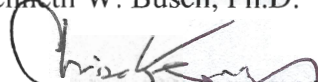
Kevin G. Pinney, Ph.D., Chairperson



Jesse W. Jones, Ph.D.

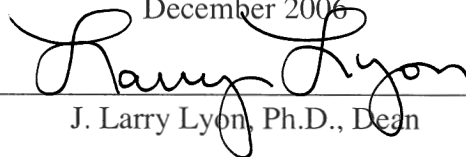


Kenneth W. Busch, Ph.D.



Christopher M. Kearney, Ph.D.

Accepted by the Graduate School
December 2006



J. Larry Lyon, Ph.D., Dean

Copyright © 2006 by Abhishek Dogra

All rights reserved

TABLE OF CONTENTS

List of Figures	vi
List of Schemes	vii
List of Abbreviations	ix
Acknowledgments	xi
Chapter One: Introduction	1
Background	1
Cancer	1
Carcinogenesis	3
Angiogenesis	3
Tumor Vasculature	5
Tumor Vascular Targeting	6
Antiangiogenics	7
Vascular Disrupting Agents	8
Biological (Ligand-directed) VDAs	11
Small Molecule VDAs	11
Flavonoids	11
Tubulin Binding Agents	12
Targeting Microtubules	12
Vinca Binding Site	15
Taxoid Binding Site	16

Colchicine Binding Site	16
Combretastatins	17
Tumor hypoxia	18
Targeting HIF-1 α	20
Hypoxia-selective Gene Therapy	21
Hypoxia-activated Prodrugs	21
Nitroheteroaromatics	21
<i>N</i> -oxides	22
Quinones	23
Indolequinones as Drug Delivery Agents	24
Mode of Action	24
Enzymatic Activation	25
Indolequinone Triggers	27
Rationale for Drug Design	29
Vascular Disrupting Agents (VDAs)	29
Bioreductive Agents	32
Chapter Two: Materials and Methods	35
General Section	35
Synthesis of Oxi6196	36
Synthesis of β -Substituted Dihydronaphthalene Analog	40
Synthesis of 3-Substituted Indolequinone Derivatives	42
Synthesis of 2-Substituted Indolequinone Derivatives	46
Synthesis of Tirapazamine Derivative	49

Chapter Three: Results and Discussion	51
Synthesis of Oxi6196	51
Synthesis of β -Substituted Dihydronaphthalene Analog	54
Synthesis of 3-Substituted Indolequinone Derivatives	60
Synthesis of 2-Substituted Indolequinone Derivatives	66
Synthesis of Tirapazamine Derivative	67
Chapter Four: Conclusions and Future Directions	70
Appendix	74
Selected NMR Spectra	75
References	105

LIST OF FIGURES

Figure

1. U.S. incidence rates (A) and mortality rates (B) 1975 – 2002	2
2. Physiological properties of a cancer cell	4
3. Tumor vasculature	6
4. Two classes of antivasular therapy	7
5. Mechanism of action for VDAs	10
6. Structures of flavonoids FAA and DMXAA	12
7. Polymerization of microtubules	13
8. Microtubule showing binding sites for three antimetabolic drugs: vinblastine (vinca binding site), colchicine (colchine binding site) and paclitaxel (taxoid binding site)	14
9. Structures of compounds binding at the vinca site	15
10. Structures of compounds binding at the taxoid site	16
11. Structures of compounds binding at the colchicine site	17
12. Structures of RB 6145 and RSU 1069	22
13. Structures of Tirapazamine and AQ4N	23
14. Structures of MMC, EO9, and RH1	23
15. Proposed mechanism of activation and DNA crosslinking of MMC	25
16. Proposed mechanism of DNA cross-linking by EO9	26
17. Mode of action for indolequinone triggers	29
18. Design paradigm for analogs of CA4	30

19. Structures of Estrogenic Receptor-binding ligands (Nafoxidene and Trioxifene), molecules developed by V. Mocharla and Z. Chen (Benzoyl-DHN) and Amino-DHN) and Oxi6196	31
20. Aryl-aryl distances for Oxi6196 and β -analog (Chem3D)	32
21. Model of a indolequinone-VDA bioconjugate drug	32
22. Mechanism of release of VDAs from 3- and 2-indolequinones	33
23. Structure of TPZ-CA4 bioconjugate	34
24. Monitoring the formation of the phenyllithium intermediate	60
25. Future compound based on the dihydronaphthalene scaffold	71
26. Future compounds based on indolequinones	73

LIST OF SCHEMES

Scheme

1. Synthesis of Oxi6196	52
2. Suggested mechanism for DDQ oxidation	53
3. Progress towards synthesis of the β -substituted dihydronaphthalene analog	55
4. Alternative strategy for the synthesis of the 2-tetralone	56
5. Model reaction for the synthesis of 2-tetralone with 1,2-dihydronaphthalene as starting material	57
6. Suggested mechanism for the formation of the 2-tetralone from the dihydronaphthalene	58
7. Synthesis of 3-(hydroxymethyl)indolequinone	61
8. Suggested mechanism for oxidation by Fremy's salt	63
9. Synthesis of 3-VDA-indolequinone bioreductive agents	64
10. Suggested mechanism for the Mitsunobu reaction	65
11. Synthesis of 2-(hydroxymethyl)indolequinone	66
12. Synthesis of 2-VDA-indolequinone bioreductive agents	67
13. Initial synthesis of CA4-TPZ bioconjugate	68
14. Synthesis of methyl ester TPZ	69
15. Alternative synthesis of methyl-TPZ dioxide	69

LIST OF ABBREVIATIONS

Å	Angstrom
ADDP	1,1'-(azodicarbonyl)dipiperidine
°C	Degrees Celsius
conc.	concentrated
δ	Chemical shift (ppm)
d	doublet
DDQ	2,3-dicyano-5,6-dichloro-parabenzoquinone
DEAD	Diethyl azodicarboxylate
DIAD	Diisopropyl azodicarboxylate
DIPEA	<i>N,N'</i> -Diisopropylethylamine
DMAP	4-dimethylaminopyridine
g	grams
h	hours
Hz	Hertz
<i>J</i>	Coupling constant
m	multiplet
min	minutes
M	Molar
MCPBA	<i>m</i> -Chloroperoxybenzoic acid
mmol	millimoles
MHz	Megahertz

nm	nanometers
p	pentet
<i>p</i> -TSA	<i>p</i> -Toluenesulfonic acid
PCC	Pyridinium chlorochromate
q	quartet
NMR	Nuclear magnetic resonance
s	singlet
SAR	Structure-activity relationship
S _N 2	bimolecular nucleophilic substitution
t	triplet
TBSCl	<i>tert</i> -Butyldimethylsilyl chloride
THF	Tetrahydrofuran
TLC	Thin layer chromatography
TMEDA	<i>N,N,N',N'</i> -Tetramethylethylenediamine
UV	Ultraviolet

ACKNOWLEDGMENTS

First and foremost, in no way would any of this be possible without the grace of my advisor Dr. Kevin G. Pinney. There are not enough words for me to express my gratitude towards him for the incredible patience, understanding and trust he has shown me during my tenure in his group. I would still like to thank him for imparting upon me his love for chemistry and showing me the way towards not only becoming a better chemist but also a better person.

I would also like to express my thanks to Dr. Carlos Manzanares for allowing me the opportunity to study chemistry at Baylor University. He has shown me more kindness than I deserve, and he has my utmost appreciation.

Special thanks also to Dr. Jesse Jones, Dr. Kenneth Busch and Dr. Christopher Kearney for serving on my committee and, more importantly, being great teachers and expanding my knowledge when I took their classes. I would like to thank other members of the organic and biochemistry divisions, Dr. Robert Kane, Dr. Charles Garner and Dr. Mary Lynn Trawick, for teaching me well at one point or another during my education.

Dr. Pennington deserves my immense gratitude for being a friend and teacher throughout my years as an undergraduate and graduate student. What I really value is his willingness to always make time for me, and I am incredibly thankful.

Nancy Kallus, Adonna Cook and Barbara Rauls also deserve my gratitude for all their help, which undoubtedly made my life much simpler. Thank you also to Andrea Johnson and Patricia Diamond for their invaluable service in the stockroom. Mrs. Sandra

Harmon also deserves my thanks for being so patient with my obvious mistakes while I was writing this thesis.

I would like to thank Baylor University, the Welch Foundation and Oxigene Inc. for their generous financial support that allowed me to accomplish my research.

Chemistry is no fun at all without friends in the lab. So, I would like to take a moment to thank past and present members of the Pinney group who have contributed extensively towards making organic chemistry so much more enjoyable: Mallinath (my first mentor), Rogelio, Graciela, Gerardo, Justin and Dr. Ming. Benson, John and Freeland, I would like to thank you just for being yourselves and allowing me to retain some sanity. And finally, I would like to thank Madhavi, whom I love as a big sister and a great friend who supported and encouraged me at all times.

Jody, I love you. I do not know where I would be without you in my life. Thank you for bringing meaning to me, my work and my life. Thank you for being everything I could ever ask for, and more.

CHAPTER ONE

Introduction

Background

Cancer

Many people believe that their risk for cancer is much greater now than it was 10, 20, or 30 years ago. It is true that the actual number of people who are diagnosed and who die of cancer each year has indeed grown, but the number has increased not because more people are at risk, but because the United States population is growing larger, and its largest segment is entering old age.

Because cancer is more common among the elderly, it is not surprising that more cases are being diagnosed as the average age of the U.S. population increases. Since 1975, the observed cancer incidence rates have increased from 400 to 495 per 100,000 cases in 2002, though death rates have declined from 200 in 1975 to 194 per 100,000 cases in the same period, which is seen in Figure 1.¹

Only a few decades ago, less than one in ten children with leukemia survived ten years after diagnosis. With modern therapies, the cure rate for these children is now almost eighty percent.² Similar progress has been made fighting Hodgkin's lymphoma, bone and kidney cancers in children, and testicular cancer.

At present, a person's risk of being diagnosed with cancer and the risk of dying of cancer both have decreased over the past few decades. More than half the people diagnosed with cancer today will survive. Some will be completely cured, and many

more people will live for years with a good quality of life, thanks to treatments that control many types of cancer.

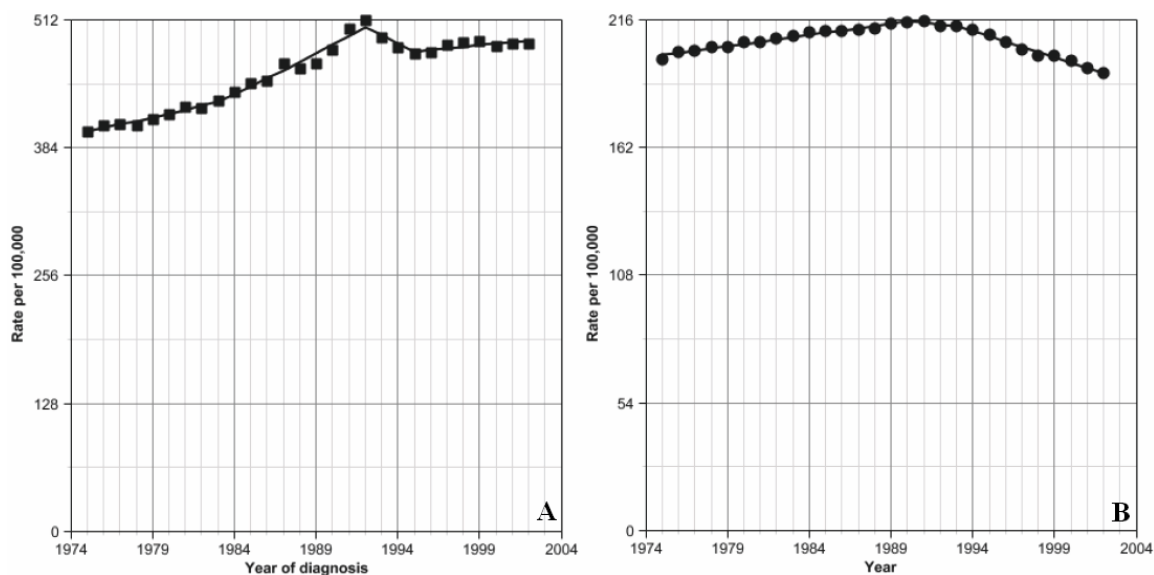


Figure 1. U.S. incidence rates (A) and mortality rates (B) 1975 – 2002 (Reproduced from reference 1.)

It is important to remember that “cancer” is not one disease but many different diseases characterized by the uncontrolled growth of abnormal cells in the body. A tumor, or neoplasm, is the result of the uncontrolled cell growth arising from malfunctions in the regulatory mechanism of cell proliferation. Malignant tumor cells have the ability to infiltrate other tissues through invasion by growth into surrounding tissue or metastasis by spreading through lymphatic or blood vessels to other tissues in the body. Mutations in DNA that lead to cancer are caused by factors such as hormones, viruses, smoking, diet and radiation. Genetic predisposition and immune status affect individual susceptibility.³

Surgery, radiation, chemotherapy and immunotherapy alone or in combination are the most common methods of cancer treatment. The choice of therapy depends on the

location and grade of the tumor and the stage of the disease, as well as the general state of the patient.³ Complete removal of the tumor with minimal damage to healthy tissue is the aim of treatment.

Carcinogenesis

At the molecular level, cancer arises as a result of several mutations that activate oncogenes and deactivate tumor suppressor genes. Oncogenes are activated by mutations in proto-oncogenes, which promote cell growth and division, and cells can then undergo excessive and uncontrollable proliferation. Tumor suppressor genes are responsible for the arrest of the cell cycle when DNA repair is necessary.⁴ Mutations in these genes cause inhibited DNA repair and hence the accumulation of genetic damage that leads to cancer.

The advent of a cancer cell is followed by a phase of avascular tumor growth. Tumor cells are supplied with oxygen and nutrients by diffusion from adjacent healthy cells, but growth is limited at a size of less than two millimeters in diameter.^{5, 6} Malignant tumor cells have some very distinct properties, as shown in Figure 2, that allow them to multiply: evading apoptosis, invading neighboring tissues, metastasizing at distant sites, and especially promoting blood vessel growth (angiogenesis).

Angiogenesis

Angiogenesis, the formation of new blood vessels from the endothelium of existing vasculature, represents an essential step in tumor proliferation, expansion and metastasis. For growth beyond the avascular phase, nutrition through diffusion is no longer sufficient, and the formation of new vasculature is necessary. The tumor can

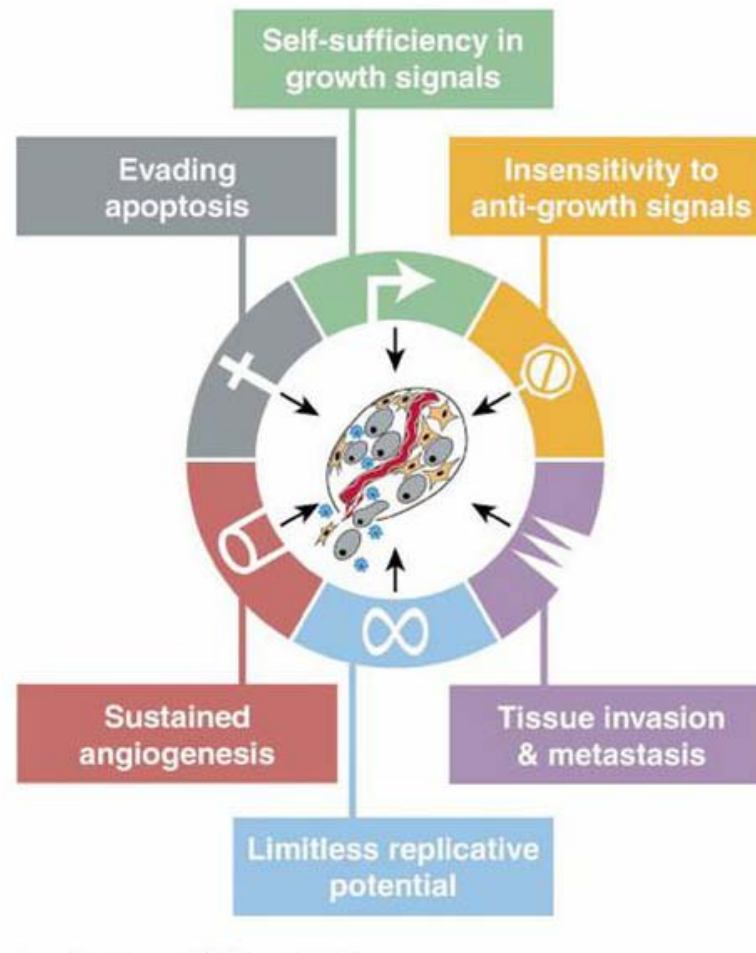


Figure 2. Physiological properties of a cancer cell (Reproduced from reference 7)

remain in a state of dormancy for years until it can stimulate the formation of a novel vascular network.⁸

It is believed that an angiogenic “switch,” controlled by the equilibrium between pro- and antiangiogenic molecules in the tumor microenvironment, is flipped when the tumor enters the vascular phase of its growth.⁹ When the proangiogenic factors are dominant, the tumor acquires an angiogenic phenotype that leads to the formation of new blood vessels. By acquiring the angiogenic phenotype, the developing tumor is able to rapidly increase its rate of growth and gain the destructive ability to metastasize.⁵

Tumor Vasculature

Ongoing angiogenesis is required by few adult tissues, such as the female reproductive organs, organs undergoing physiological growth, or injured tissue.⁹ The point at which these normal processes differ from pathological angiogenesis is in the tightly regulated balance of pro- and antiangiogenic signals. During normal physiological angiogenesis, blood vessels rapidly mature and become stable. By contrast, tumors have lost the appropriate balances between positive and negative controls. One characteristic feature of tumor blood vessels is that they fail to become quiescent, enabling the constant growth of new tumor blood vessels. Therefore, the tumor vasculature develops unique characteristics and becomes quite distinct from the normal blood supply system.

The vascular network that forms in tumors is often leaky and hemorrhagic, partly due to an angiogenic molecule, vascular endothelial growth factor (VEGF), which plays a critical role in the angiogenic process. VEGF exerts its angiogenic effects by interacting with specific receptors on endothelial cells stimulating their growth and differentiation into blood vessels. Tumor hypoxia, oncogenes, cytokines and hormones, among other pro-angiogenic factors, are important stimuli that cause the increased production of tumor VEGF.^{6,9}

Tumor blood vessels are architecturally different from their normal counterparts, illustrated in Figure 3. They are irregularly shaped, dilated, tortuous and can have dead ends. They are not organized into definitive venules, arterioles and capillaries, but rather share chaotic features of all of them. Blood flows irregularly in tumor vessels, moving more slowly and sometimes even oscillating, which leads to dysfunctional capillaries.

Aberrant blood flow contributes to micro-regional hypoxia. The tumor is also nutrient starved, acidic, and under oxidative stress as its blood supply lags behind the aggressively expanding tumor mass.

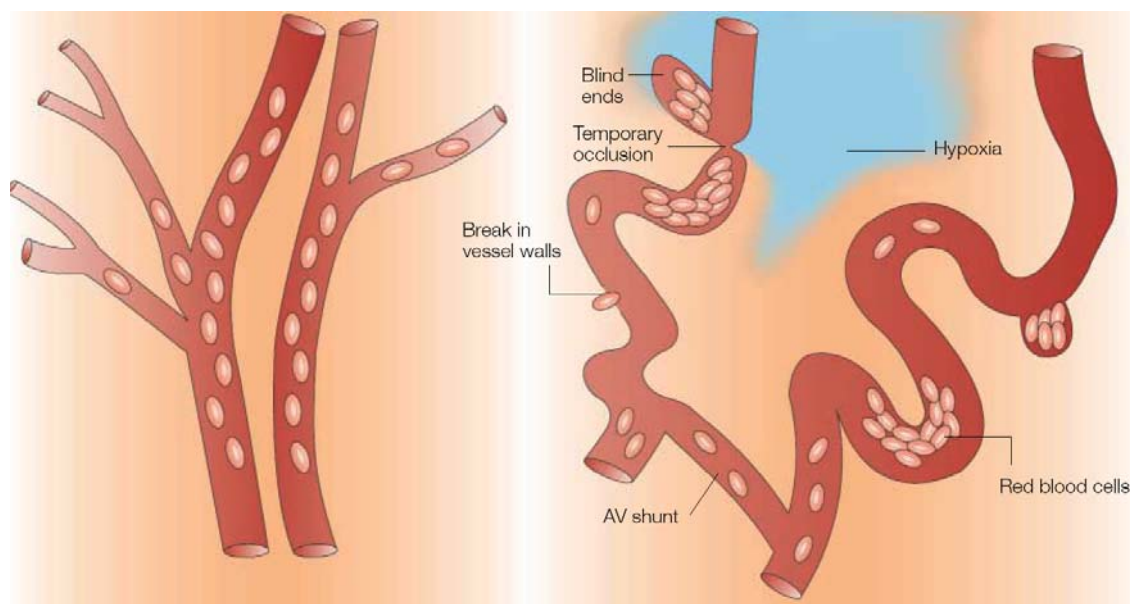


Figure 3. Tumor vasculature (Directly reproduced from reference 54.)

Tumor Vascular Targeting

Given its pivotal role in growth and survival, the tumor vasculature represents an attractive target for anticancer therapy. Conventional cancer treatments, such as radiation, exert their antitumor effect by targeting the rapidly growing neoplastic cell population. However, physiological conditions in the tumor microenvironment, arising as a consequence of the tumor's anomalous vascular network, are significant contributors towards resistance to non-surgical anticancer treatments. For example, hypoxia has been long known to have a detrimental effect on the radiation response of tumor cells.^{10, 11}

The primary reason for pursuing the tumor vasculature as a therapeutic target involves the inherent differences between blood vessels in tumors and normal tissues.

These variations allow for the provision of unique targets in the design of novel therapeutics that are highly selective for the cancer itself. Two key approaches to targeting the tumor blood vessel network have been developed (Figure 4). The first approach, antiangiogenics, aims to inhibit the angiogenic process itself.^{12, 13} The alternative approach, vascular disrupting agents (VDAs), involves the use of therapeutic agents to selectively destroy the established tumor vessel network.^{12, 14}

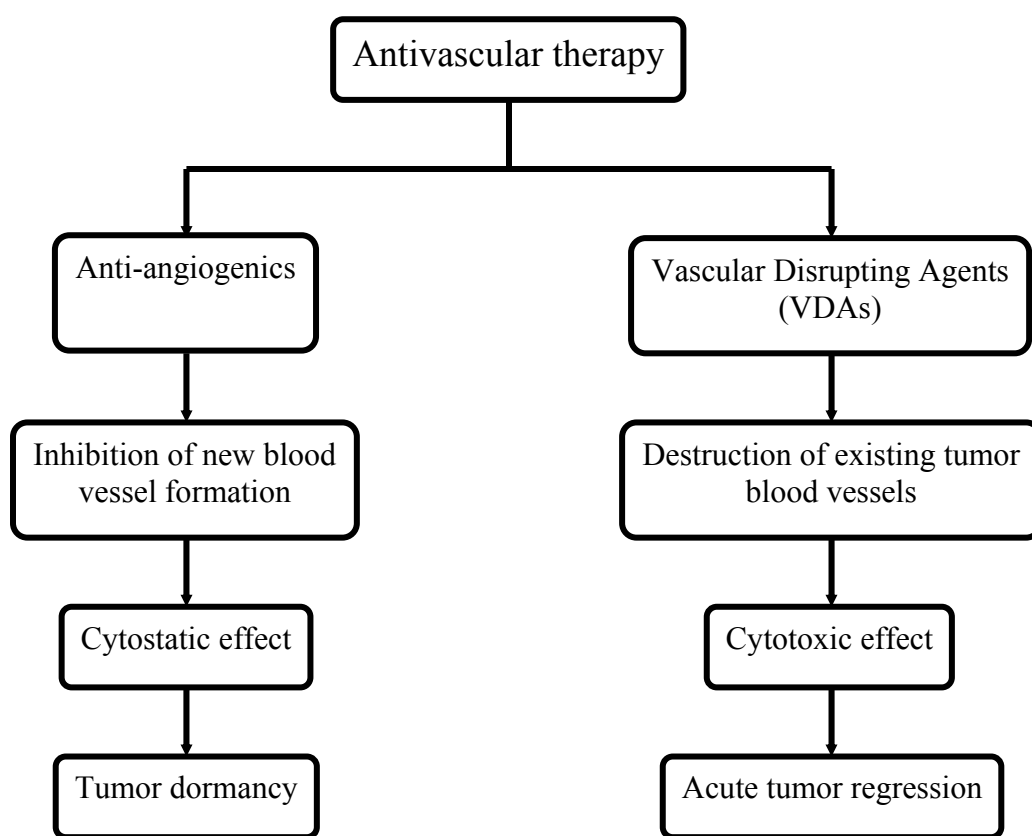


Figure 4. Two classes of antivascular therapy (Reproduced from reference 5)

Antiangiogenics

The fundamental goal of antiangiogenic strategies is to interfere with the proangiogenic balance in the tumor in order to prevent the formation of new blood

vessels thereby inhibiting the tumor's growth and metastatic ability. Antiangiogenic agents affect at least one of the several important stages of angiogenesis, such as basement membrane degradation, endothelial cell proliferation and tube formation.

Many relevant antiangiogenic agents focus on the inhibition of the proangiogenic growth factor VEGF because of the crucial role it plays in tumor neovascularization.¹⁵ Suppression of VEGF-signaling has been targeted with a variety of strategies, including monoclonal antibodies (e.g. Bevacizumab¹⁵) and small molecule VEGF receptor tyrosine kinase inhibitors (e.g. ZD6474¹⁶ and PTK787¹⁷). In addition to the aforementioned antiangiogenics, numerous other drugs have been developed with a similar mode of action, including matrix metalloproteinase inhibitors (MMPs), natural peptide inhibitors (e.g. angiostatin and endostatin) and inhibitors with an unknown mechanism (e.g. thalidomide).^{5, 18, 19} Many of these agents are currently undergoing clinical evaluation.

Antiangiogenics have been shown to significantly curtail primary tumor growth and establishment of metastases in several preclinical minimal disease models, but overt shrinkage of large, well-established tumors was less common.⁶ Therefore, successful clinical application of the angiogenesis inhibitors will likely be in patients with micrometastatic disease.

Vascular Disrupting Agents

Vascular disruption as an antivascular strategy was first proposed by Juliana Denekamp in the early 1980s.²⁰ She observed that endothelial cells in tumors proliferate much faster than endothelial cells in normal tissues and that the obstruction of the blood vessels of solid tumors in mice caused tumor regressions. Hence, the idea that VDAs could be created, which were selectively targeted towards the occlusion of tumor blood

vessels, was a result of her observations.²¹ Later studies involving immunotherapy with antibodies directed towards tumor vascular endothelium, which led to excellent responses in mice, and tubulin-binding drugs, which have vascular targeting properties, confirmed this idea.^{14, 22}

Destruction of the tumor endothelium leads to the death of tumor cells from oxygen and nutrient starvation owing to the occlusion of tumor blood vessels, which is shown in Figure 5. This halts blood flow in most of the tumor vessels, thereby eliciting secondary tumor cell death through ischemia. In contrast to antiangiogenic treatment, this approach has the potential to destroy existing tumor masses, as well as preventing progression. Thus, VDAs can be more active in large tumors.

There are some notable advantages of VDAs over other classes of anticancer treatment. Most significantly, a bystander effect may occur, as one single blood vessel may provide oxygen and nutrients for thousands of tumor cells. Blockage or destruction of this solitary vessel may then result in thousands of downstream cell deaths. Also, VDAs do not need to exert their effects for long. Studies suggest that a tumor can be almost completely destroyed within a few hours of ischemia.²⁴

VDAs have also been shown to produce a characteristic pattern of widespread central necrosis, which can extend to as much as 95% of the tumor leaving a thin rim of viable tumor cells on the periphery of the tumor.^{11, 14, 25} This viable rim can then later rapidly repopulate the tumor. It has been postulated that for VDAs to be most effective, they should be combined with other treatment options so that the entire tumor cell population can be completely destroyed. Several studies involving the use of VDAs in conjunction with conventional chemotherapeutic agents and radiotherapy have been

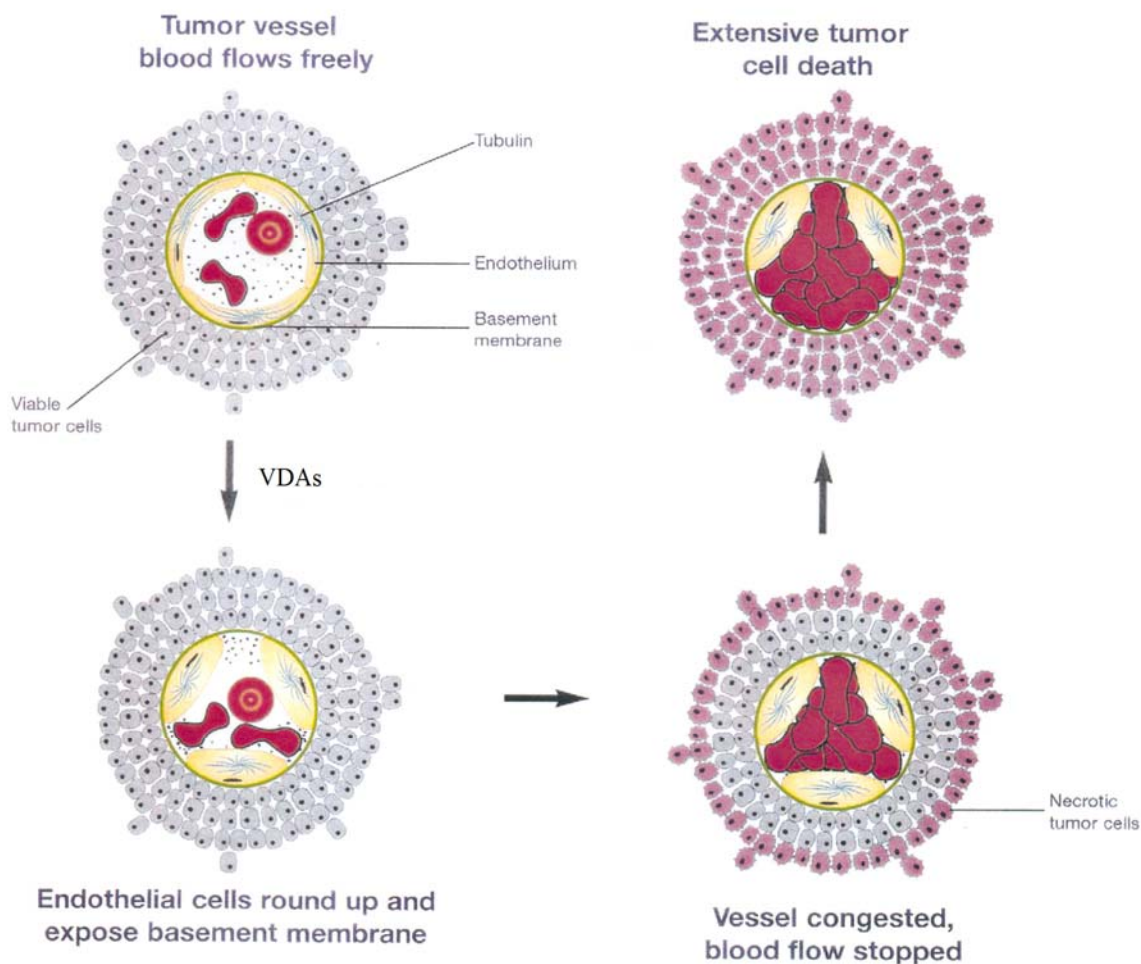


Figure 5. Mechanism of action for VDAs (Directly reproduced from reference 23)

reported in a variety of tumor models.^{11, 26, 27} Most of these studies demonstrated marked enhancements in antitumor activity when VDAs were administered within a few hours of conventional treatment.

Two broad classes of VDAs are currently being developed: the biological or ligand-directed VDAs, which include antibodies or peptides that deliver toxins and procoagulant and proapoptotic effectors to the tumor endothelium, and small molecule VDAs, which can take advantage of differences in normal and tumor endothelium to induce vascular shutdown of tumor blood vessels.

Biological (Ligand-directed) VDAs

The strategy behind this approach is to use ligands that bind selectively to components of tumor blood vessels to target agents that occlude those vessels. Ligand-directed VDAs, therefore, are composed of a targeting moiety, usually an antibody, specific peptide or growth factor, which is specific to an upregulated marker on tumor endothelium cells. The targeting moiety is complexed with immunomodulatory, procoagulant or cytotoxic molecules that act as effectors. The result may be thrombosis within tumor vasculature caused by direct action or apoptosis, initiation of an immune attack on the tumor vasculature or a change of conformation of the tumor endothelium, which leads to blood vessel occlusion.

Despite a proven mode of action and antitumor efficacy in experimental animal models,¹⁴ the difficulties involved in producing these complex compounds in large scale have prevented biological VDAs from realizing their clinical potential.

Small Molecule VDAs

Small molecule VDAs do not localize selectively to tumor vessels but utilize physiological differences in tumor and normal endothelial tissue to the detriment of tumor vasculature. These differences include the increased proliferation and permeability of the tumor endothelium, as well as its reliance on a tubulin cytoskeleton to maintain cell shape. This class of VDAs is divided into flavonoids that are cytokine inducers and tubulin binding agents.

Flavonoids. Flavone acetic acid (FAA) is a synthetic flavonoid that was found to possess unexpectedly high antitumor activity in murine models due to antivasular action

via the induction of tumor necrosis factor α (TNF α).²⁸ However, the lack of clinical activity of FAA led to the development of DMXAA (5,6-dimethylxanthenone-4-acetic acid) as a more potent analog. DMXAA is sixteen times as dose-potent as FAA,^{24, 25} and it is currently the leading candidate in clinical trials from this class of VDAs. The structures of both drugs are shown in Figure 6.

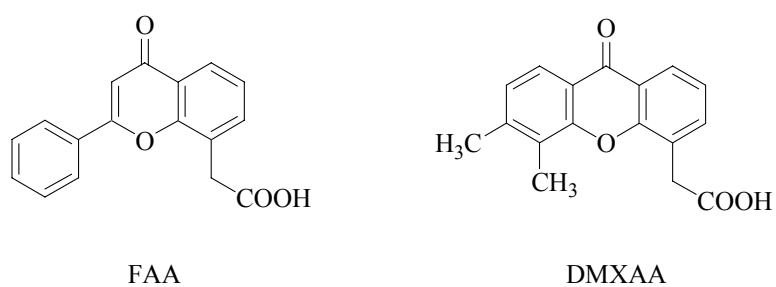


Figure 6. Structures of flavonoids FAA and DMXAA

Tubulin Binding Agents. The rapidly proliferating and immature tumor endothelial cells rely on a tubulin cytoskeleton to maintain their cell shape. Disruption of these microtubule filaments as the antivascular and antimitotic effects of tubulin binding agents leads to the inhibition of spindle formation (mitotic arrest) and reduced tumor blood flow.^{11, 29}

Targeting Microtubules

Microtubules are one of the major components of the cytoskeleton found in all eukaryotic cells. They are crucial in the development and maintenance of cell shape, in the transport of vesicles, mitochondria and other cell components, in cell signaling, and in cell division and mitosis. Microtubules are composed of two structurally similar protein subunits, α - and β -tubulin, arranged head-to-tail at 80 Å intervals to form a linear

protofilament.³⁰ The structural organization of tubulin is shown in Figure 7. A single microtubule is composed of thirteen protofilaments, forming a hollow structure about 240 Å in diameter.³¹ Each tubulin monomer is composed of approximately 440 amino acids (50 kDa) forming a core of two β -sheets surrounded by α -helices.^{32, 33}

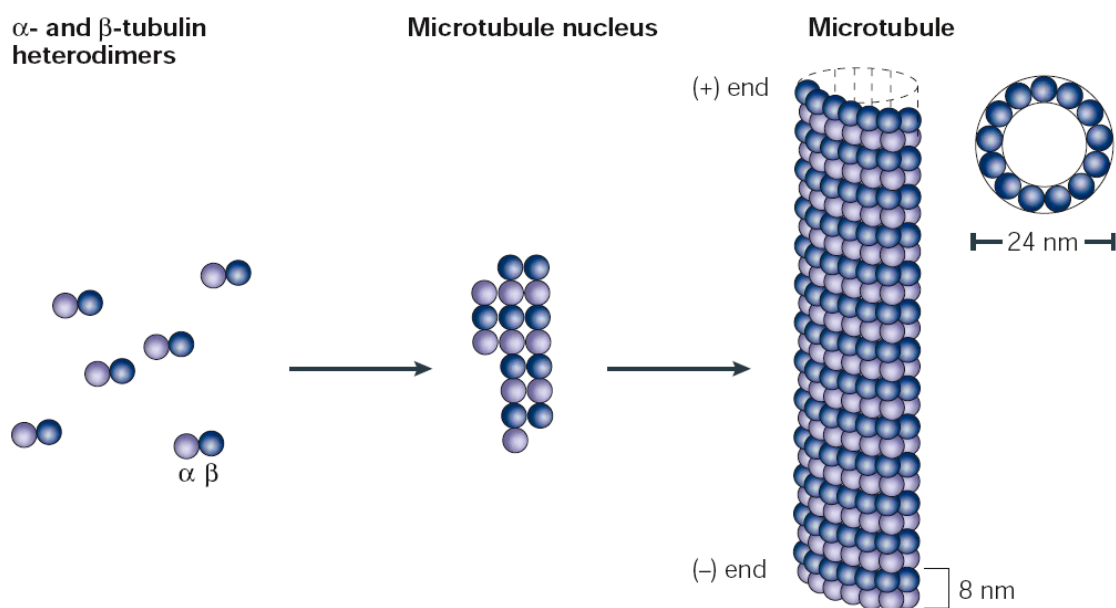


Figure 7. Polymerization of microtubules. (Directly reproduced from reference 34.)

In order to respond to the rapidly changing requirements of the cell, microtubules have to assume a vast array of stability states and degrees of organization, which are regulated by numerous factors including the intrinsic ability of microtubule subunits, tubulin heterodimers, to form nonequilibrium, dynamic polymers.³⁴ Microtubules display two kinds of nonequilibrium dynamics that use energy provided by the hydrolysis of GTP when a tubulin dimer, with bound GTP, attaches to the microtubule ends.

One kind of dynamic behavior that is prominent in cells, called “dynamic instability,” is a process in which the individual microtubule ends switch between phases of growth and shortening.³⁵ The two ends of a microtubule are not equivalent – one end,

called the plus end, grows and shortens more rapidly and more extensively than the other (the minus end). The second dynamic behavior, called “treadmilling,” is net growth at one microtubule end and balanced net shortening at the opposite end. It involves the flow of tubulin subunits from the plus end of the microtubule to the minus end.³⁶

Compounds that selectively target tubulin, microtubule protein systems interfere with this dynamic process of assembly and disassembly by binding to three distinct sites (Figure 8), which include the vinca alkaloid binding site, taxoid binding site and colchicine binding site.³⁷⁻³⁹ The vinca alkaloid site is found at the plus end of β -tubulin. The taxoid binding site is located at the interior surface of the microtubule between contiguous filaments, and the colchicine binding site is found at the interface of α - and β -tubulin heterodimer.

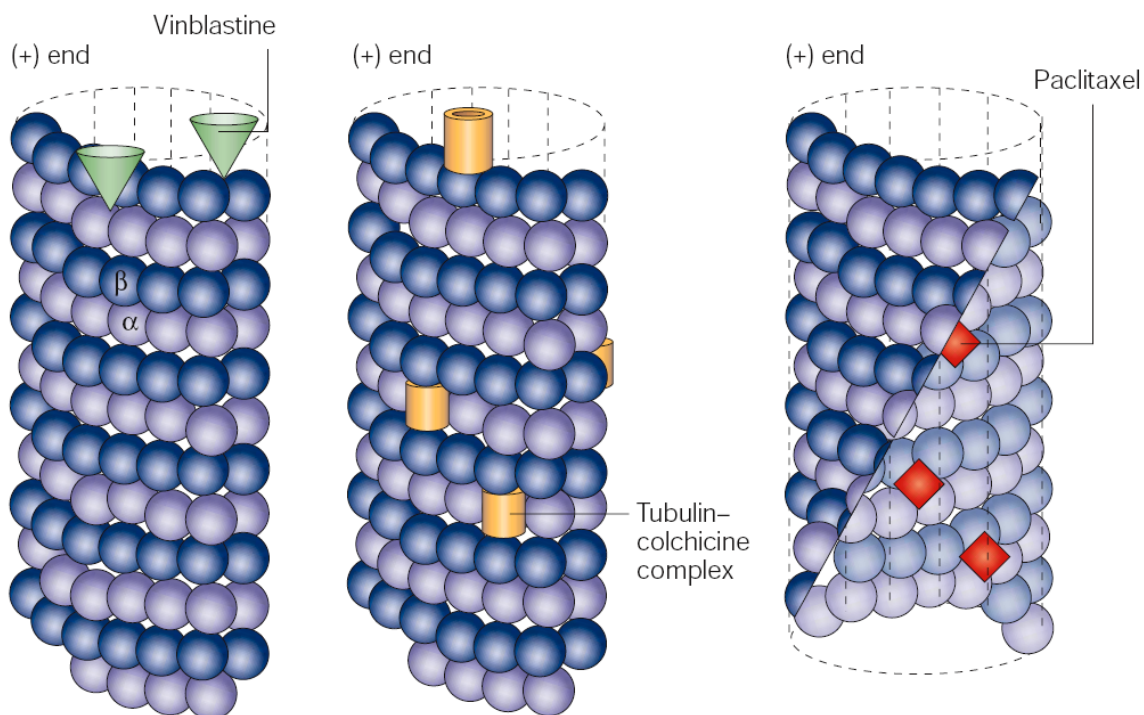


Figure 8. Microtubule showing binding sites for three antimitotic drugs: vinblastine (vinca binding site), colchicine (colchine binding site) and paclitaxel (taxoid binding site) (Directly reproduced from reference 34.)

Vinca Binding Site

Vinca alkaloids (Figure 9), such as the naturally occurring vincristine and vinblastine, bind strongly to this site on β -tubulin, depolymerizing tubulin and causing it to form indefinite spirals and paracrystalline aggregates that compete with microtubule formation, leading to mitotic arrest and subsequent apoptosis.³⁸ In addition to the two natural products, which have been widely used as clinical agents in the treatment of leukemias, lymphomas and some solid tumors, their semi-synthetic analogs, vindesine and vinorelbine, have also shown antitumor efficacy.^{34, 39} Various other chemotherapeutic drugs, such as cryptophycin and dolastatin, also bind in this region and appear to work by the same mechanism.

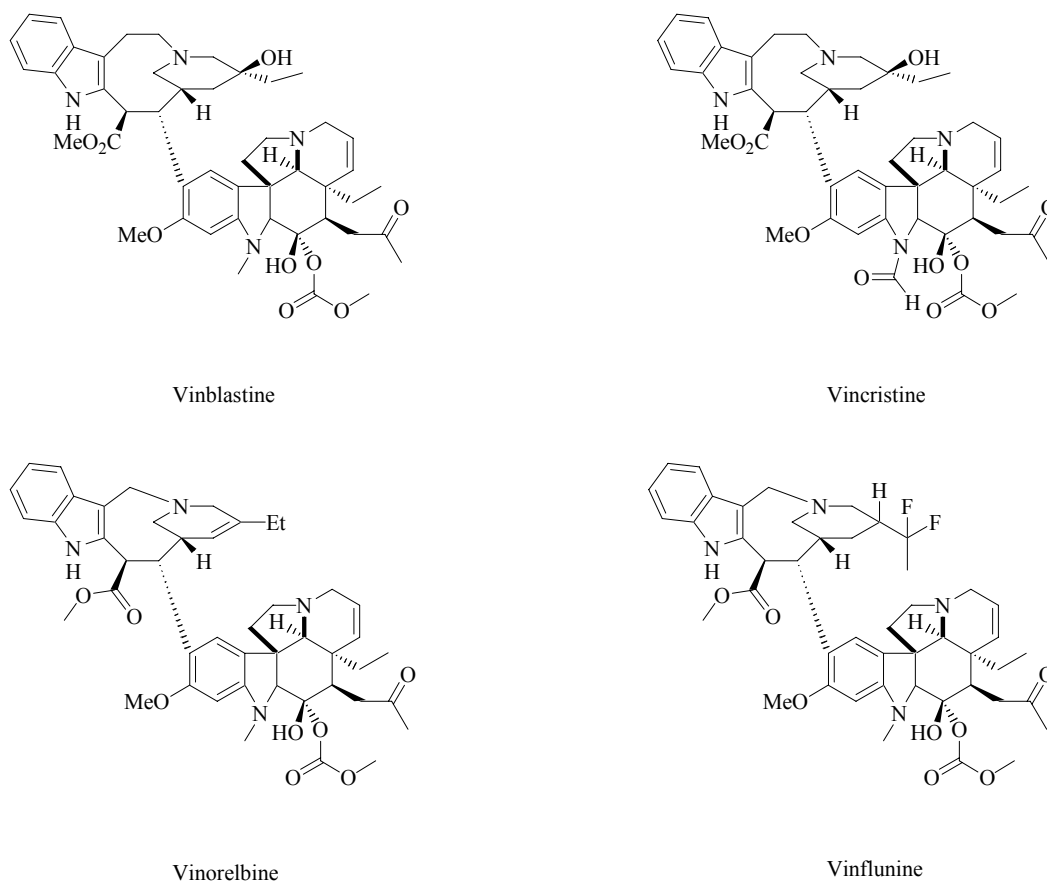


Figure 9. Structures of compounds binding at the vinca site.

Taxoid Binding Site

Drugs that bind to this site are known to act as microtubule stabilizing agents. Paclitaxel was the first compound found to promote the assembly of tubulin heterodimers into microtubules and stabilize them. As with the vinca alkaloids, the suppression of microtubule dynamics prevents the dividing cancer cells from completing mitosis, the cells eventually die by apoptosis. Paclitaxel and docetaxel (Figure 10), a semi-synthetic derivative, are now considered established drugs for the treatment of breast cancer and other malignancies.

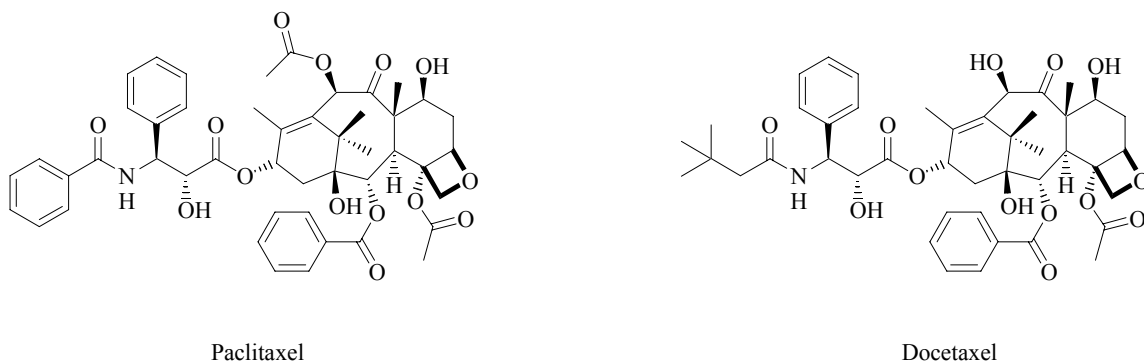


Figure 10. Structures of compounds binding at the taxoid site.

Colchicine Binding Site

Colchicine was the first drug known to bind to tubulin and was one of the first antimetabolic agents investigated. It is used in the treatment of gout, but its high toxicity prevents its use in other therapies. Colchicine changes the secondary structure of tubulin by binding to a high affinity site on the tubulin heterodimer. This binding, which is temperature dependent and irreversible, induces a change in dimer structure and inhibits tubulin assembly.³⁷ Several colchicine analogs (Figure 11), especially the naturally occurring combretastatins, are currently under investigation for cancer treatment.

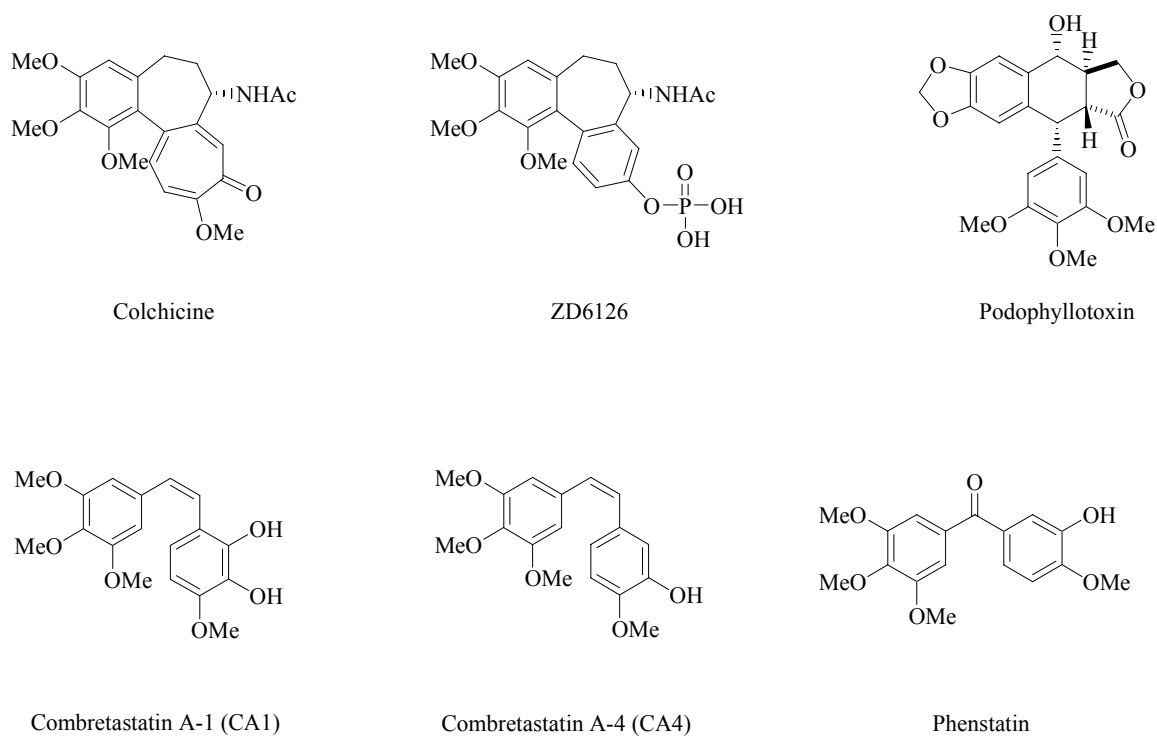


Figure 11. Structures of compounds binding at the colchicine site: colchicine,^{37,40} ZD6126,^{23,41} podophyllotoxin,⁴² phenstatin,⁴³ CA1⁴⁶ and CA4⁴⁶

Colchicine-site binding agents are known to activate RhoA, a guanosine nucleotide triphosphate, by an uncertain mechanism. The activation of RhoA can then lead to the further activation of downstream effectors, such as RhoA kinase. Consequentially, morphological changes in the endothelial cells instigate blood vessel occlusion and tumor cell death.^{44,45}

Combretastatins

The combretastatins are a family of approximately twenty natural compounds that are remarkable for their pronounced biological activity and structural simplicity. These compounds were originally discovered by Professor George R. Pettit (Arizona State University) and isolated from the bark of the South African bush willow tree known as *Combretum caffrum*.⁴⁶

Of the compounds isolated, combretastatin A-4 (CA4) and combretastatin A-1 (CA1), members of the *cis*-stilbenoid A-series of combretastatins, were found to be the most active.⁴⁷ Structurally similar to colchicine, containing two phenyl rings tilted at 50-60° to each other and linked by a two carbon bridge, these compounds are potent inhibitors of tubulin. The *cis* configuration of these combretastatins, and other structural features, has proven important for biological activity. Limited water-solubility of CA-1 and CA4 hindered their progress until the development of their sodium phosphate salts, CA1P and CA4P, in the mid-1990s.^{48, 49} The salts act as prodrugs, which are cleaved to their active forms by endogenous, nonspecific phosphatases that are then taken up into cells. Preclinical studies have reported that the combretastatins uniquely compromise tumor vasculature,^{47, 50} and in contrast to colchicine and other tubulin binding drugs, their *in vivo* antivasular effects are apparent well below the maximum tolerated dose (MTD),⁵¹ offering a wide therapeutic window.

A wide variety of synthetic analogs have been designed that are based on CA1 and CA4. Some of these bear the stilbenoid nature of the original combretastatins, whereas others are based on different molecular scaffolds.

Tumor Hypoxia

Hypoxia, a reduction in the normal level of tissue oxygen tension, produces cell death when it is severe or prolonged. Tumors become hypoxic because of their abnormal blood vessels and irregular blood flow. Hypoxia is toxic to both cancer cells and normal cells, but cancerous cells undergo genetic and adaptive changes in order to survive and even proliferate in a hypoxic environment.

The presence of hypoxia in human tumors was postulated by Thomlinson and Gray fifty years ago based on the observations that tumor cells that were located more than 180 μm away from blood vessels were victim to necrosis.⁵² This is similar to the calculated distance that oxygen diffuses as it passes from the capillary to cells before it is completely metabolized. Tumors outgrow their oxygen supply because of uncontrolled proliferation, and this limit in oxygen diffusion was termed “chronic hypoxia.” Another type of hypoxia, known as “acute” or “perfusion-limited” occurs when aberrant blood vessels are shut down, which can also cause blood flow to be reversed.⁵³ Both diffusion and perfusion-limited hypoxia have been shown to confer radiation resistance in experimental models because response to radiotherapy requires free radicals from oxygen to destroy cells.^{54, 55}

To adapt to hypoxia, cells generate a variety of biological responses including the activation of key genes whose products support anaerobic metabolism and facilitate increased oxygen delivery to the oxygen-deprived regions. Hypoxia also induces the release of erythropoietin (EPO) to increase red blood cell production and the production of growth factors like VEGF that stimulate angiogenesis.

Hypoxic cells are considered resistant to most anticancer drugs for several reasons: first, hypoxic cells are distant from blood vessels and are not adequately exposed to some anticancer drugs. Also, cellular proliferation decreases as a function of distance from blood vessels, and hypoxia selects for cells that have lost sensitivity to p53-mediated apoptosis, which might lessen sensitivity to certain drugs. Furthermore, hypoxia upregulates genes involved in drug resistance.⁵⁴

As a result, hypoxia plays a negative role in cancer therapy because it causes resistance to conventional therapies, and it advances a malignant tumor phenotype. However, the low oxygen levels and presence of necrosis are features unique to solid tumors and, thus, can be exploited by anticancer agents. Three general classes of hypoxia-selective therapies are currently in development: targeting the hypoxia-inducible transcription factor 1 (HIF-1), hypoxia-selective gene therapy and hypoxia-activated prodrugs (bioreductives).

Targeting HIF-1 α

HIF-1 plays an important role in the response of cells to a hypoxic environment. The protein is a heterodimer that consists of the hypoxic response factor HIF-1 α and the aryl hydrocarbon receptor nuclear translocator (ARNT), which is also known as HIF-1 β . In the absence of oxygen, HIF-1 binds to hypoxia-response elements (HREs), thereby activating various hypoxia-response genes, such as VEGF.⁵⁶

Therapies are under development to block HIF-1 α itself or HIF-1 α -interacting proteins. Blocking the interaction between HIF-1 α and its transcriptional coactivator CBP/p300 led to the attenuation of hypoxia-inducible gene expression and inhibition of tumor growth in a mouse xenograft model.⁵⁷ Antagonists to HIF-1 α , as peptides or small molecules, have also been reported.^{53, 54} Anaerobic bacteria provide another method of delivering genes specifically to hypoxic cells. They have shown tumor-specific proliferation in animal models and inhibited tumor growth.⁵⁴

Hypoxia-selective Gene Therapy

Hypoxia regulated gene therapy exploits the activation of HIF-1 under low oxygen conditions. Introducing a HRE in a gene delivery vehicle affords hypoxic regulation of the expressed gene. This offers a level of selectivity to standard gene-directed enzyme prodrug therapy (GDEPT). Expression of an enzyme that is not normally found in the human body could, under the control of a hypoxia-responsive promoter, convert a non-toxic prodrug into a toxic drug in the tumor. Promoters using HREs from hypoxia-responsive genes have been developed, and *in vivo* activity has been observed in experimental models.^{54, 58}

Hypoxia-activated Prodrugs

Bioreductive drugs are prodrugs that are only activated under hypoxic conditions. They were primarily developed to be used in combination therapy with radiation. The selectivity is based on the ability of molecular oxygen to reverse the bioreductive activation, so the final cytotoxic product is prevented from harming normal cells. Also, selectivity is accorded by the presence of elevated levels of specific reductase enzymes in cancer cells. The differences in enzyme activity between normal and tumor tissue allow the development of enzyme-directed bioreductives. The three main classes of bioreductive drugs are the nitroheteroaromatics, the *N*-oxides and the quinones.

Nitroheteroaromatics. This class of bioreductives was developed on the basis that the nitro functionality would be reduced under hypoxia, utilizing various reductive enzymes to yield reactive intermediates.⁵⁹ The formation of the hydroxylamino group, or amino group, after reduction, triggers the release of the therapeutic drug. The

nitroheteroaromatics also include bioreductive drugs based on nitroimidazole, like RB 6145⁶⁰ and RSU 1069⁶¹ (Figure 12) that are reduced by one electron reducing enzymes to form cytotoxic metabolites.

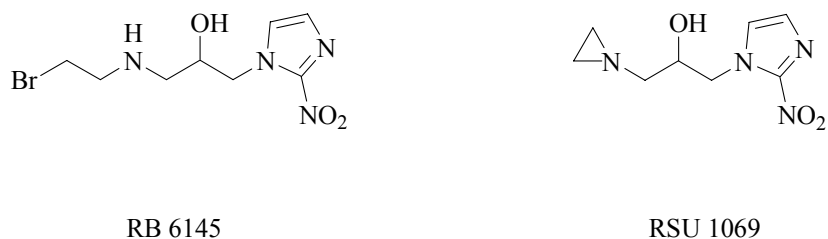


Figure 12. Structures of RB 6145 and RSU 1069

N-oxides. Tirapazamine (TPZ), an aromatic *N*-oxide, is probably the best known member of this category and its structure is given in Figure 13. Compared to 10-15 fold difference seen for nitroimidazoles, TPZ has a 50-200 fold differential toxicity toward hypoxic cells compared to normal cells.⁵⁴ It also has a wider range of oxygen levels, where it maintains toxicity toward hypoxic cells.⁶² Cytochrome P450 reductase, among other reducing enzymes, is suggested to play an important role in the one electron reduction of TPZ to form a highly reactive radical that is able to react with DNA to abstract hydrogen, leading to strand breaks.

AQ4N, shown in Figure 13, is an anthraquinone prodrug that contains aliphatic *N*-oxides. The activity of this drug is based on the reduction of the tertiary *N*-oxides to form an active DNA-binding agent and a potent inhibitor of DNA topoisomerase II. AQ4N has been shown to be effective against experimental models in combination with radiotherapy.⁶²

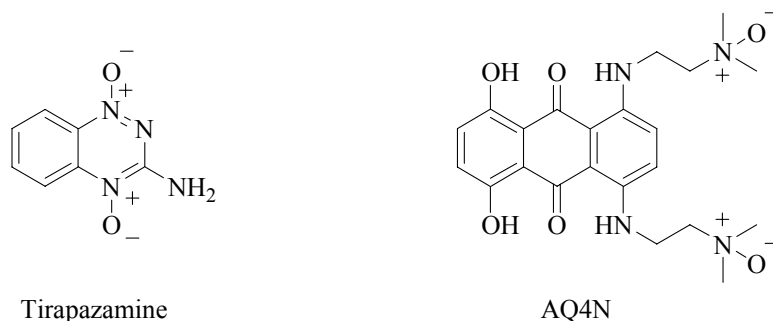


Figure 13. Structures of Tirapazamine and AQ4N

Quinones. The para-quinone containing compounds, including various forms of indolequinones, benzoquinones and naphthaquinones, are one of the major bioreductive classes of anticancer therapeutics. These compounds were developed as a result of the identification of natural products, such as mitomycin C (MMC), streptonigrin and adriamycin, that are currently in use as anticancer agents. Other agents developed as partial structures of the naturally occurring quinones, such as EO9 and RH1 (Figure 14), show enhanced cytotoxicity in experimental tumor models.^{59, 63}

The quinone prodrug can be reduced by a two-electron reducing enzyme (e.g. NQO1) to afford the hydroquinone species that may form drug-DNA adducts. Alternatively, reduction through a one-electron reductase (e.g. P450R) forms the semiquinone radical species, that, itself exerts a cytotoxic effect but can be further reduced to the hydroquinone.

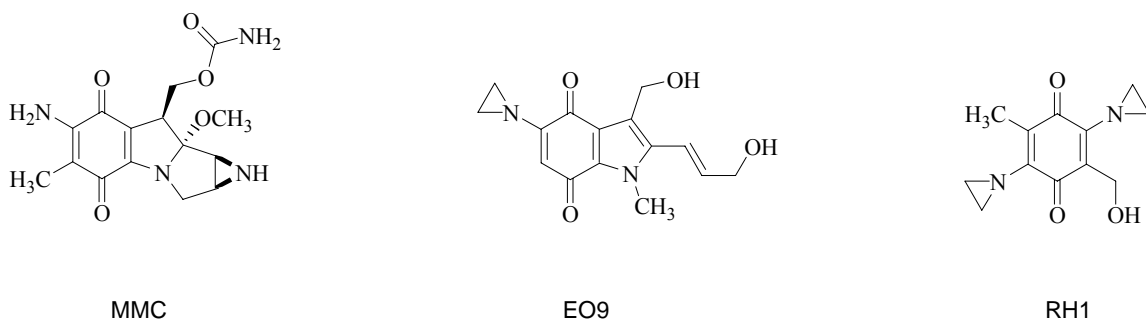


Figure 14. Structures of MMC, EO9, and RH1

Indolequinones as Drug Delivery Agents

A large range of indolequinone bioreductive analogs has been synthesized based on the clinically-relevant naturally occurring antitumor drug mitomycin C (MMC), which is considered to be the archetypal bioreductive drug. MMC is usually used in combination with other drugs or radiotherapy. The bioreductive indolequinone EO9 was synthesized in 1987 by Oostveen and Speckamp as part of a project designed to develop new analogs of MMC.⁶⁴ It was considered for clinical evaluation based on a novel mechanism and potent *in vitro* activity. Unfortunately, EO9 showed high toxicity and no antitumor activity (possibly due to rapid plasma clearance); however, some concerns were raised about the design of the trials.^{63, 65} These included the failure to evaluate EO9 in combination with radiation and failure to measure the levels of enzymes that are critical to the activation of the drug.

Mode of Action

The reduction of the *p*-quinone substructure of MMC results in electron movement from the hydroquinone or semiquinone activated species to form an electrophilic site initially at the C-1 position and subsequently at the C-10 position. These sites would then be attacked by DNA to form mainly adducts at the N-2 position of guanine leading to crosslinking. This mechanism is shown in Figure 15.

The indolequinone EO9 has shown improved antitumor properties over MMC, which have been attributed to its aziridinyl moiety and the formation of the iminium intermediate upon reductive activation. Mechanistic studies have indicated that, to cause DNA damage, reduction of EO9 must occur in a fashion similar to MMC.⁶³ The C-3 position (equivalent to the C-10 in MMC) is activated for nucleophilic attack by the

movement of the lone pair of electrons from the N-1 position followed by the elimination of the 3-hydroxymethyl substituent. The C-2 position of EO9 (equivalent to the C-1 in MMC) is also thought to be activated by a similar mechanism in which, following bioreduction and electron transfer, a quinone methide is generated that can be attacked by DNA, as seen in Figure 16.

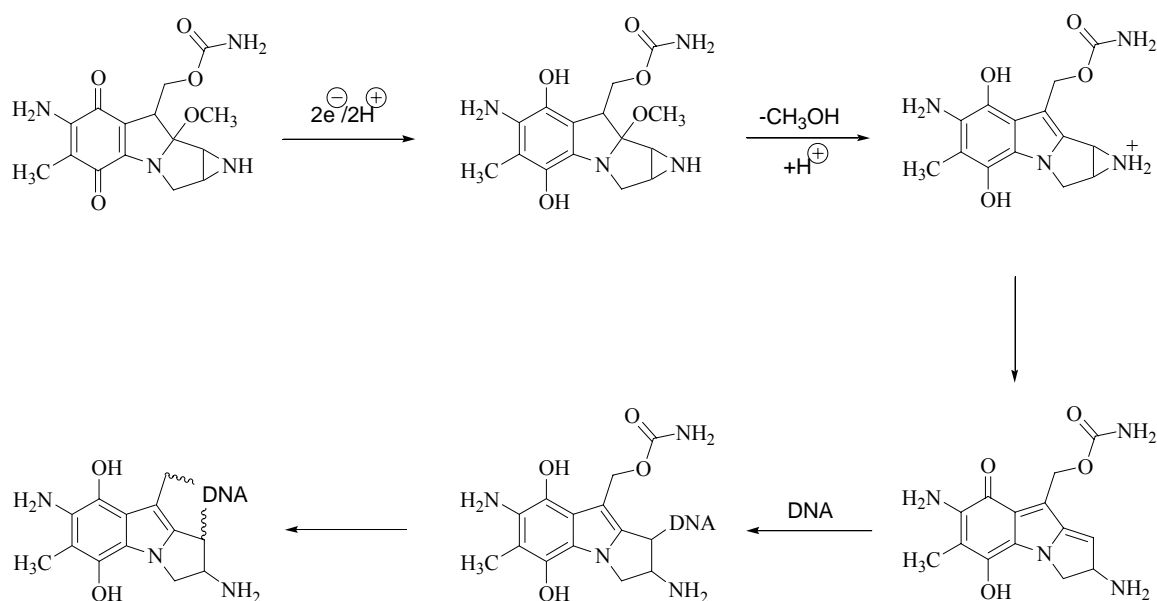


Figure 15. Proposed mechanism of activation and DNA crosslinking of MMC⁶⁶

Recently, EO9 has been observed to form both DNA strand breaks and interstrand crosslinks, which may be accounted for by this mechanism and involves the C-3 position. The C-5 aziridiny substituent of EO9 can alkylate DNA by protonation of the aziridine group followed by nucleophilic attack. Following reduction, the aziridiny moiety is activated due to an increase in pK_a and becomes more prone to attack by DNA.⁶⁶

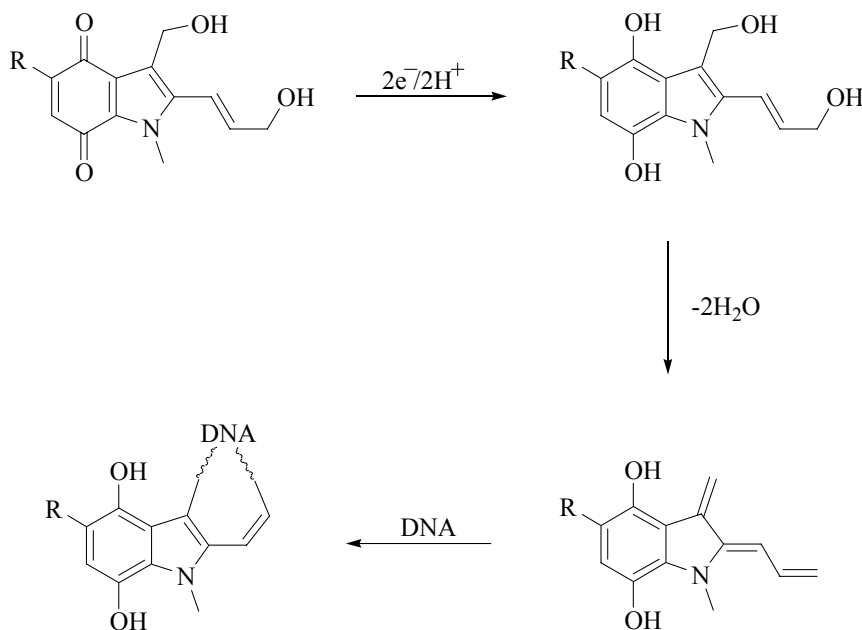


Figure 16. Proposed mechanism of DNA cross-linking by EO9⁶⁶

Enzyme Activation

Activation of the indolequinone bio-reductives is catalyzed by enzymes such as NAD(P)H: quinone oxidoreductase (NQO1), which is an oxygen-independent two-electron reducing enzyme, and NAD(P)H: cytochrome *c* P450 reductase (P450R), a one-electron reducing enzyme. Unlike reduction by NQO1, drug activation by P450R involves oxygen-sensitive reduction chemistry that protects oxidative tissue. Other bio-reductive enzymes are also involved in the activation of these agents. Cellular responses to indolequinone bio-reductive agents depend on a complex relationship between enzymatic activity and oxygenation levels.

There is now substantial evidence that NQO1 is overexpressed in a variety of tumor types,⁶⁷ and it is extensively implicated in the activation of MMC, EO9, and derivative indolequinones, using NAD(P)H as a cofactor.⁶³ Expansive studies of the structure-activity relationship of indolequinones, as NQO1-specific prodrugs, have

elicited structural features that are key to NQO1-mediated activity.^{65, 68} Modifications at the C-2 position of the indole ring, for instance, impact substrate specificity because they are located at the entrance to the active site. Also, analogs with bulky groups at the C-3 position limit enzyme activity, and the aziridinyl moiety at the C-5 position markedly increases drug potency.

Under aerobic conditions, a good correlation exists between NQO1 activity and chemosensitivity to EO9. However, under hypoxic conditions, EO9 shows highly potent cytotoxicity only against cells with low NQO1 levels. It has been stipulated that EO9 remains active in a hypoxic environment, despite low NQO1 activity, because of activation by one electron reductases that lead to a more efficient reduction and the generation of the more toxic semiquinone species. NQO1 reduction of EO9 in hypoxic cells may in fact reduce cytotoxicity due to the formation of the hydroquinone, which has to back-oxidize to the more reactive semiquinone. NQO1, then, appears to be the major reductase involved in the activation of the cytotoxic effects of indolequinones under aerobic conditions, while P450R is predominantly involved in the activation and subsequent cytotoxic effects under hypoxic conditions. Indolequinones are therefore an uncommon class of bioreductive drugs that have the potential to kill the aerobic fraction of NQO1-rich tumors or the hypoxic fraction of NQO1-deficient tumors.

Indolequinone Triggers

Based on the mechanistic propensity of their C-3 substituents to undergo elimination, indolequinones have been studied extensively to examine their potential to release a cytotoxic agent in a reductive environment. Consequently, the bioreductive has a secondary effect in addition to the iminium derivative, which is an electrophilic DNA-

alkylating agent, formed upon reduction and elimination. The potential for bioreductive drug targeting this way has been demonstrated by the reductive elimination of compounds, such as aspirin⁶⁹ or coumarin,⁷⁰ from indolequinones.

The two pathways to drug activation involve either the NQO1-directed two-electron reduction, via hydride transfer, to form the hydroquinone, or the P450R-directed one-electron reduction to form the semiquinone intermediate. Both pathways result in the release of the leaving group and formation of the iminium intermediate (Figure 17). The process of enzymatic reduction localizes electron density onto the N-1 position, and a cascade of electron movements results in the release via a Michael-type elimination from the (indol-3-yl)methyl position of the indole ring. This mechanism was further confirmed when a cytotoxic indolequinone, 5-aziridiny-3-hydroxymethyl-1-methylindole-4,7-dione, bearing an aziridiny substituent at the C-5 position crosslinked DNA.⁷¹ This observation increased when the drug was incubated under hypoxic conditions or when evaluated in tumor cell lines overexpressing NQO1.

Alternatively, the C-2 position is also capable of drug release, which has been demonstrated by the elimination of phosphoramidate drugs under the control of two-electron and one-electron reductases.⁷² Also, bulkier groups at the 2-position are thought to increase substrate specificity for NQO1-mediated activity. The drug is released from the indolequinone via an *ortho*-quinodimethane type intermediate.

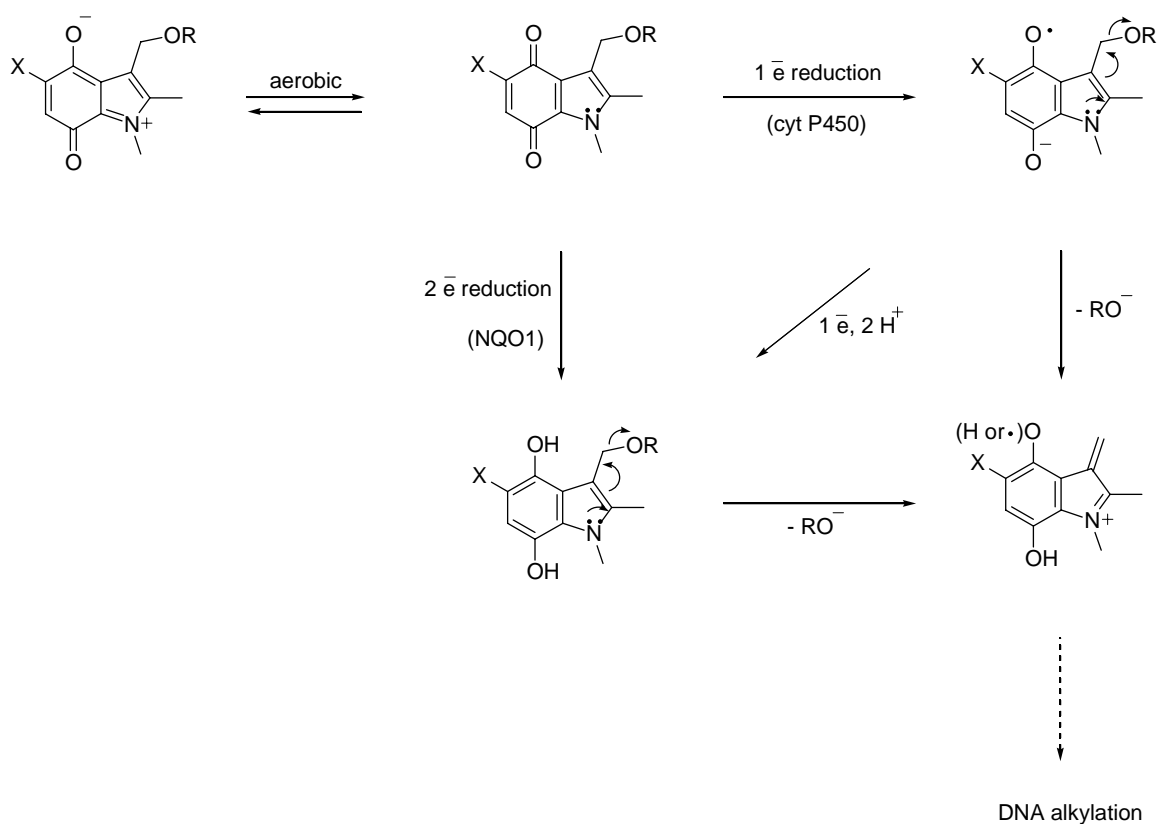


Figure 17. Mode of action for indolequinone triggers.

Rationale for Drug Design

Vascular Disrupting Agents (VDAs)

A simple model (Figure 18), based on work by Hamel and co-workers,⁷³ details features key to the development of active analogs of combretastatin. This model was based on structure-activity studies on early analogs of combretastatin. The trimethoxyphenyl ring, for example, is believed to be paramount because of its role in tubulin binding. Also, the methoxy group at the 4'-position of CA4 is considered to be important, therefore, many CA4 analogs contain the methoxy group at an analogous position in their structures. Even though the bridge between the two phenyl rings can vary, combretastatin derivatives usually adopt a *cis*-conformation because of good activity

as inhibitors of tubulin inhibition. An aryl-aryl distance of approximately 5 Å between the two rings is also recommended.

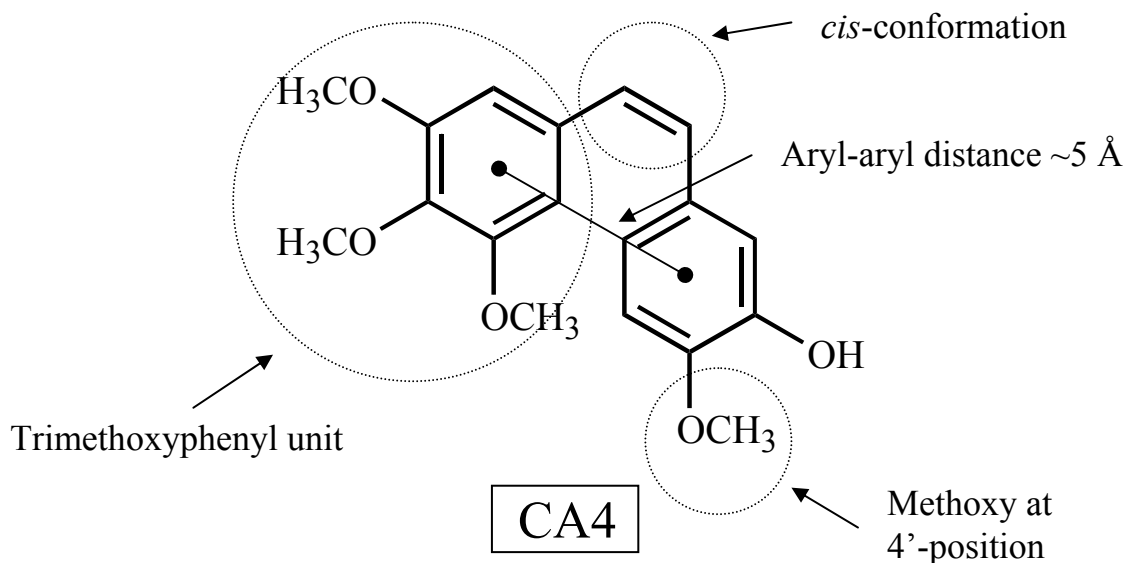


Figure 18. Design paradigm for analogs of CA4

The dihydronaphthalene scaffold, like the benzo[*b*]thiophene and indole scaffolds also used in the Pinney group, can be utilized in the synthesis of effective tubulin-binding agents and vascular disrupting agents because of the restriction of the molecule to the *cis*-conformation. Furthermore, certain estrogenic compounds, such as 2-methoxyestradiol that binds to the estrogen receptor (ER), were found to interfere with microtubule assembly, as well as mitosis.^{74, 75} Previous graduate students in the Pinney group, Zhi Chen⁷⁶ and Vani Mocharla,⁷⁴ had developed some dihydronaphthalene derivatives of combretastatin upon structural modification of ER-binding molecules, such as such as the dihydronaphthalene-based ligands nafoxidene and trioxifene (Figure 19). The synthesis of Oxi6196⁷⁹ was developed as a consequence of their work by Pinney and co-workers.

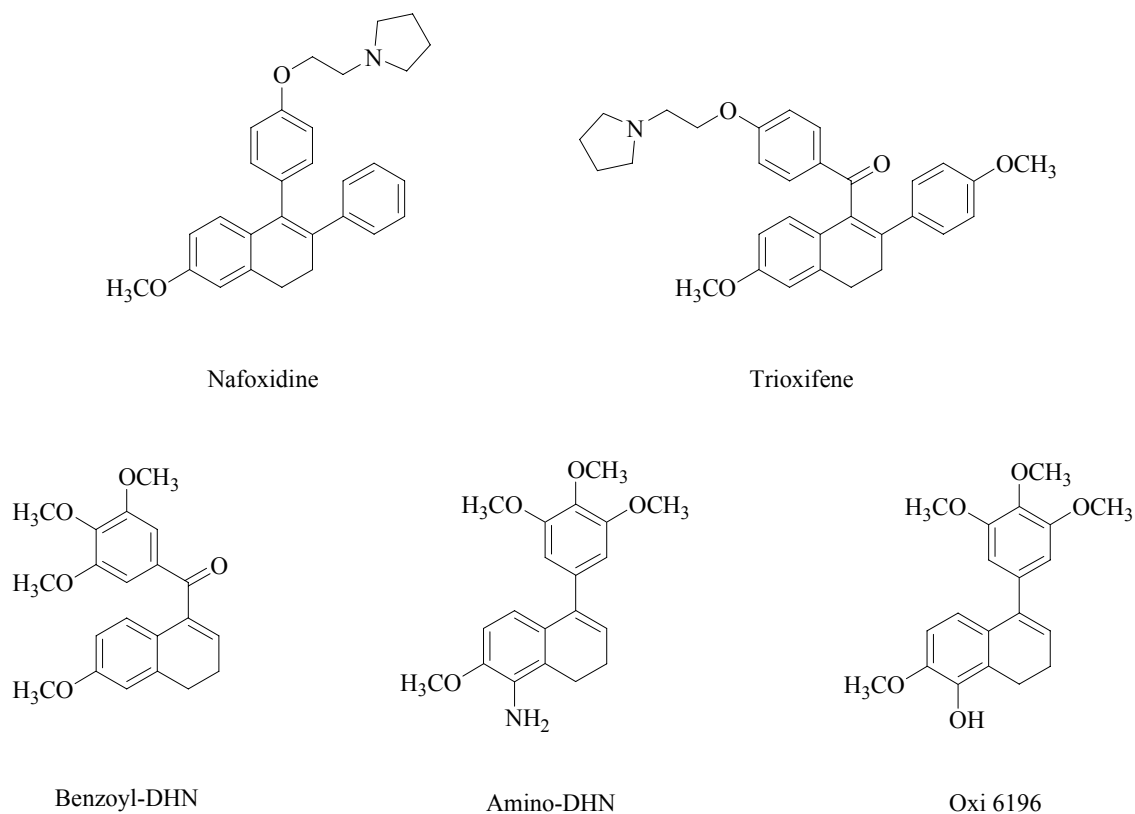


Figure 19. Structures of ER-binding ligands (Nafoxidene and Trioxifene),⁷⁷ molecules developed by V. Mocharla⁷⁴ and Z. Chen⁷⁶ (Benzoyl-DHN) and Amino-DHN) and Oxi6196⁷⁹

The first project involved the re-synthesis of Oxi6196, an extremely potent inhibitor of tubulin assembly ($IC_{50} = 0.5 \mu M$), as an individual project, as well as a part of a team-based scale-up. The second project in this series of dihydronaphthalene derivatives of combretastatin involved the synthesis of a β -Substituted dihydronaphthalene analog, which is structurally very similar to Oxi6196. Rudimentary molecular modeling, with Chem3D and MM2 energy minimization, depicted a longer aryl-aryl distance of 6.5 Å for the β -analog as opposed to 5.1 Å for Oxi6196, which is shown in Figure 20.

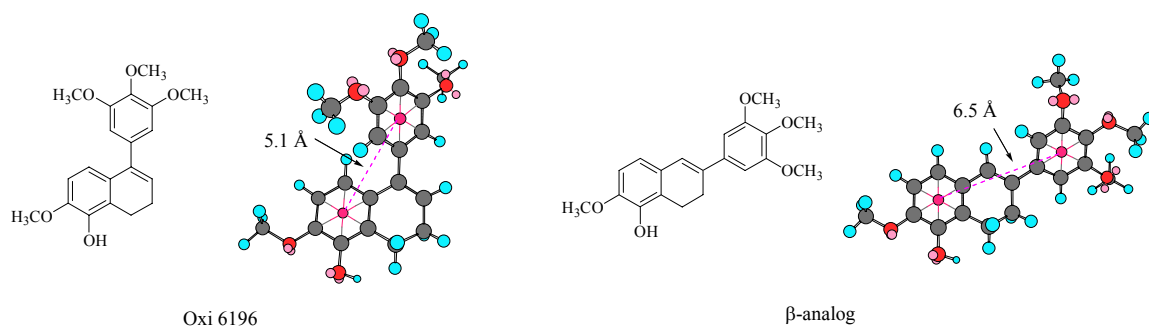


Figure 20. Aryl-aryl distances for Oxi6196 and β -analog (Chem3D)

A novel synthesis for the β -analog was developed and attempted in order to investigate the final product for any potential for tubulin-inhibition and to elucidate any structure-activity data with respect to molecular recognition of the colchicine binding site on β -tubulin.

Bioreductive Agents

Two classes of indolequinones were synthesized as potential triggers to release attached VDAs in a bioreductive environment. The indolequinone, upon activation, can release an effective drug, such as CA4, and form an active species, the iminium intermediate that can act as a DNA alkylating agent, from the bioreductive prodrug, shown in Figure 21.

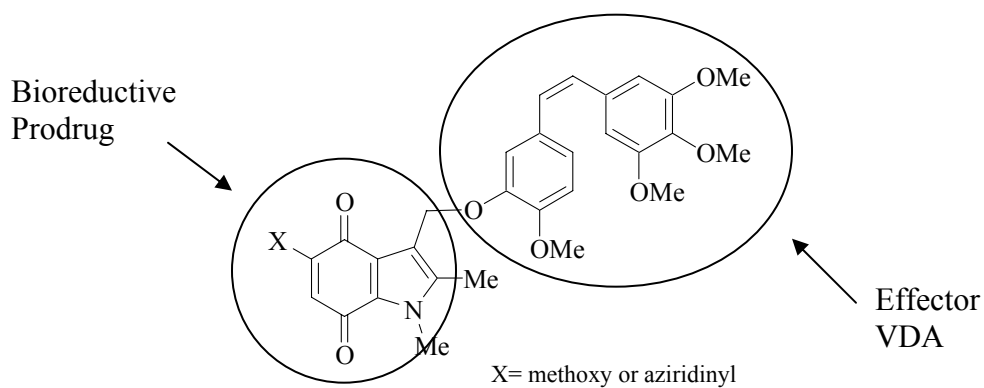


Figure 21. Model of an indolequinone-VDA bioconjugate drug

With the addition of an aziridinyl group, which can also alkylate DNA upon nucleophilic ring opening, this type of drug has the potential of becoming a tri-functional anticancer agent. The mechanisms for the release of VDAs from the 3- and 2-indolequinones are shown below in Fig. 22.

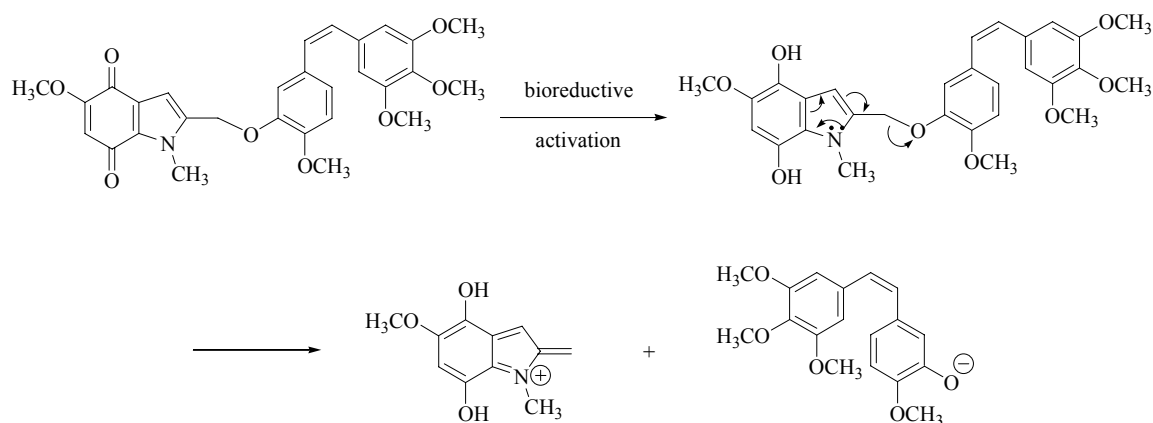
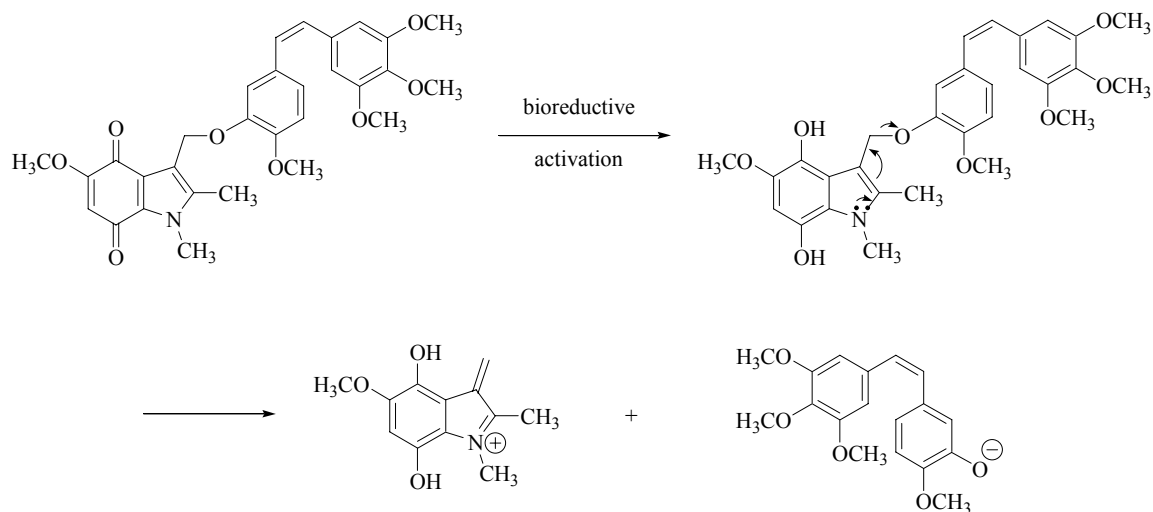


Figure 22. Mechanism of release of VDAs from 3- and 2-indolequinones

The idea of an indolequinone-VDA trigger evolved from another project – coupling the bioreductive Tirapazamine (TPZ) with CA4 (Figure 23) via an ester linkage that can be broken by hydrolases in the cellular environment. The CA4 may then be able to exert its vascular disrupting effect, and the TPZ moiety could be hypoxically activated and interfere with DNA.

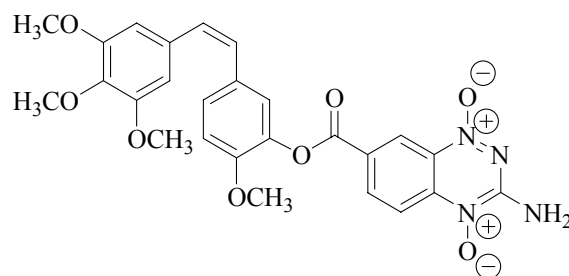


Figure 23. Structure of TPZ-CA4 bioconjugate

CHAPTER TWO

Materials and Methods

General Section

Chemicals were obtained from commercial sources such as Acros Chemicals, Aldrich Chemical Company, Alfa Aesar, Lancaster Chemicals and Fisher Scientific. Reactions that involved air or moisture sensitive reagents were performed in oven-dried glassware under nitrogen atmosphere using dried needles and cannulas to transfer solvents and reagents. Reactions were monitored by thin layer chromatography (TLC) using Merck Kieselgel 60 F₂₅₄ glass backed plates. The plates were visualized by the use of a multiband 254/365 nm UV lamp or iodine. Compounds were purified by column chromatography, using silica gel (230-400 mesh) and alumina (150 mesh), prep TLC, or recrystallization. Solvents used for reactions, chromatography and workup were purchased from the aforementioned companies. Hexanes and dichloromethane were dried over calcium chloride. Ethyl acetate, diethyl ether, methanol, ethanol, THF, and other solvents were purchased as anhydrous solvents and used without further purification.

Structural elucidation of compounds was carried out using NMR on either Bruker DPX-300 or Varian 500 spectrometers. ¹H NMR spectra were recorded at 300 or 500 MHz, and ¹³C spectra were recorded at 75 or 125 MHz. All NMR were recorded in CDCl₃ unless noted otherwise. Chemical shifts are expressed in ppm (δ). NMR patterns are recorded as singlets (s), doublets (d), triplets (t), quartets (q), pentets (p), or multiplets (m), and the coupling constants (J) are reported in Hz.

*Synthesis of Oxi6196*⁷⁹*5-Hydroxy-6-methoxy-1,2,3,4-tetrahydronaphthalene (1)*^{78, 79}

To a solution of 6-methoxy-1,2,3,4-tetrahydronaphthalene (10.00 g, 61.6 mmol) in TMEDA (17 mL), *sec*-butyllithium (1.0 M, 92.5 mmol) was added dropwise at 0 °C. The mixture was allowed to stir for 45 min at room temperature. Trimethyl borate (9.61 g, 92.5 mmol) was added dropwise at 0 °C, and then the mixture was allowed to stir at room temperature for 1h. The reaction was cooled down to 0 °C and acetic acid (7 mL) was added dropwise, followed by dropwise addition of hydrogen peroxide (35%, 13 mL). The mixture was allowed to stir overnight at room temperature, quenched with saturated NH₄Cl, and extracted with EtOAc. The organic layer was dried (Na₂SO₄) and concentrated *in vacuo*. The crude product was purified by column chromatography (hexanes/EtOAc, 98:2) to yield the title product (2.22 g, 12.5 mmol, 20%).

¹H NMR (300 MHz, CDCl₃) δ 6.67 (1H, d, *J* = 8.2 Hz, ArH), 6.58 (1H, d, *J* = 8.2 Hz, ArH), 5.65 (1H, s, OH), 3.85 (3H, s, OCH₃), 2.70 (4H, t, *J* = 6.2 Hz, CH₂), 1.76 (4H, m, CH₂).

5-Acetoxy-6-methoxy-1,2,3,4-tetrahydronaphthalene (2)^{78, 79}

To a solution of 5-hydroxy-6-methoxy-1,2,3,4-tetrahydronaphthalene (2.20 g, 12.3 mmol) in CH₂Cl₂ (40 mL) was added DIPEA (2.39 g, 18.5 mmol), acetic anhydride (1.89 g, 18.5 mmol) and DMAP (0.20 g, 1.6 mmol). The reaction mixture was allowed to stir overnight and then concentrated *in vacuo*. The crude product was purified by column chromatography (hexanes/EtOAc, 9:1) to yield the title product (2.26 g, 10.3 mmol, 83%).

^1H NMR (300 MHz, CDCl_3) δ 6.93 (1H, d, $J = 8.1$ Hz, ArH), 6.76 (1H, d, $J = 8.1$ Hz, ArH), 3.79 (3H, s, OCH_3), 2.72 (2H, m, CH_2), 2.57 (2H, m, CH_2), 2.33 (3H, s, COCH_3), 1.75 (4H, m, CH_2).

5-Acetoxy-6-methoxy-3,4-dihydro-2H-naphthalen-1-one (**3**)^{78, 79}

A solution of DDQ (4.67 g, 20.5 mmol) in dioxane (5 mL) was added dropwise to a solution 5-acetoxy-6-methoxy-1,2,3,4-tetrahydronaphthalene (2.26 g 10.3 mmol) in a mixture of water/dioxane (5 mL, 5:95). EtOAc was used to extract the organic layer, which was concentrated, and saturated NaHCO_3 (10 mL) was added. The crude product was extracted with diethyl ether, and purification by column chromatography (hexanes/EtOAc, 4:1) yielded the title product (1.23 g, 5.3 mmol, 51%).

^1H NMR (300 MHz, CDCl_3) δ 7.98 (1H, d, $J = 8.8$ Hz, ArH), 6.92 (1H, d, $J = 8.8$ Hz, ArH), 3.88 (3H, s, OCH_3), 2.78 (2H, t, $J = 6.1$ Hz, CH_2), 2.59 (2H, dd, $J = 7.4$ Hz, 5.9 Hz, CH_2), 2.35 (3H, s, COCH_3), 2.10 (4H, p, $J = 6.5$ Hz, CH_2).

5-Hydroxy-6-methoxy-3,4-dihydro-2H-naphthalen-1-one (**4**)^{78, 79}

To a solution of 5-acetoxy-6-methoxy-1-tetralone (1.23 g, 5.3 mmol) in MeOH (30 mL) was added potassium carbonate (1.45 g, 10.5 mmol) and water (1.5 mL). The suspension was stirred overnight at room temperature. The solvent was removed *in vacuo*, and saturated NaHCO_3 (50 mL) was added. The reaction mixture was acidified with the addition of concentrated HCl and then extracted with CH_2Cl_2 and EtOAc. The combined organic layers were dried (Na_2SO_4) and concentrated to yield the title product (0.92 g, 4.8 mmol, 91%) as a brown crystalline solid.

^1H NMR (300 MHz, CDCl_3) δ 7.68 (1H, d, $J = 8.6$ Hz, ArH), 6.84 (1H, d, $J = 8.6$ Hz, ArH), 5.71 (1H, s, OH), 3.96 (3H, s, OCH₃), 2.93 (2H, t, $J = 6.3$ Hz, CH₂), 2.63 (2H, t, $J = 6.0$, CH₂), 2.11 (2H, m, CH₂).

*5-(tert-Butyldimethylsilyl)-oxy-6-methoxy-1-tetralone (5)*⁷⁹

Triethylamine (0.73 g, 7.2 mmol) and DMAP (0.06 g, 0.5 mmol) were added to a solution of 5-hydroxy-6-methoxy-1-tetralone (0.92 g, 4.8 mmol) in anhydrous CH_2Cl_2 at 0 °C. The mixture was stirred for 5 min, followed by the addition of TBSCl (1.08 g, 7.2 mmol), and was allowed to stir overnight at room temperature. The mixture was quenched with water. The organic layer was separated, dried (Na_2SO_4) and concentrated. The crude product was purified by column chromatography (hexanes/EtOAc, 95:5) to yield the title product (0.99 g, 3.2 mmol, 67%).

^1H NMR (300 MHz, CDCl_3) δ 7.73 (1H, d, $J = 8.7$ Hz, ArH), 6.82 (1H, d, $J = 8.7$ Hz, ArH), 3.85 (3H, s, OCH₃), 2.90 (2H, t, $J = 6.0$ Hz, CH₂), 2.57 (2H, dd, $J = 7.5$ Hz, $J = 6.0$ Hz, CH₂), 2.07 (2H, m, CH₂).

*5-(tert-Butyldimethylsilyloxy)-1-hydroxy-6-methoxy-1-(3',4',5'-trimethoxyphenyl)-2,3,4-trihydronaphthalene (6)*⁷⁹

To a solution of 3,4,5-trimethoxybromobenzene (1.20 g, 4.8 mmol) in dry ether (75 mL), n-butyllithium (0.9 M, 5.4 mL) was added dropwise at -78 °C. The temperature was gradually allowed to reach -30 °C. A solution of 5-(tert-butyldimethylsilyl)-oxy-6-methoxy-1-tetralone (0.99 g, 3.2 mmol) in ether (25 mL) was added dropwise, and the mixture was allowed to stir for 2 h at room temperature. The reaction was quenched with water, and extracted with ether. The organic layer was dried (Na_2SO_4) and concentrated

in vacuo. Purification by column chromatography yielded the title product (1.01 g, 2.1 mmol, 66%).

^1H NMR (300 MHz, CDCl_3) δ 6.70 (1H, s, ArH), 6.60 (1H, s, ArH), 3.82 (3H, s, OCH₃), 3.77 (9H, s, OCH₃), 2.92 (2H, m, CH₂), 2.10 (2H, m, CH₂), 1.61 (2H, s, CH₂), 1.01 (9H, s, CCH₃), 0.23 (3H, s, SiCH₃), 0.20 (3H, s, SiCH₃).

*5-(tert-Butyldimethylsilyloxy)-6-methoxy-1-(3',4',5'-trimethoxyphenyl)-3,4-dihydronaphthalene (8)*⁷⁹

A mixture of HOAc (23 mL) and water (140 mL) was added to 5-(tert-butyldimethylsilyloxy)-1-hydroxy-6-methoxy-1-(3',4',5'-trimethoxyphenyl)-2,3,4-trihydronaphthalene (1.01 g, 2.1 mmol). The mixture was refluxed overnight and extracted with CH_2Cl_2 . The organic extract was dried (Na_2SO_4), filtered and concentrated to yield the title product (0.98 g, 2.2 mmol), which was used directly in the next step without further purification.

Tetrabutylammonium fluoride in THF (1.0 M, 3.2 mL) was added dropwise to the intermediate (0.98 g, 2.2 mmol) in CH_2Cl_2 (25 mL) at 0 °C. The reaction was monitored by TLC and completed in 10 min. Water was added, and the mixture was extracted with CH_2Cl_2 . Purification by column chromatography yielded the title product (0.50 g, 1.5 mmol, 71%) as an off-white powder.

^1H NMR (300 MHz, CDCl_3) δ 6.63 (1H, d, $J = 8.5$ Hz, ArH), 6.59 (2H, d, $J = 8.51$ Hz, ArH), 5.98 (1H, s, CH), 5.71 (1H, s, OH), 3.88 (6H, s, OCH₃), 3.84 (6H, s, OCH₃), 2.89 (2H, t, $J = 7.71$, CH₂), 2.39 (2H, m, CH₂).

^{13}C NMR (75 MHz, CDCl_3) δ 152.87, 145.82, 141.98, 139.51, 137.05, 136.87, 128.98, 125.34, 122.28, 117.34, 107.24, 105.94, 60.89, 56.09, 55.92, 22.79, 20.20.

*Synthesis of β -Substituted Dihydronaphthalene Analog**5-Isopropoxy-6-methoxy-1,2,3,4-tetrahydronaphthalene (9)*

To a solution of 5-hydroxy-6-methoxy-1,2,3,4-tetrahydronaphthalene (1.21 g, 6.8 mmol) in dry acetone (125 mL) was added Cs₂CO₃ (17.7 g, 54.3 mmol) and 2-bromopropane (8.35 g, 67.9 mmol), and the mixture was refluxed overnight. The reaction mixture was filtered, and the solvent was removed from the filtrate *in vacuo*. Purification by column chromatography (hexanes/EtOAc, 99:1) yielded the title product (1.41 g, 6.4 mmol, 94%).

¹H NMR (300 MHz, CDCl₃) δ 6.73 (1H, d, $J = 8.3$ Hz, ArH), 6.67 (1H, d, $J = 8.3$ Hz, ArH), 4.46 (1H, m, CH), 3.76 (3H, s, CH₃), 2.70 (4H, d, $J = 11.0$ Hz, CH₂), 1.70 (4H, m, CH₂), 1.27 (3H, s, CH₃), 1.25 (3H, s, CH₃).

5-Isopropoxy-6-methoxy-3,4-dihydro-2H-naphthalen-1-one (10)

A solution of DDQ (2.90 g, 12.8 mmol) in dioxane (35 mL) was added dropwise to a solution of 5-isopropoxy-6-methoxy-1,2,3,4-tetrahydronaphthalene (1.41 g, 6.4 mmol) in a mixture of water/dioxane (35 mL, 5:95). EtOAc was used to extract the organic layer, which was concentrated, and saturated NaHCO₃ (10 mL) was added. The crude product was extracted with diethyl ether, and purification by column chromatography (hexanes/EtOAc, 4:1) yielded the title product (1.04 g, 4.4 mmol, 69%).

¹H NMR (300 MHz, CDCl₃) δ 7.84 (1H, d, $J = 8.7$ Hz, ArH), 6.86 (1H, d, $J = 8.7$ Hz, ArH), 4.45 (1H, m, CH), 3.89 (3H, s, CH₃), 2.95 (2H, t, $J = 6.0$ Hz, CH₂), 2.58 (2H, t, $J = 6.0$ Hz, CH₂), 2.06 (2H, p, $J = 6.6$ Hz, CH₂), 1.30 (3H, s, CH₃), 1.28 (3H, s, CH₃).

5-Isopropoxy-6-methoxy-1,2,3,4-tetrahydronaphthalen-1-ol (11)

To a solution of 5-isopropoxy-6-methoxy-3,4-dihydro-2H-naphthalen-1-one (1.04 g, 4.4 mmol) in anhydrous methanol (60 mL) was added NaBH₄ (0.30 g, 7.7 mmol) at 0 °C. The reaction mixture was then allowed to stir at room temperature for one hour. The mixture was quenched with saturated NaHCO₃ before undergoing rotary evaporation, and the product was extracted from the aqueous layer by diethyl ether. The organic layer was dried (Na₂SO₄) and concentrated to yield the title product (0.99 g, 4.2 mmol, 94%) without further purification.

¹H NMR (300 MHz, CDCl₃) δ 7.12 (1H, d, *J* = 8.5 Hz, ArH), 6.79 (1H, d, *J* = 8.5 Hz, ArH), 4.73 (1H, s, CH), 4.47 (1H, m, CH), 3.82 (3H, s, CH₃), 2.84 (1H, m, CH₂), 2.62 (1H, m, CH₂), 1.89 (2H, m, CH₂), 1.78 (2H, m, CH₂), 1.28 (3H, s, CH₃), 1.26 (3H, s, CH₃).

8-Isopropoxy-7-methoxy-1,2-dihydronaphthalene (12)

Acetic acid (25 mL) was added to 5-isopropoxy-6-methoxy-1,2,3,4-tetrahydronaphthalen-1-ol (0.99 g, 4.2 mmol) in water (100 mL), and the reaction mixture was refluxed overnight. The mixture was extracted with CH₂Cl₂, and the combined organic extracts were dried (Na₂SO₄), filtered and concentrated *in vacuo*. The crude product was purified by column chromatography (hexanes/EtOAc, 99:1) to yield the title product (0.86 g, 3.9 mmol, 94%).

¹H NMR (300 MHz, CDCl₃) δ 6.73 (1H, d, *J* = 8.2 Hz, ArH), 6.68 (1H, d, *J* = 8.2 Hz, ArH), 6.40 (1H, dt, *J* = 7.7 Hz, *J* = 1.8 Hz, CH), 5.90 (1H, dt, *J* = 9.6 Hz, *J* = 4.4 Hz, CH), 4.38 (1H, m, CH), 3.81 (3H, s, CH₃), 2.80 (2H, t, *J* = 7.9, CH₂), 2.23 (2H, m, CH₂), 1.29 (3H, s, CH₃), 1.27 (3H, s, CH₃).

5-Isopropoxy-6-methoxy-3,4-dihydro-1H-naphthalen-2-one (14)

To a solution of 8-isopropoxy-7-methoxy-1,2-dihydronaphthalene (0.94 g, 4.3 mmol) in CH₂Cl₂ (25 mL), MCPBA (0.97 g, 5.6 mmol) in CH₂Cl₂ (65 mL) was added dropwise at 0 °C, and the reaction mixture was stirred at 0 °C for 12 h. The mixture was washed once with saturated NaHCO₃ and 3% NaHSO₃ and twice with water. The organic layer was dried (Na₂SO₄), and the solvent was removed by rotary evaporation (bath temperature 25 °C).

To the crude product, dissolved in dry toluene (70 mL), was added *p*-toluenesulfonic acid monohydrate (150 mg), and the reaction mixture was refluxed for 1.5 h. After cooling to room temperature, diethyl ether was added, and the organic extracts were washed twice with water, dried (Na₂SO₄), and the solvent removed *in vacuo*. Purification by column chromatography (hexanes/EtOAc, 95:5) yielded the title product (0.28 g, 1.2 mmol, 28%).

¹H NMR (300 MHz, CDCl₃) δ 6.81 (1H, d, *J* = 8.3 Hz, ArH), 6.77 (1H, d, *J* = 8.3 Hz, ArH), 4.43 (1H, m, CH), 3.84 (3H, s, CH₃), 3.51 (2H, s, CH₂), 3.11 (2H, t, *J* = 6.5 Hz, CH₂), 2.46 (2H, t, *J* = 6.1 Hz, CH₂), 1.30 (3H, s, CH₃), 1.28 (3H, s, CH₃).

*Synthesis of 3-Substituted Indolequinone Derivatives**Ethyl 5-methoxy-1,2-dimethylindole-3-carboxylate (15)*

Ethyl 5-hydroxy-2-methylindole-3-carboxylate (2.00 g, 9.1 mmol) in DMF (17 mL) was added to a stirring suspension of NaH (0.66 g, 27.4 mmol) in DMF (50 mL) at 0 °C. Iodomethane (3.88 g, 27.4 mmol) was added dropwise at 0 °C, and the mixture was allowed to warm to room temperature. The reaction was monitored by TLC and was

completed within 2 h. Saturated ammonium chloride solution was added and the mixture extracted with EtOAc. The EtOAc layer was washed with water, dried (Na_2SO_4), and concentrated to yield the title compound as a tan solid (2.23 g, 9.1 mmol, quant.).

^1H NMR (300 MHz, CDCl_3) δ 7.66 (1H, d, $J = 2.5$ Hz, ArH), 7.17 (1H, d, $J = 8.8$ Hz, ArH), 6.87 (1H, dd, $J = 8.8$ Hz, 2.6 Hz, ArH), 4.39 (2H, q, $J = 7.1$ Hz, $\text{CO}_2\text{CH}_2\text{CH}_3$), 3.89 (3H, s, OCH_3), 3.67 (3H, s, NCH_3), 2.75 (3H, s, CH_3), 1.45 (3H, t, $J = 7.1$ Hz, $\text{CO}_2\text{CH}_2\text{CH}_3$).

Ethyl 5-methoxy-1,2-dimethyl-4-nitroindole-3-carboxylate (16)

To a solution of ethyl 5-methoxy-1,2-dimethylindole-3-carboxylate (2.23 g, 9.0 mmol) in HOAc (40 mL), cooled to -10 °C, was added a mixture of concentrated HNO_3 (6 mL) and HOAc (20 mL). The mixture was stirred at room temperature for 2 h. A yellow suspension was obtained which was poured onto an ice/water mixture, and the crystals obtained were filtered off and dried. The crude product was purified by column chromatography (hexanes/EtOAc, 4:1) to yield the title compound as a yellow powder (0.53 g, 1.8 mmol, 20%).

^1H NMR (300 MHz, CDCl_3) δ 7.35 (1H, d, $J = 9.0$ Hz, ArH), 6.98 (1H, d, $J = 9.0$ Hz, ArH), 4.29 (2H, q, $J = 7.2$ Hz, $\text{CO}_2\text{CH}_2\text{CH}_3$), 3.93 (3H, s, OCH_3), 3.71 (3H, s, NCH_3), 2.73 (3H, s, CH_3), 1.36 (3H, t, $J = 7.2$ Hz, $\text{CO}_2\text{CH}_2\text{CH}_3$).

Ethyl 4-amino-5-methoxy-1,2-dimethylindole-3-carboxylate (17)

To a suspension of ethyl 5-methoxy-1,2-dimethyl-4-nitroindole-3-carboxylate (0.53 g, 1.8 mmol) in EtOH (46 mL) were added tin powder (0.97 g, 8.2 mmol) and HCl (3 M, 13 mL). The mixture was heated under reflux for 30 min. Upon cooling the

solution was decanted from the excess tin and neutralized with NaHCO₃ (aqueous). The suspension obtained was added to an equal volume of water. The precipitate and aqueous layer were stirred overnight with CH₂Cl₂ and filtered through Celite to separate the layers. The organic product was dried (Na₂SO₄) and concentrated to yield the title compound as an off-white crystalline solid (0.43 g, 1.6 mmol, 89 %).

¹H NMR (300 MHz, CDCl₃) δ 6.88 (1H, d, *J* = 8.7 Hz, ArH), 6.53 (1H, d, *J* = 8.7 Hz, ArH), 5.75 (2H, br s, NH₂), 4.36 (2H, q, *J* = 7.1 Hz, CO₂CH₂CH₃), 3.87 (3H, s, OCH₃), 3.60 (3H, s, NCH₃), 2.66 (3H, s, CH₃), 1.41 (3H, t, *J* = 7.1 Hz, CO₂CH₂CH₃).

4-Amino-3-(hydroxymethyl)-5-methoxy-1,2-methylindole (18)

To a suspension of LiAlH₄ in THF (2 M, 6.6 mmol, 3.3 mL) at 0 °C was added a solution of ethyl 4-amino-5-methoxy-1,2-dimethylindole-3 carboxylate (0.43 g, 1.6 mmol) in THF (5 mL). The mixture was allowed to warm to room temperature and stirred for 30 min. The mixture was cooled to 0 °C and reaction quenched by the addition of water (0.5 mL), 1 M NaOH and silica gel (3 g). The granular precipitate was filtered off through a pad of Celite. The filtrate was dried (Na₂SO₄) to yield the title product as a dark-brown solid (0.32 g, 1.4 mmol, 88%).

¹H NMR (300 MHz, CDCl₃) δ 6.87 (1H, d, *J* = 8.6 Hz, ArH), 6.62 (1H, d, *J* = 8.6 Hz, ArH), 4.86 (2H, s, 3-CH₂), 3.87 (3H, s, OCH₃), 3.57 (3H, s, NCH₃), 2.35 (3H, s, CH₃).

3-(Hydroxymethyl)-5-methoxy-1,2-dimethylindole-4,7-dione (19)

To a solution of 4-amino-3-(hydroxymethyl)-5-methoxy-1,2-methylindole (0.32 g, 1.4 mmol) in Me₂CO (110 mL) was added a solution of potassium nitrosodisulfonate (1.6 g,

5.8 mmol) in sodium dihydrogen phosphate buffer (0.3 M, pH 7, 110 mL). The mixture was stirred at room temperature for 1 h. The excess Me₂CO was removed *in vacuo*. The resulting residue was extracted with CH₂Cl₂ and washed with water. The organic layer was dried (Na₂SO₄) and concentrated. The crude product was purified by column chromatography (CH₂Cl₂/EtOAc, 1:1) to yield the title compound as an orange/red solid (0.23 g, 1.0 mmol, 67%).

¹H NMR (300 MHz, CDCl₃) δ 5.64 (1H, s, CH), 4.61 (2H, d, *J* = 7.0 Hz, CH₂OH), 4.00 (2H, t, *J* = 7.0 Hz, OH), 3.89 (3H, s, OCH₃), 3.83 (3H, s, NCH₃), 2.23 (3H, s, CH₃).

5-Methoxy-3-{2-methoxy-5-[2-(3,4,5-trimethoxy-phenyl)-vinyl]-phenoxyethyl}-1,2-dimethyl-indole-4,7-dione (20)

To a mixture of 3-(hydroxymethyl)-5-methoxy-1,2-dimethylindole-4,7-dione (0.16 g, 0.7 mmol), CA4 (0.20 g, 0.6 mmol), and ADDP (0.16 g, 0.6 mmol) dissolved in dry benzene (20 mL), was added tributyl phosphine (0.16 mL, 0.6 mmol) dropwise and stirred for 48 h at room temperature. The excess benzene was removed *in vacuo*. The resulting residue was extracted with CH₂Cl₂ and washed with water. The organic layer was dried (Na₂SO₄) and concentrated. The crude product was purified by column chromatography (CH₂Cl₂/EtOAc, 4:1) to yield the title product as a bright orange solid (0.16 g, 0.3 mmol, 42%).

¹H NMR (300 MHz, CDCl₃) δ 7.02 (1H, d, *J* = 1.7 Hz, ArH), 6.87 (1H, dd, *J* = 8.4 Hz, 1.8 Hz, ArH), 6.74 (1H, d, *J* = 8.3 Hz, ArH), 6.50 (2H, s, ArH), 6.49 (1H, d, *J* = 11.8 Hz, HC=CH), 6.41 (1H, d, *J* = 11.8 Hz, HC=CH), 5.57 (1H, s, CH), 5.11 (2H, s,

CH_2), 3.86 (3H, s, OCH_3), 3.79 (6H, s, OCH_3), 3.77 (3H, s, NCH_3), (6H, s, OCH_3), 2.27 (3H, s, CH_3).

^{13}C NMR (125 MHz, CDCl_3) δ 159.8, 153.1, 138.4, 133.2, 130.2, 130.0, 129.1, 122.5, 117.2, 115.7, 111.7, 106.9, 106.1, 61.8, 61.1, 56.6, 56.2, 56.1, 32.5.

5-Methoxy-3-[2-methoxy-5-(3,4,5-trimethoxy-phenyl)-7,8-dihydro-naphthalen-1-ylloxymethyl]-1,2-dimethyl-1H-indole-4,7-dione (21)

To a mixture of 3-(hydroxymethyl)-5-methoxy-1,2-dimethylindole-4,7-dione (0.05 g, 0.2 mmol), Oxi6196 (0.07 g, 0.2 mmol), and ADDP (0.05 g, 0.2 mmol) dissolved in dry benzene (10 mL), was added tributyl phosphine (0.05 mL, 0.2 mmol) dropwise and stirred for 48 h at room temperature. The excess benzene was removed *in vacuo*. The resulting residue was extracted with CH_2Cl_2 and washed with water. The organic layer was dried (Na_2SO_4) and concentrated. The crude product was purified by column chromatography (hexanes/EtOAc, 3:2) to yield the title product as an orange solid (0.03 g, 0.05 mmol, 21%).

^1H NMR (300 MHz, CDCl_3) δ 6.81 (1H, d, $J = 8.5$ Hz, ArH), 6.69 (1H, d, $J = 8.5$ Hz, ArH), 6.57 (2H, s, ArH), 5.97 (1H, t, $J = 4.6$ Hz, CH), 5.64 (1H, s, CH), 5.14 (2H, s, CH_2), 3.93 (3H, s, OCH_3), 3.89 (6H, s, OCH_3), 3.85 (6H, s, OCH_3), 3.83 (3H, s, NCH_3), 2.97 (2H, t, $J = 7.8$ Hz, CH_2), 2.43 (3H, s, CH_3), 2.35 (2H, m, CH_2).

Synthesis of 2-Substituted Indolequinone Derivatives

Ethyl 5-methoxy-1-methylindole-2-carboxylate (22)

Ethyl 5-methoxyindole-2-carboxylate (1.00 g, 4.5 mmol) in DMF (9 mL) was added to a stirring suspension of NaH (0.33 g, 13.6 mmol) in DMF (30 mL) at 0 °C.

Iodomethane (1.93 g, 13.6 mmol) was added dropwise at 0 °C, and the mixture was allowed to warm to room temperature. The reaction was monitored by TLC and was completed within 2 h. Saturated ammonium chloride solution was added and the mixture extracted with EtOAc. The EtOAc layer was washed with water, dried (Na₂SO₄), and concentrated to yield the title compound as a tan solid (0.96 g, 4.1 mmol, 91%).

¹H NMR (300 MHz, CDCl₃) δ 7.66 (1H, d, *J* = 2.5 Hz, ArH), 7.17 (1H, d, *J* = 8.8 Hz, ArH), 6.87 (1H, dd, *J* = 8.8 Hz, 2.6 Hz, ArH), 4.39 (2H, q, *J* = 7.1 Hz, CO₂CH₂CH₃), 3.89 (3H, s, OCH₃), 3.67 (3H, s, NCH₃), 2.75 (3H, s, CH₃), 1.45 (3H, t, *J* = 7.1 Hz, CO₂CH₂CH₃).

Ethyl 5-methoxy-1-methyl-4-nitroindole-2-carboxylate (23)

To a crude suspension of ethyl 5-methoxy-1-methylindole-2-carboxylate (0.48 g, 2.1 mmol) in HOAc (9 mL) was added a solution of concentrated HNO₃ (1.1 mL) in HOAc (5 mL) at 0 °C. Following the addition, the reaction mixture was warmed to room temperature and stirred for 2 h. The reaction mixture was poured over ice and filtered, and the yellow precipitate was washed with water. The crude product was recrystallized (hexanes/EtOAc, 1:1) to yield the title product as a bright yellow solid (0.28 g, 1.0 mmol, 48%).

¹H NMR (300 MHz, CDCl₃) δ 7.58 (1H, d, *J* = 9.1 Hz, ArH), 7.54 (1H, s, ArH), 7.18 (1H, d, *J* = 9.2 Hz, ArH), 4.40 (2H, q, *J* = 7.1 Hz, CO₂CH₂CH₃), 4.11 (3H, s, OCH₃), 4.02 (3H, s, NCH₃), 1.42 (3H, t, *J* = 7.14 Hz, CO₂CH₂CH₃).

Ethyl 4-amino-5-methoxy-1-methylindole-2-carboxylate (24)

To a suspension of ethyl 5-methoxy-1-methyl-4-nitroindole-2-carboxylate (0.28 g, 1.0 mmol) in EtOH (45 mL) was added tin powder (1.33 g, 11.2 mmol), followed by HCl (5 mL, 12 M). The reaction was stirred at room temperature for 2 h, and neutralized with saturated NaHCO₃. The suspension obtained was added to an equal volume of water. The precipitate and aqueous layer were stirred with CH₂Cl₂ for 3 h and filtered through Celite to separate the layers. The organic layer was extracted with CH₂Cl₂, dried (Na₂SO₄) and concentrated to yield the title product (0.19 g, 0.8 mmol, 77%).

¹H NMR (300 MHz, CDCl₃) δ 7.64 (1H, d, *J* = 9.2 Hz, ArH), 7.37 (1H, d, *J* = 9.2 Hz, ArH), 7.36 (1H, s, ArH), 4.88 (2H, s, NH₂), 4.40 (2H, q, *J* = 7.1 Hz, CO₂CH₂CH₃), 4.10 (3H, s, OCH₃), 4.02 (3H, s, NCH₃), 1.47 (3H, t, *J* = 7.1 Hz, CO₂CH₂CH₃).

2-Hydroxymethyl-5-methoxy-1-methylindole-4,7-dione (25)

To a suspension of ethyl 4-amino-5-methoxy-1-methylindole-2-carboxylate (0.19 g, 0.8 mmol) in THF (5 mL) was added LiAlH₄ in THF (2.0 M, 0.98 mL, 1.95 mmol). The reaction was then heated at reflux for 15 min, quenched by the addition of water (0.5 mL), 1 M NaOH (0.5 mL) and silica gel (5 g). The granular precipitate was filtered off through a pad of Celite. The filtrate was dried (Na₂SO₄) and concentrated *in vacuo* to yield 2-hydroxymethyl-5-methoxy-1-methylindole, as a dark brown solid, which was used directly in the next step without further purification.

To a solution of the intermediate (0.30 g, 1.4 mmol) in acetone (18 mL) was added a solution of potassium nitrosodisulfonate (1.36 g, 5.1 mmol) in sodium dihydrogen phosphate buffer (0.4 M, pH 6, 30 mL). The reaction mixture was stirred for 1 h at room temperature. The excess acetone was removed *in vacuo*, and water and

CH₂Cl₂ were added. The organic layer was extracted, dried (Na₂SO₄) and concentrated. The crude product was purified by column chromatography (hexanes/EtOAc, 1:1) to yield the title product as a pale orange solid (0.15 g, 0.7 mmol, 88%).

¹H NMR (300 MHz, CDCl₃) δ 6.55 (1H, s, CH), 5.65 (1H, s, CH), 4.67 (2H, d, *J* = 4.6 Hz, CH₂OH), 4.02 (3H, s, OCH₃), 3.82 (3H, s, NCH₃), 1.89 (1H, s, OH).

5-Methoxy-2-{2-methoxy-5-[2-(3,4,5-trimethoxy-phenyl)-vinyl]-phenoxy-methyl}-1-methyl-1H-indole-4,7-dione (26)

To a mixture of 2-hydroxymethyl-5-methoxy-1-methylindole-4,7-dione (0.16 g, 0.7 mmol), CA4 (0.05 g, 0.2 mmol), and ADDP (0.06 g, 0.2 mmol) dissolved in dry benzene (10 mL), was added tributyl phosphine (0.5 mL, 0.2 mmol) dropwise and stirred for 48 h at room temperature. The excess benzene was removed *in vacuo*. The resulting residue was extracted with CH₂Cl₂ and washed with water. The organic layer was dried (Na₂SO₄) and concentrated. The crude product was purified by column chromatography (hexanes/EtOAc, 3:2) to yield the title product as an orange solid (0.02 g, 0.05 mmol, 21%).

¹H NMR (300 MHz, CDCl₃) δ 6.55 (3H, m, ArH), 6.53 (1H, s, ArH), 6.52 (2H, s, ArH), 6.47 (2H, s, CH), 5.68 (1H, s, CH), 4.85 (2H, s, CH₂), 4.00 (3H, s, OCH₃), 3.82 (9H, s, OCH₃), 3.73 (3H, s, NCH₃).

Synthesis of Tirapazamine Derivative

Methyl 4-amino-3-nitrobenzoate (27)

To 4-amino-3-nitrobenzoic acid (0.93 g, 5.1 mmol) was added MeOH (13 mL) and H₂SO₄ (0.5 mL), and the mixture was refluxed for 2 h. The mixture was extracted with

CH₂Cl₂, washed with water, dried (Na₂SO₄), and concentrated to yield the title product (1.00 g, 5.1 mmol, quant.) without further purification.

¹H NMR (300 MHz, CDCl₃) δ 8.85 (1H, d, *J* = 1.9 Hz, ArH), (1H, dd, *J* = 8.7 Hz, *J* = 1.9 Hz, ArH), 6.83 (1H, d, *J* = 8.7 Hz, ArH), 6.40 (2H, br s, NH₂).

7-Methyl-benzo-1,2,4-triazin-3-amine 1-Oxide (28)

4-Methyl-2-nitroaniline (0.51 g, 3.4 mmol) and cyanamide (0.71 g, 16.8 mmol) were heated melted together at 120 °C, cooled to ca. 50 °C, and conc. HCl (12 N, 4 mL) was added carefully. The mixture was stirred until the heat subsided then stirred at 120 °C for 2 h. The reaction mixture was cooled to 20 °C and made strongly basic with 7.5 M NaOH solution (40 mL), prior to further heating at 120 °C for 1 h and then cooling to 20 °C and diluting with water (100 mL). The precipitate was filtered, washed with water and ethanol and dried. The crude mixture was recrystallized in ethanol to yield the title product (0.32g, 1.8 mmol, 54 %).

¹H NMR (300 MHz, (CD₃)₂SO) δ 7.94 (1H, s, ArH), 7.64 (1H, d, *J* = 8.7 Hz, ArH), 7.46 (1H, d, *J* = 8.6 Hz, ArH), 7.14 (2H, s, NH₂), 3.34 (3H, s, CH₃).

CHAPTER THREE

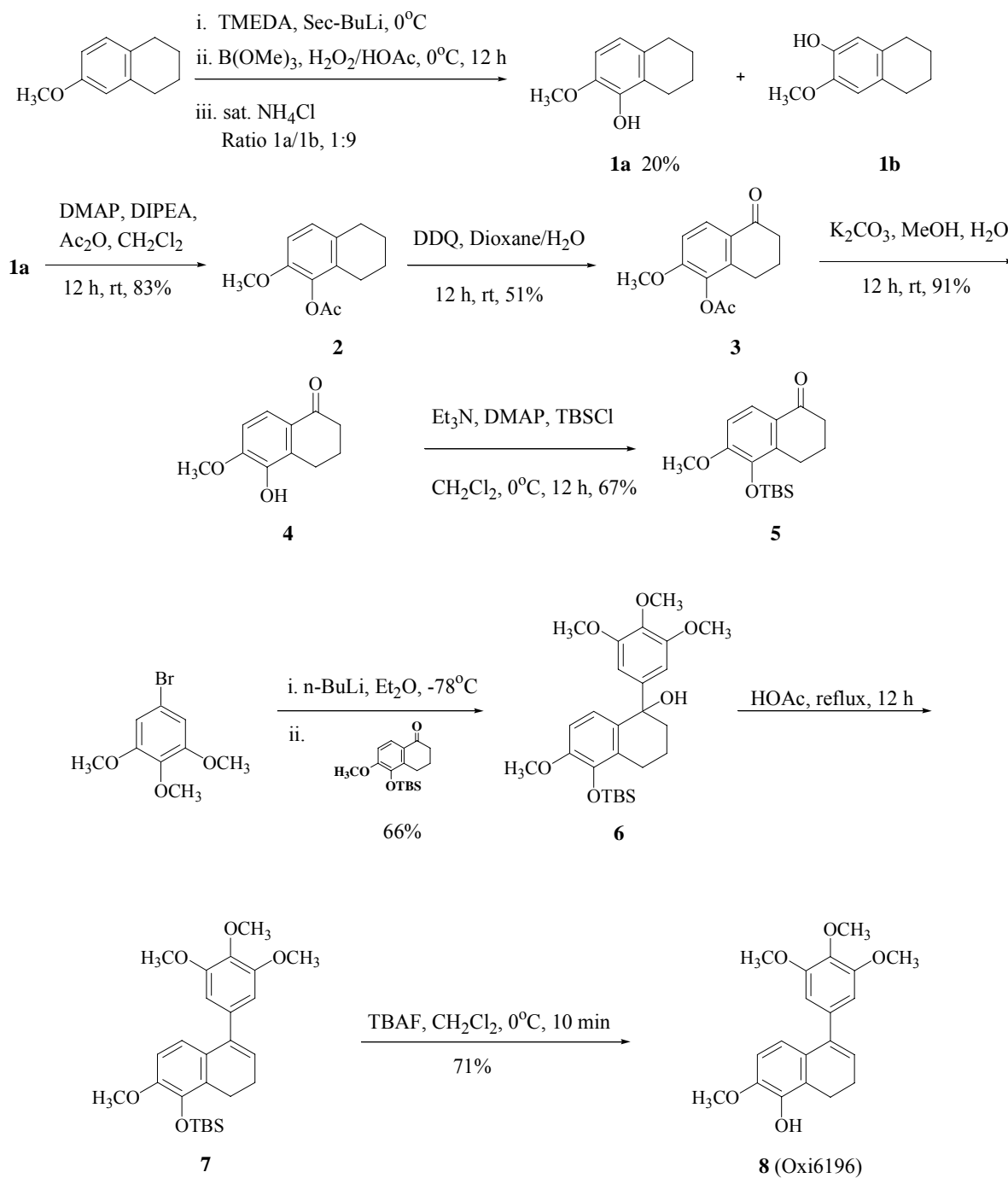
Results and Discussion

Synthesis of Oxi6196

This project, detailed below in Scheme 1, involved the re-synthesis of the dihydronaphthalene drug, Oxi6196 **8**, according to the procedures previously reported by Pinney and co-workers.^{78, 79} Initial hydroxylation at the 5-position of 6-methoxy-1,2,3,4-tetrahydronaphthalene was carried out by using a slightly modified procedure by Beak and co-workers,⁸⁰ which was first tried by a post-doctoral fellow, Dr. Anjan Ghatak, in the Pinney group at Baylor University.

This reaction utilized trimethyl borate to selectively introduce a hydroxyl group at a position *ortho* to the methoxy group. The major product for the reaction was found to be the 7-hydroxy isomer **1b**, and the 5-hydroxy isomer **1a** was found to be the minor product possibly due to steric hindrance. The ratio of the 7- and 5-hydroxy products was observed to be approximately 9:1, which differs from the 2:1 ratio specified by Dr. Ghatak.⁷⁸ The 5-hydroxy product could only be separated from the crude mix after two columns and a recrystallization. Early attempts of this reaction resulted in low yields of under 10% for the 5-hydroxy product, however, fresh distillation of TMEDA, titration of *sec*-BuLi with *N*-benzyl benzamide, and the usage of brand new trimethyl borate resulted in increased yields of 20%.

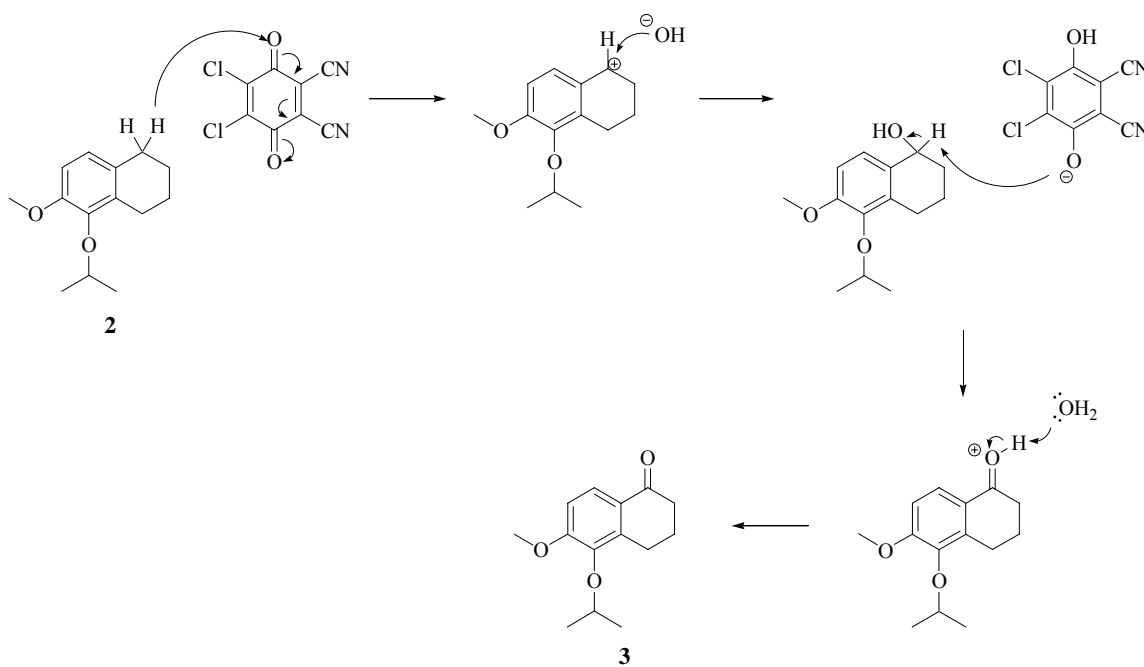
By reaction with acetic anhydride, the 5-hydroxy isomer was protected with the acetoxy group in high yield. In the following step, the reaction of the acetoxytetrahydronaphthalene **2** with DDQ in dioxane-water led to the introduction of the



Scheme 1. Synthesis of Oxi6196

keto group at the benzylic position, which was the desired 1-tetralone **3**. The formation of the ketone at the benzylic position was due to the *para*-directing effect of the methoxy

group.⁸¹ A suggested mechanism for the formation of this intermediate is give in Scheme 2. Initially, the mechanism involves a hydride transfer to quinone oxygen followed by the attack of a hydroxide ion. Deprotonation by the DDQ phenolate at the 1-position and the ensuing deprotonation of the oxygen affords the tetralone intermediate. This intermediate was deprotected and then re-protected with the TBS group to afford the tert-butylsilyl protected tetralone **5**. The TBS protection was done so that the acetoxy group would not later hinder the addition of the trimethoxyphenyl unit.



Scheme 2. Suggested mechanism for DDQ oxidation

The coupling of the phenyl ring to the TBS-protected tetralone was carried out through a halogen-metal exchange between 3,4,5-trimethoxyphenyl bromide and *n*-BuLi, followed by addition of the tetralone **5**. Refluxing with acetic acid caused the elimination of the hydroxyl group and without further purification, the crude product was reacted

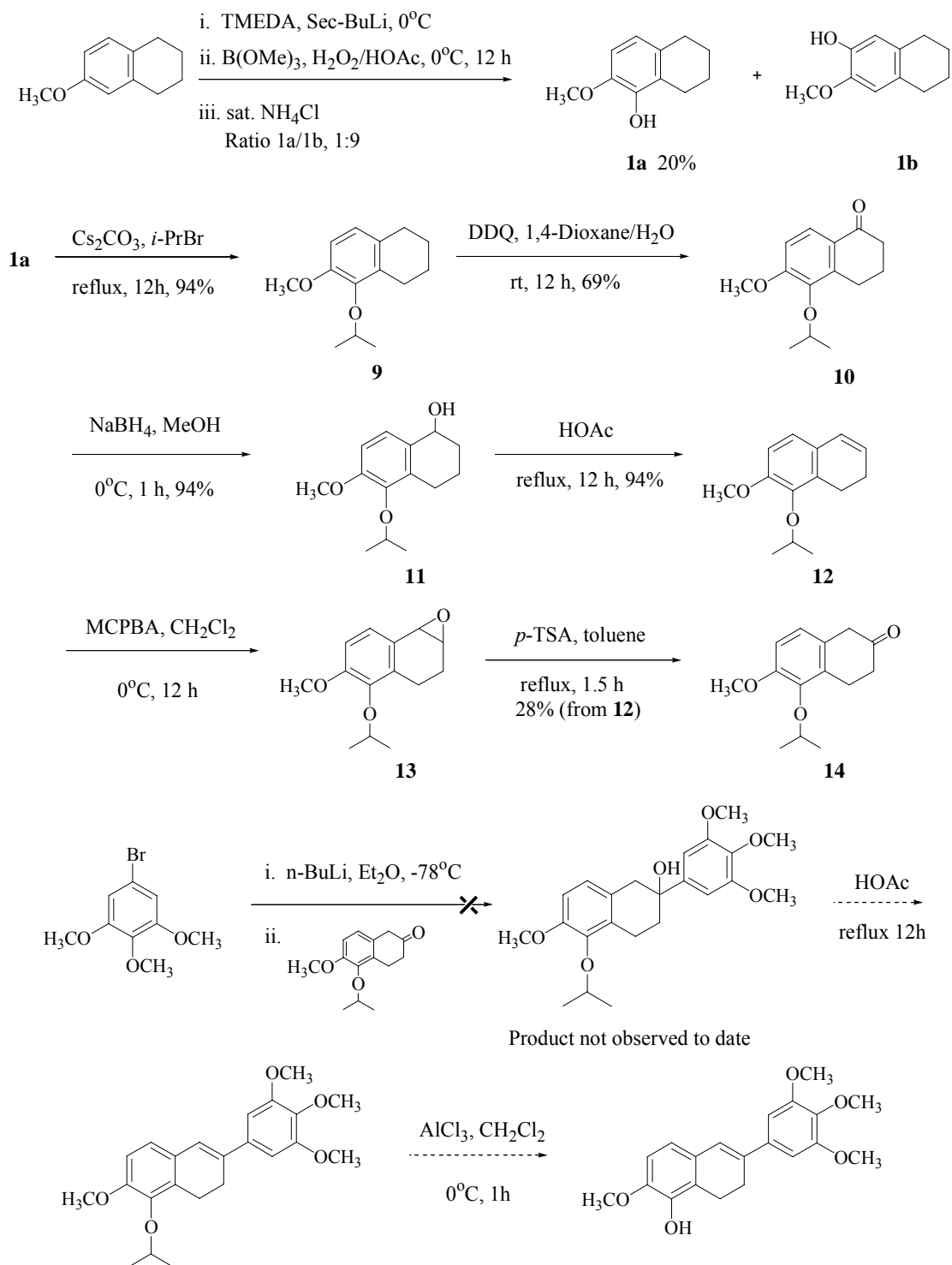
with TBAF in order to deprotect the TBS-protected intermediate **7** and yield Oxi6196. The overall yield for this scheme was determined to be a little over 2%.

Synthesis of β -Substituted Dihydronaphthalene Analog

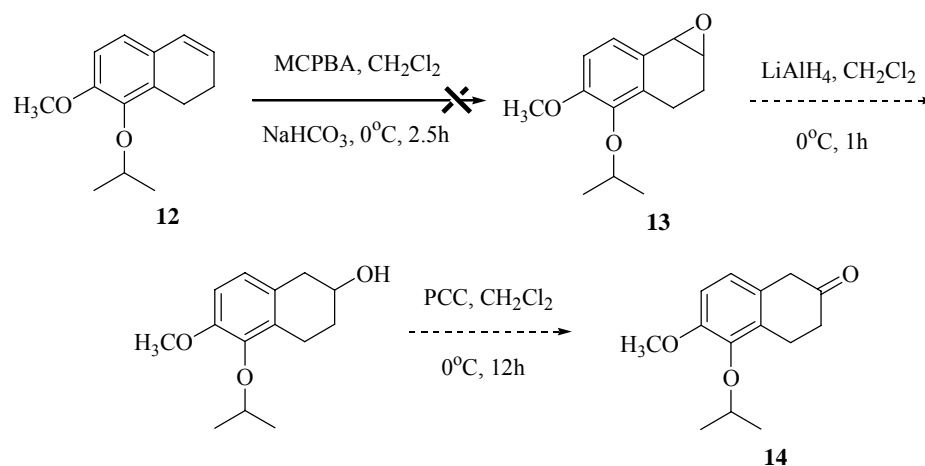
The synthesis of the novel analog of Oxi6196, depicted in Scheme 2, involved the trimethoxyphenyl unit substituted at the β -position of the dihydronaphthalene. In addition to any activity against tubulin binding that may be observed, this compound was designed and synthesized to elucidate further structure-activity relationship data with respect to molecular recognition of the colchicine binding site on β -tubulin.

The first step in this synthesis was analogous to that of Oxi6196, wherein the desired 5-hydroxy product **1a** was formed. The intermediate was then protected with the isopropyl group using cesium carbonate to yield the isopropyl protected tetrahydronaphthalene **9**. The isopropyl group was selected as the protecting group for two reasons. First, in lieu of the acetyl group, the isopropyl group could also exert a directing effect in order to yield the 1-tetralone intermediate. Secondly, isopropyl protection would avoid the extra steps deprotection of the acetyl group and reprotection with the TBS group.

Oxidation of the isopropyl-protected intermediate **9** with DDQ in dioxane-water afforded the 1-tetralone **10**, which was then reduced by NaBH₄ to yield the tetrahydronaphthalenol **11** with a hydroxyl group at the 1-position. Elimination of the hydroxyl group by reaction with acetic acid yielded the isopropyl-protected dihydronaphthalene **12**.

Scheme 3. Progress towards synthesis of β -substituted Dihydronaphthalene Analog

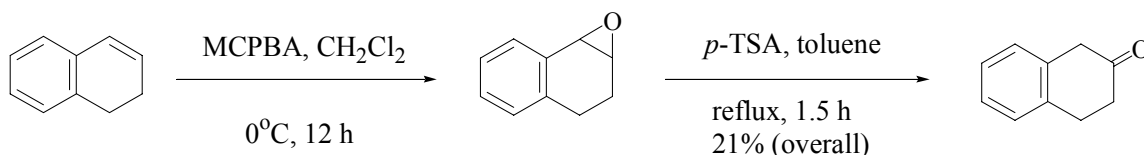
The 2-tetralone **14** was identified as a key intermediate in this synthetic scheme. To achieve this intermediate, epoxidation of the dihydronaphthalene and selective ring opening was determined to be a sound strategy. Initially, the epoxidation reaction was based on a paper by Hara, Sasada and co-workers⁸² that employed MCPBA as the epoxidizing agent, and the ring-opening to yield the 2-hydroxy group would be mediated by LiAlH_4 , which was based on a paper by Rao and co-workers.⁸³ Subsequent oxidation by PCC would be expected to afford the 2-tetralone, as seen in Scheme 3. However, epoxidation with MCPBA did not succeed using either CH_2Cl_2 or diethyl ether as a solvent. Purification of the crude mixture, on basic alumina or silica gel, did not yield the desired epoxide, possibly due to degradation on the column. No product was recovered after purification on alumina gel; and purification on silica gel yielded three compounds, which were neither the starting material **12** nor the desired product **13**. At that point, no other epoxidizing agents were tried.



Scheme 4. Alternative strategy for the synthesis of the 2-tetralone

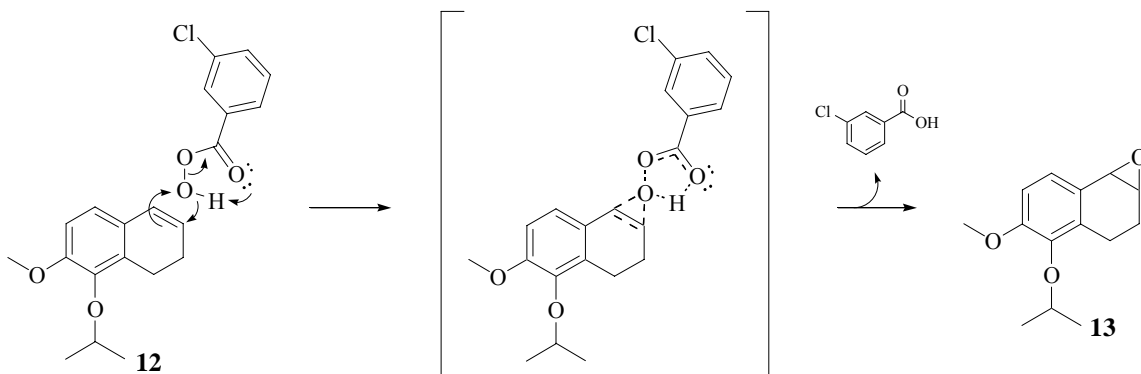
Fortunately, a German procedure, by Braun and co-workers,⁸⁴ was found detailing the formation of the 2-tetralone via an epoxide intermediate. The procedure was first

tested by this researcher on a model system, namely 1,2-dihydronaphthalene, by reacting the starting material with MCPBA in CH_2Cl_2 , and the crude product was then refluxed with a catalytic amount of *p*-TSA to afford the 2-tetralone in 21% yield. The reaction on the model system is shown in Scheme 5.

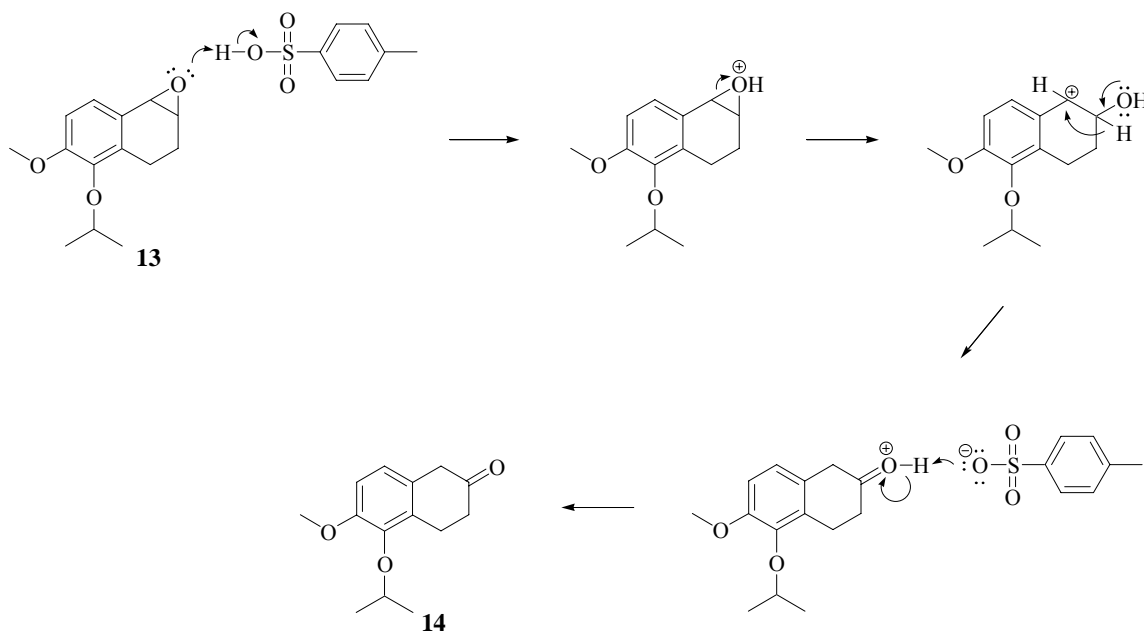


Scheme 5. Model reaction for the synthesis of 2-tetralone with 1,2-dihydronaphthalene as starting material

The same reaction was then attempted with the isopropyl-protected dihydronaphthalene **12**, which resulted in the formation of the desired 2-tetralone **14**. As opposed to the epoxidation attempted with MCPBA earlier, shown in Scheme 4, it is believed that epoxidation with the same reagent succeeded in the new procedure due to the extended length of the reaction. A suggested mechanism by which the dihydronaphthalene is converted into the 2-tetralone is detailed in Scheme 6. The first part of the mechanism shows the epoxidation by MCPBA via a “Butterfly Mechanism.”⁸⁵ The reaction proceeds through a transition state involving the simultaneous addition of the oxygen and shift of the hydrogen. After the first stage, the epoxide oxygen is protonated by *p*-TSA. Ring opening yields a hydroxyl group at the 2-position and a positive charge at the benzylic carbon. Following a hydride shift, the *p*-TSA fulfils a catalytic role when its conjugate base abstracts a proton, subsequently yielding a keto group affording the 2-tetralone **14**.



Stage I: Epoxidation



Stage II: Formation of 2-Tetralone

Scheme 6. Suggested mechanism for the formation of the 2-tetralone from the dihydronaphthalene

The following step, the addition of the trimethoxyphenyl ring, presented a problem due to the nature of the 2-tetralone. The compound, at room temperature, exists as a suspension of white solid in yellow oil, and it did not completely dissolve in either diethyl ether or THF, which are the preferred solvents for the halogen-metal exchange. The compound was soluble in CDCl_3 , and subsequent analysis by NMR showed that the

compound was pure. TLC analysis also ensured that no impurities were present in the compound.

The trimethoxyphenyl addition was first attempted by adding a suspension of the 2-tetralone in ether to the lithiated benzene moiety, but the reaction did not yield the desired product. The reagent, *n*-BuLi, and solvent, ether, may not have been moisture-free and may have compromised the reaction. Also, the insolubility of the starting material in ether may have contributed to the failure of the reaction. Therefore, three approaches were devised in order to continue the scheme:

1. The reaction would be repeated with new and dry ether and *n*-BuLi;
2. The lithiated intermediate would be added dropwise to the starting material, in ether, via canula;
3. The reaction would be repeated using the starting material dissolved in chloroform.

The reaction still did not succeed after using the first two methods, however, one cause of the reaction failure was determined to be the incomplete formation of the phenyllithium intermediate. A third and final reaction with the last of the starting material was set up, and the almost complete formation of the phenyllithium intermediate was monitored by NMR, which is seen below in Figure 24. The NMR sample was prepared by extracting a small aliquot of the reaction mixture, washing with water, and extracting the organic phase with ether. The organic phase was concentrated and then dissolved in CDCl₃. The water workup would have displaced the lithium from the phenyllithium intermediate forming trimethoxybenzene, which was then observed by NMR.

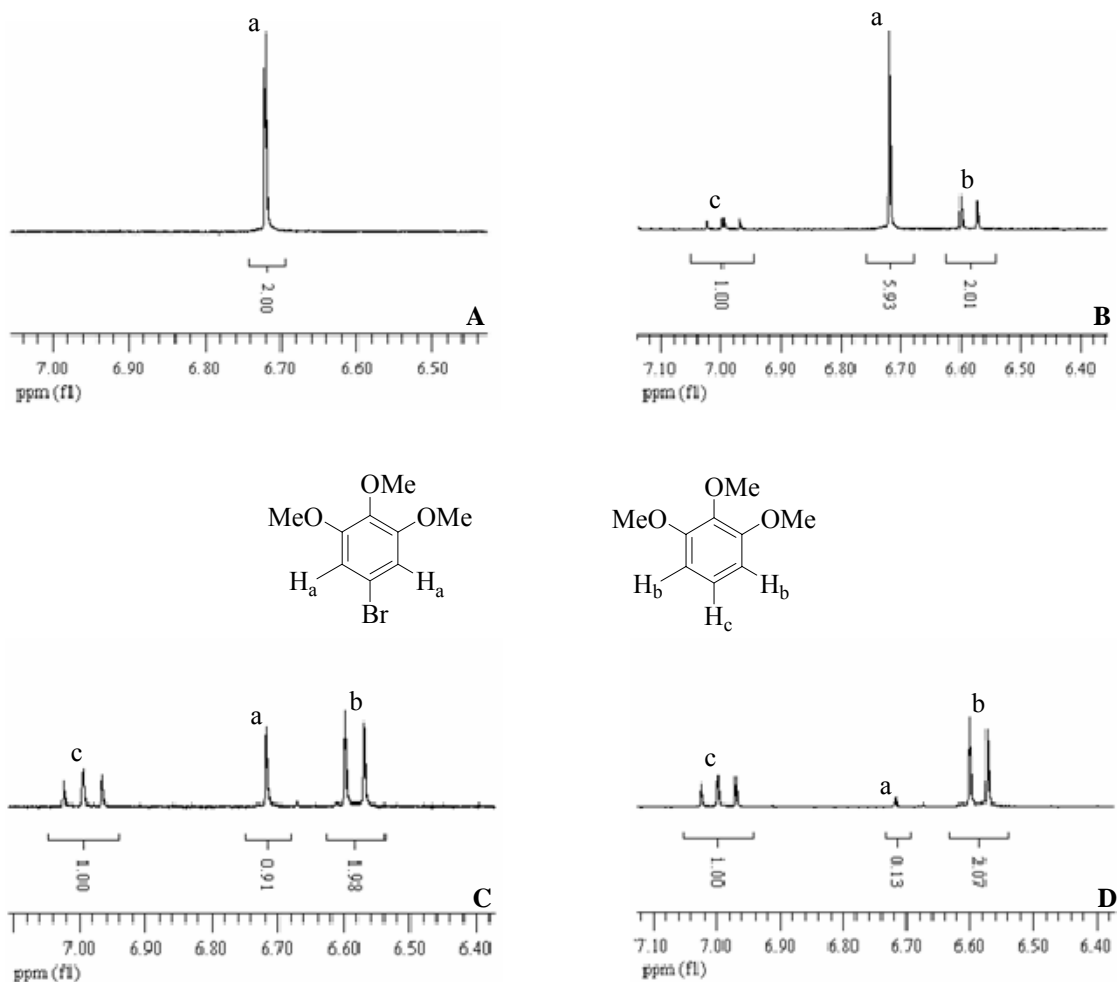


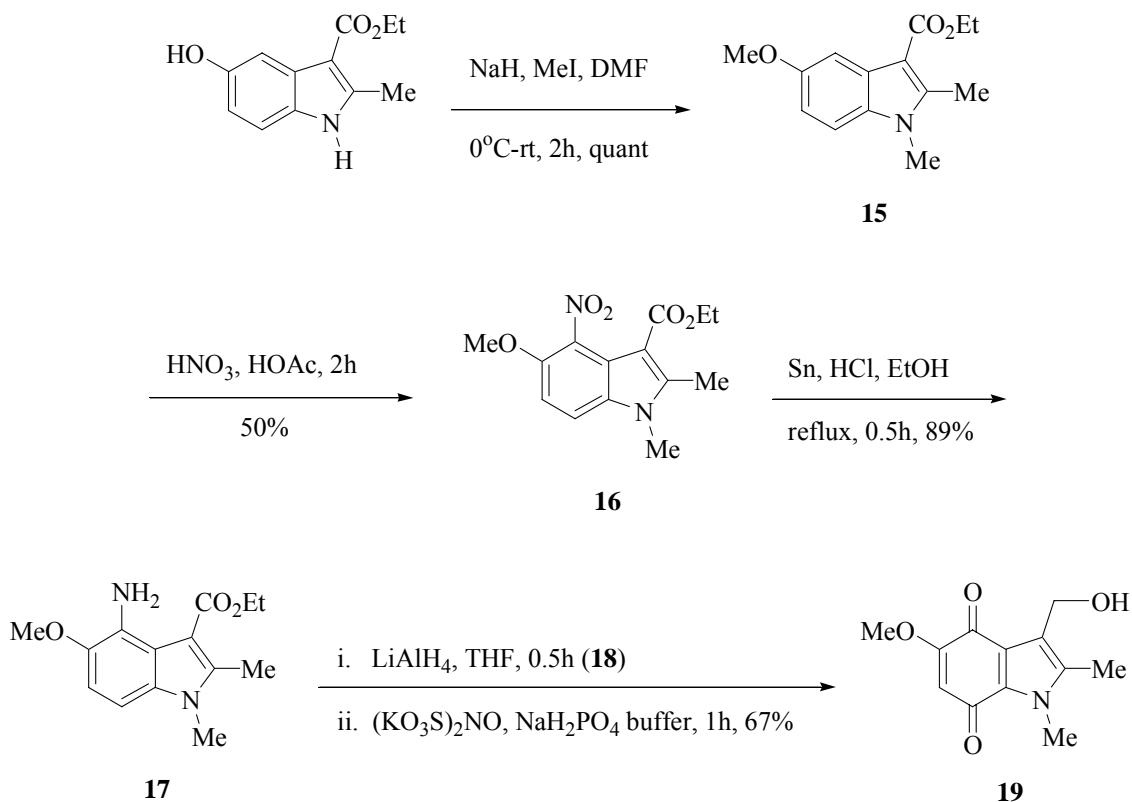
Figure 24. Monitoring the formation of the phenyllithium intermediate, characterized by the observation of trimethoxybenzene, at 1 h (A), 3 h (B), 5 h (C) and 7 h (D)

The determination of the presence of the phenyllithium prompted the addition of the 2-tetralone, which was dissolved in THF. Frustratingly, the reaction did not succeed; therefore, further attempts at synthesizing the target are necessary.

Synthesis of 3-Substituted Indolequinone Derivatives

The synthetic route towards 3-(hydroxymethyl)indolequinone **19**, shown in Scheme 7, details the formation of a key intermediate in this process that was coupled to VDAs in order to create multi-functional drugs that contain a bioreductive prodrug and

the capability for vascular disruption. This procedure is based on work that was originally published by Naylor and co-workers,⁸⁶ and all the intermediates until the indolequinone **19** are known in the literature.



Scheme 7. Synthesis of 3-(hydroxymethyl)indolequinone

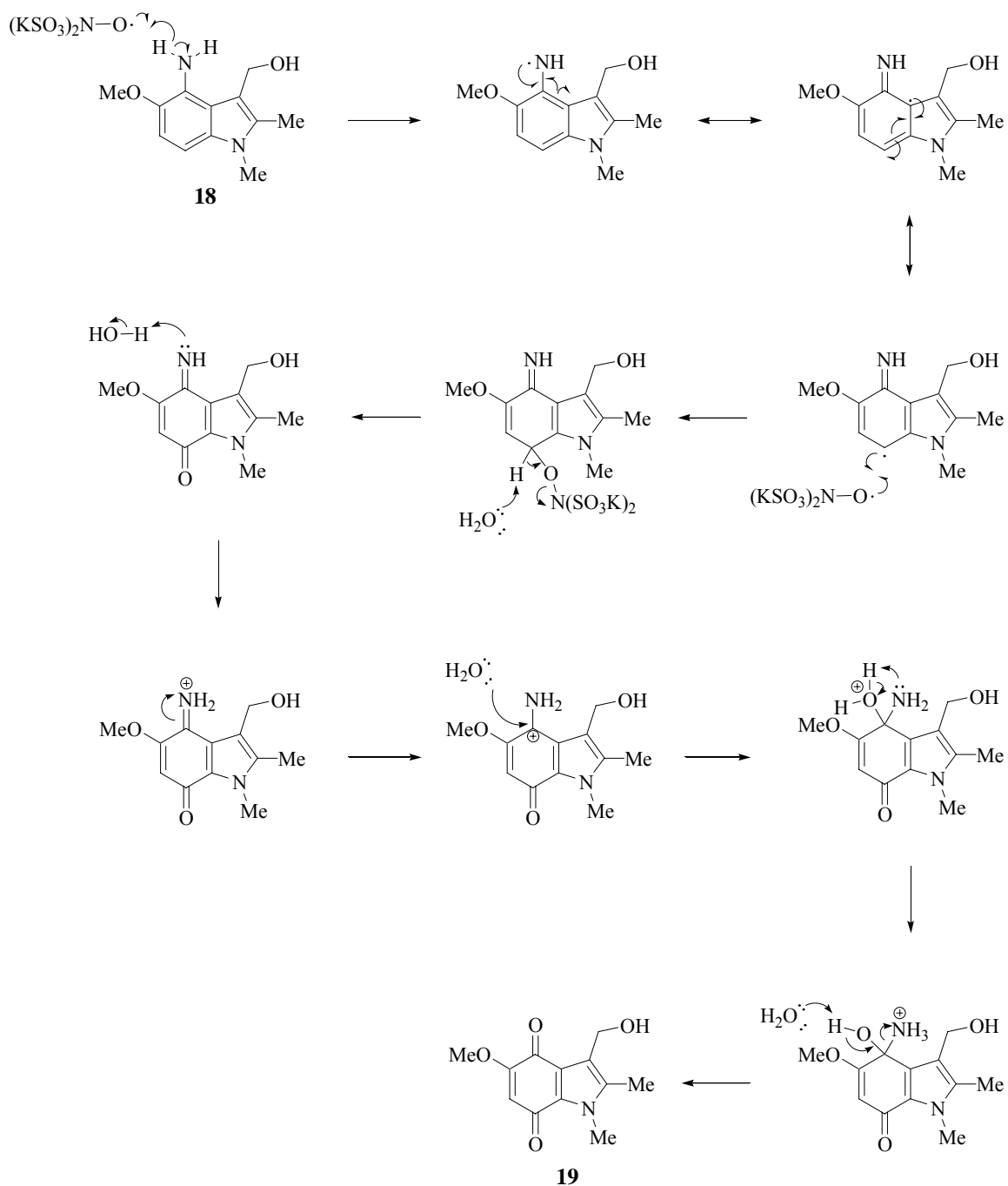
Firstly, the commercially available ethyl 5-hydroxy-2-methylindole-3-carboxylate underwent a dimethylation at both the 1- and 5-position to afford the methylated intermediate **15**. To deprotonate the *N*-hydrogen, NaH was employed as a strong base. Subsequent nitration at the 4-position was effected by mixture of nitric and acetic acid.

Due to the concerns of this researcher regarding a possible nitration at the 6-position, this reaction was monitored by TLC to ensure that the starting material was undergoing only a mono-nitration and to investigate whether nitration was occurring at

the 4- or the 6-position. After 2 hours of reaction time, only one product spot was visible. However, after 4 hours, another spot of equal intensity had appeared on the TLC plate above the previous spot. By NMR spectroscopy, the first (lower) spot was identified as the desired 4-dinitro product **16**, and the second (upper) spot was identified as the 4,6-dinitro product. After 4 hours, the mono- and dinitro products were formed in a 1:1 yield. No evidence was seen of a 6-nitro compound, so the reaction time was maintained at 2 hours.

Subsequent reduction afforded the 4-amino intermediate **17**, which underwent a LiAlH₄-catalyzed ester hydrolysis to yield the hydroxymethylindole **18**. Without further purification, the crude product was oxidized by Fremy's salt to yield the indolequinone **19**. Fremy's salt (potassium nitrosodisulfonate) is a radical oxidizing agent that is commonly used to oxidize phenols to their corresponding benzoquinones.⁸⁷ The suggested mechanism by which the oxidation of amine proceeds towards the indolequinone is shown in Scheme 8. The initial step is the abstraction of the *N*-1 hydrogen by Fremy's salt to form the nitrogen radical, which is trapped at C-7, after resonance, by another molecule of Fremy's salt. Then, the N-O bond is cleaved leading to the formation of the iminoquinone. Hydrolysis of the imine then results in the formation of the dione **19**.

In order to take advantage of the trigger capability of the indolequinone upon bioreductive activation, to release effector VDAs, the Mitsunobu reaction was employed as a method of coupling the 3-hydroxymethyl group to the free phenol of either CA4 or Oxi6196, as seen in Scheme 9. The Mitsunobu reaction utilizes Ph₃P and an azodicarboxylic derivative (DEAD or DIAD) to activate the alcohol substituent on the

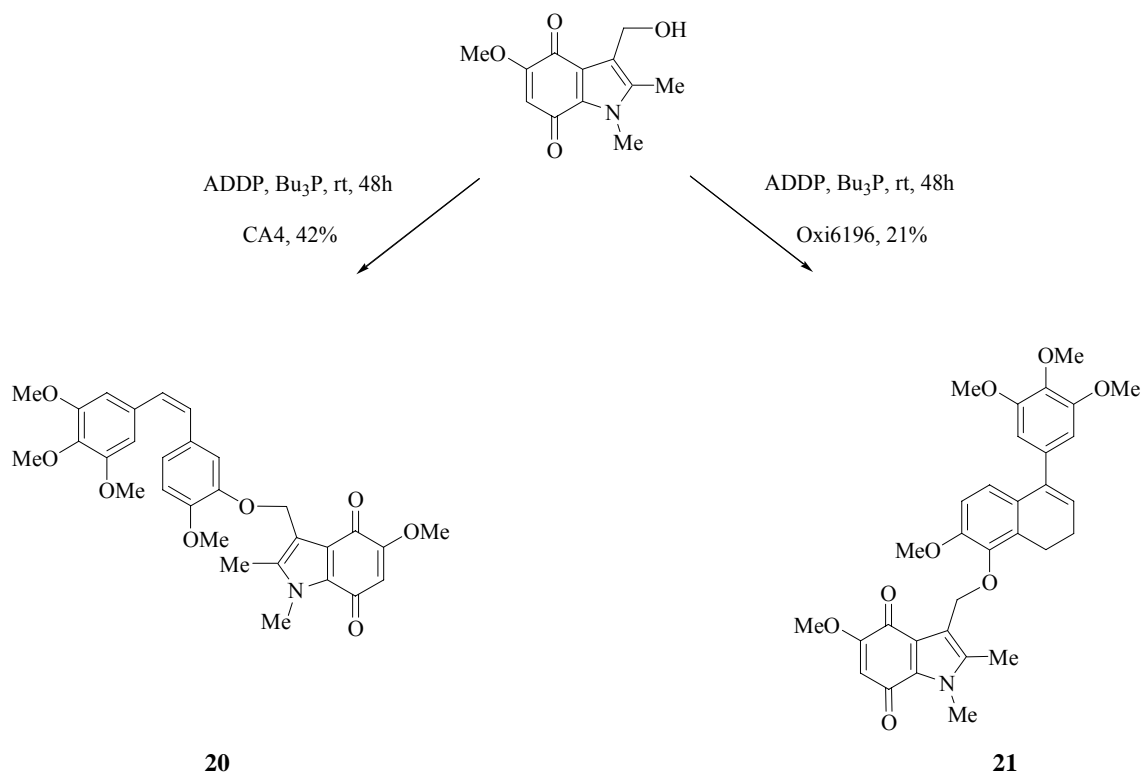


Scheme 8. Suggested mechanism for oxidation by Fremy's salt

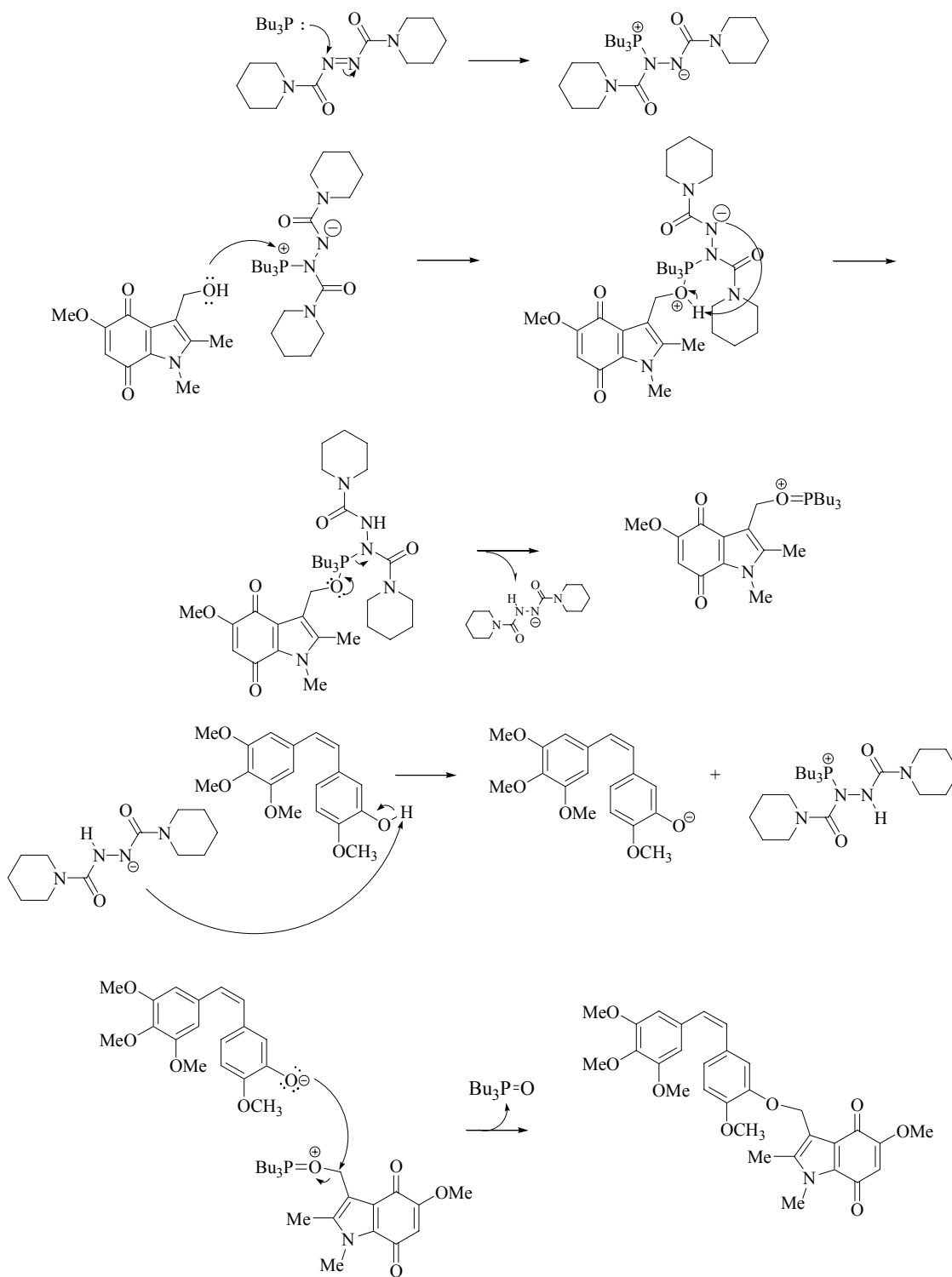
substrate and make it susceptible to nucleophilic attack. A different set of reagents, 1,1'-(azodicarbonyl)-dipiperidide (ADDP) and Bu_3P ,⁸⁸ were used for the coupling of the indolequinones and VDAs, however, the mild conditions of the reaction were maintained.

These reagents were used after higher yields, compared to the more conventional DEAD and Ph_3P , were reported by Graciela Miranda in the Pinney group.⁸⁹ A mechanism for this coupling is suggested in Scheme 10. The DEAD and Bu_3P combine to activate CA4 as a nucleophile by deprotonating its phenol. The alkoxyphosphonium intermediate generated binds to the hydroxyl group of the indolequinone and activates it as a leaving group. The CA4 phenoxide ion then attacks the indolequinone in an $\text{S}_{\text{N}}2$ fashion forming the arylalkylether, the CA4-indolequinone coupled product **20**, and giving tributylphosphine oxide as a side product.

The coupling of the indolequinone and CA4 afforded the bioconjugate trigger **20** in 42% yield. However, the coupling of the indolequinone and Oxi6196 resulted in the desired product **21** in a lower yield of 21%, although the reaction was performed at a smaller scale.



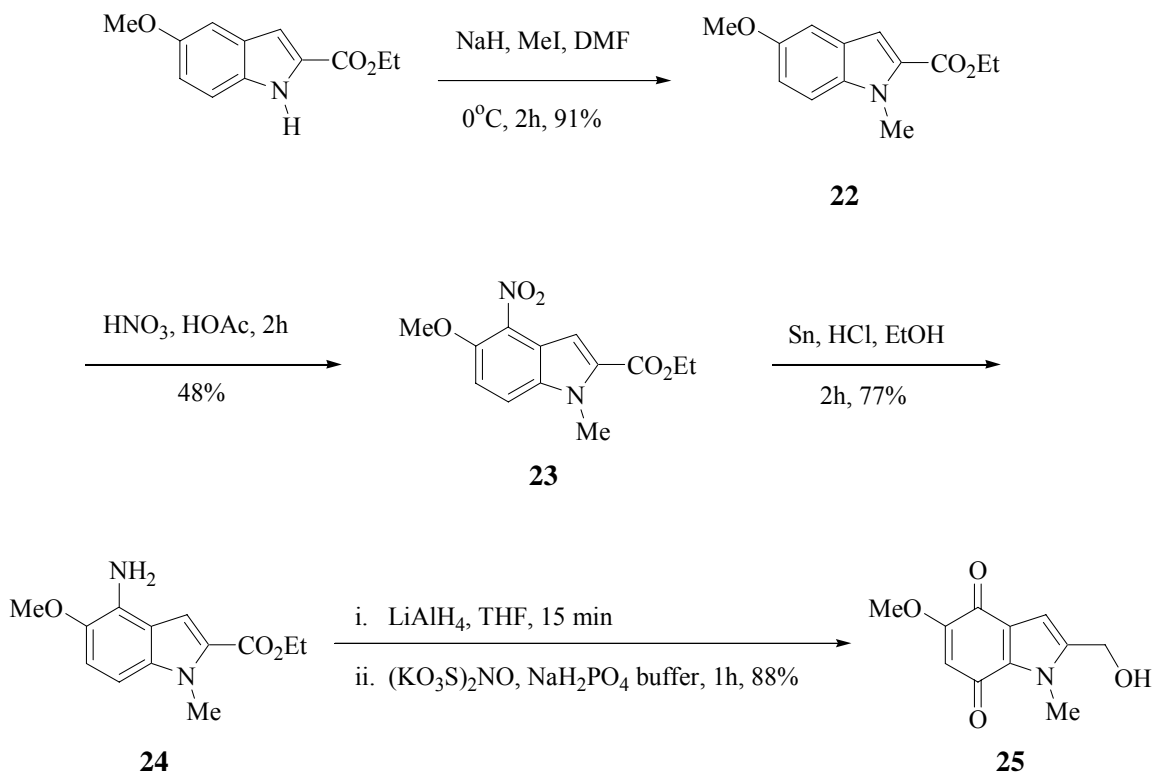
Scheme 9. Synthesis of 3-VDA-indolequinone bioconjugative agents



Scheme 10. Suggested mechanism for the Mitsunobu reaction

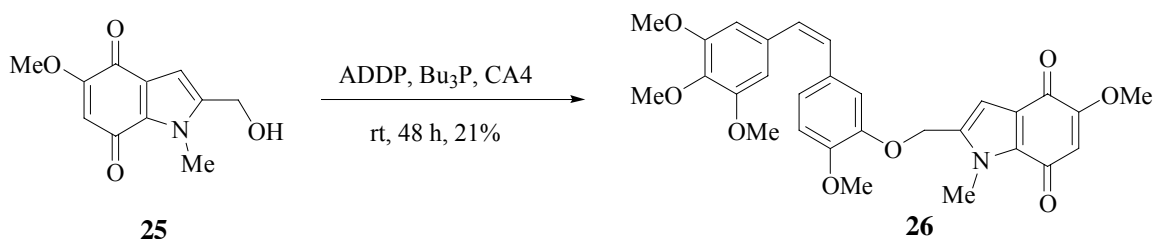
Synthesis of 2-Substituted Indolequinone Derivatives

The 2-indolequinone was synthesized, based on a procedure by Borch and co-workers,⁹⁰ in an analogous fashion to the 3-indolequinone. The procedure for the formation of 2-(hydroxymethyl)indolequinone **25** is shown in Scheme 11. First, ethyl 5-methoxyindole-2-carboxylate was methylated by treatment with NaH, followed by iodomethane to yield the methylated indole **22**. Nitration of the ethyl ester **22**, to form the nitrated intermediate **23**, was followed by the reduction of the nitro substituent using Sn/HCl yielded the corresponding amine intermediate **24**. The ester moiety of this intermediate was reduced using LiAlH₄. The indolequinone **25** was then obtained by oxidation of the crude mix using Fremy's salt.



Scheme 11. Synthesis of 2-(hydroxymethyl)indolequinone

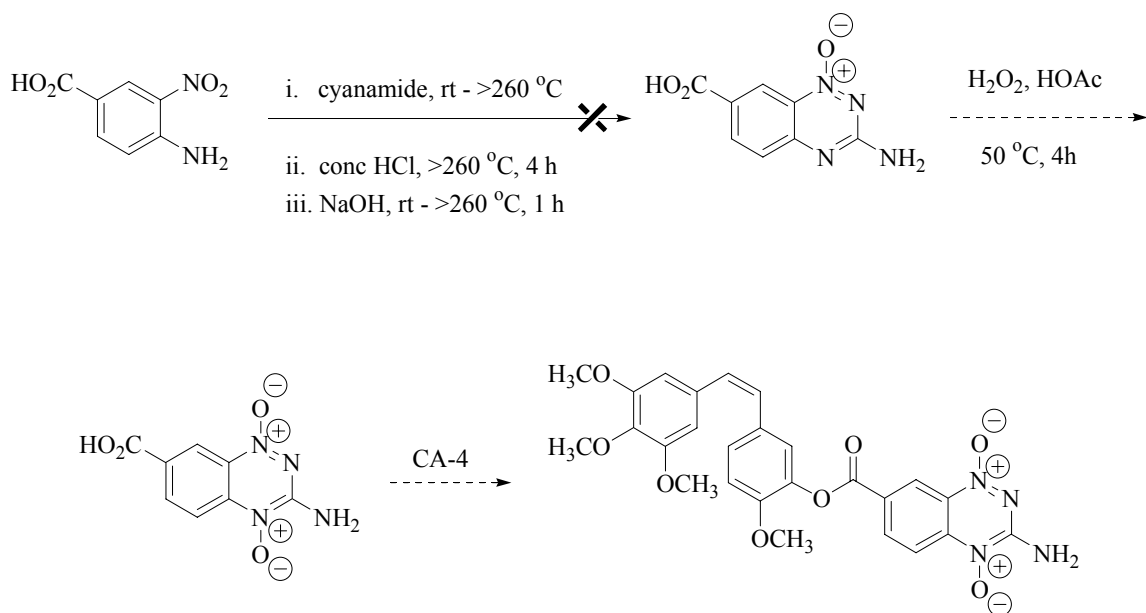
Coupling the 2-(hydroxymethyl)indolequinone **25** to CA4, depicted in Scheme 12, was also attempted using the new set of reagents, Bu₃P and ADDP, in the Mitsunobu reaction. Flash column chromatography yielded a compound that was identified by NMR spectroscopy as the desired product in an impure form **26**. Even recrystallization, attempted twice, and purification by preparative TLC did not afford the product in pure form. The impurities in the compound are, as yet, unknown, and further studies need to be performed to determine the nature of the impurities and the most effective method of their removal.



Scheme 12. Synthesis of 2-VDA-indolequinone bioconjugate

Synthesis of Tirapazamine Derivative

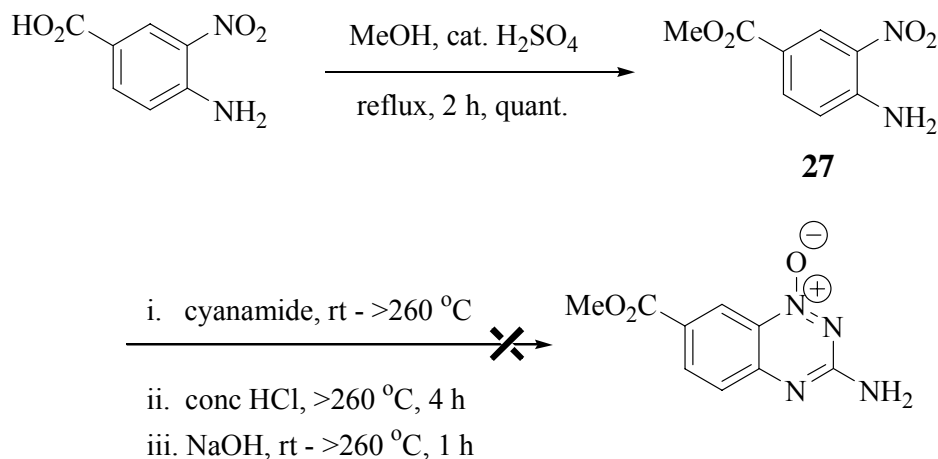
This purpose of this project was to synthesize a bioconjugate drug combining the bioconjugate drug tirapazamine and CA4 through an ester linkage that would be hydrolyzed, enzymatically or otherwise, to release both drugs. Initially, as depicted in Scheme 13, 4-amino-3-nitrobenzoic acid would be cyclized with cyanamide to form the carboxyl mono-*N*-oxide, based on a procedure by Hay and co-workers,⁹¹ but the reaction was not successful, possibly because of the formation of the sodium salt after the addition of NaOH during the reaction. Although the mixture was then acidified to regain the carboxylic acid, the desired product was not found.



Scheme 13. Initial synthesis of CA4-TPZ bioconjugate

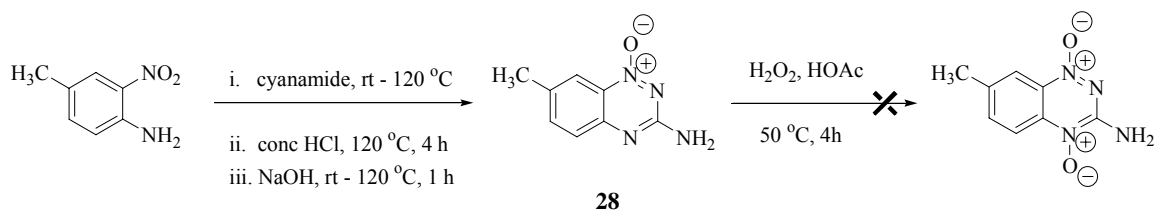
To avoid the possible salt formation, the starting material, 4-amino-3-nitrobenzoic acid, was reacted with methanol and a catalytic amount of H₂SO₄, to yield the methyl ester **26**, which is seen in Scheme 12. The methyl dioxide ester would have been reacted with CA4 in a transesterification to yield the target bioconjugate drug. Cyclization with cyanamide to form the mono-*N*-oxide, though, remained unsuccessful. This may have been because of the high temperature at which the reaction took place, due to the high melting point of the starting material (m.p. = 284 °C).

Another strategy employed towards achieving the coupled target, seen in Scheme 15, was to begin with 4-methyl-2-nitroaniline as the starting material, with a melting point of 114 °C, which would allow the reaction to occur at a much lower temperature.



Scheme 14. Synthesis of methyl ester TPZ

The cyclization was successful, affording the mono-*N*-oxide **28** in a yield of 54%. Therefore, the product was subjected to further oxidation by H₂O₂ in the hope that not only the dioxide would result but the methyl group would be oxidized to a carboxyl group, which could then be coupled with CA4. Unfortunately, the desired product was not formed. Greater efforts are necessary towards achieving this target.



Scheme 15. Alternative synthesis of methyl-TPZ dioxide

CHAPTER FOUR

Conclusions and Future Directions

Vascular disrupting agents, such as CA4P (the phosphate prodrug of CA4), show great promise in the field of anticancer research and can prove to be effective inhibitors of tubulin assembly. The dihydronaphthalene framework, as evidenced by Oxi6196, has proven to be an effective scaffold towards inhibiting tubulin assembly. The synthesis of two compounds based on the dihydronaphthalene framework was attempted: Oxi6196 and a β -dihydronaphthalene analog.

The project involving the re-synthesis of the previously designed Oxi6196, was successfully completed, though limited yields were encountered in the first step, which reduced the overall yield. Synthesis of the novel β -dihydronaphthalene analog was temporarily discontinued after the formation of the 2-tetralone, which was the key intermediate in the synthetic scheme. However, the procedure elicited some important chemistry, such as the finding and successful application of a relatively simple method of transposing the keto group from the 1- to the 2-position. The major benefit of this method, aside from a lesser number of steps, was the avoidance of purifying the epoxide, which had proven unsuccessful on alumina and silica until that point. Also, using the isopropyl group as a protecting group, in lieu of the TBS group, yielded the protected 1-tetralone in two fewer steps than in the Oxi6196 synthesis, which would shorten the procedure and raise the overall yield.

The continued synthesis of the β -dihydronaphthalene analog is recommended to investigate its role as a possible inhibitor of tubulin assembly, as well as to provide SAR data with respect to the molecular recognition of the colchicine binding site. Another molecule of interest for future consideration, seen below in Figure 25, is similar to the aryl chromene framework worked on by Physllis Arthasery (dissertation in the Pinney group, Baylor University), and it is the β -substituted analog of a dihydronaphthalene developed by Vani Mocharla⁷³ that showed significant inhibition of tubulin assembly ($IC_{50} \sim 1.5 \mu M$).

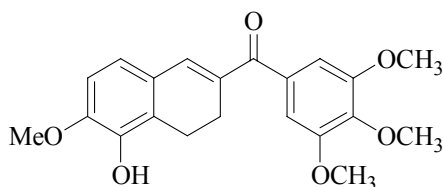


Figure 25. Future compound based on the dihydronaphthalene scaffold

Bioreductive compounds that are selectively activated at the site of the tumor offer a myriad of options as to their utilization as effective anticancer drugs. Their synthesis has become a focal point of research in the Pinney group. A wide variety of bioreductives, employing a number of mechanisms and playing different roles, have been researched and synthesized. Among them, the indolequinones remain an intriguing class of molecules because of their potential to trigger the release of an attached drug and their subsequent transformation into a DNA-alkylating agent. The idea to attach a VDA and design an indolequinone prodrug then occurred. Two analogs of indolequinones, with the ability to couple to drugs at the 3- or the 2- position, were synthesized.

The 3-indolequinone was synthesized and successfully coupled to CA4 and Oxi6196 via the Mitsunobu reaction. The 2-indolequinone was also synthesized efficiently and coupled to CA4. Although the product was purified by flash column chromatography and identified by NMR, impurities still remained, and the product resisted further attempts at purification. The Mitsunobu reaction was carried out with slightly more unconventional reagents, ADDP and Bu₃P,⁸⁹ and it seemed to provide better yields at a higher scale of reaction.

An extension of the research into indolequinones is encouraged and should include the coupling of other effective VDAs to the 3- and 2-indolequinones. In addition, the replacement of the 5-methoxy group on the indolequinone with an aziridinyl group, which can also become a DNA-alkylating agent upon nucleophilic ring opening, can afford the indolequinone prodrug a third functionality. Some molecules for further consideration are shown in Figure 26. In addition to biological evaluation of these indolequinone compounds, however, exposure of these compounds to chemically reductive conditions may also be important to confirm the elimination of the attached VDA upon reductive activation.

The design of a compound incorporating CA4 coupled to the bioreductive tirapazamine via an ester linkage was an initial attempt at creating a bifunctional drug with both VDA and bioreductive capabilities. The formation of the mono-*N*-oxide, albeit with a substituted methyl instead of a carboxyl, was finally a success after multiple attempts. The compound remains an interesting target because of the innate simplicity of its design.

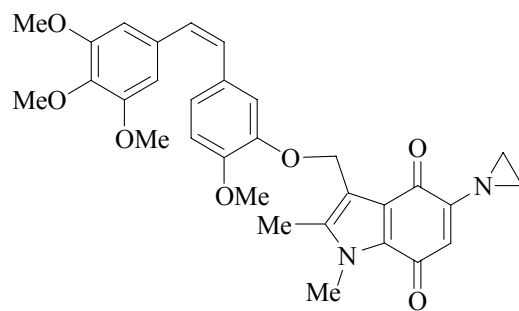
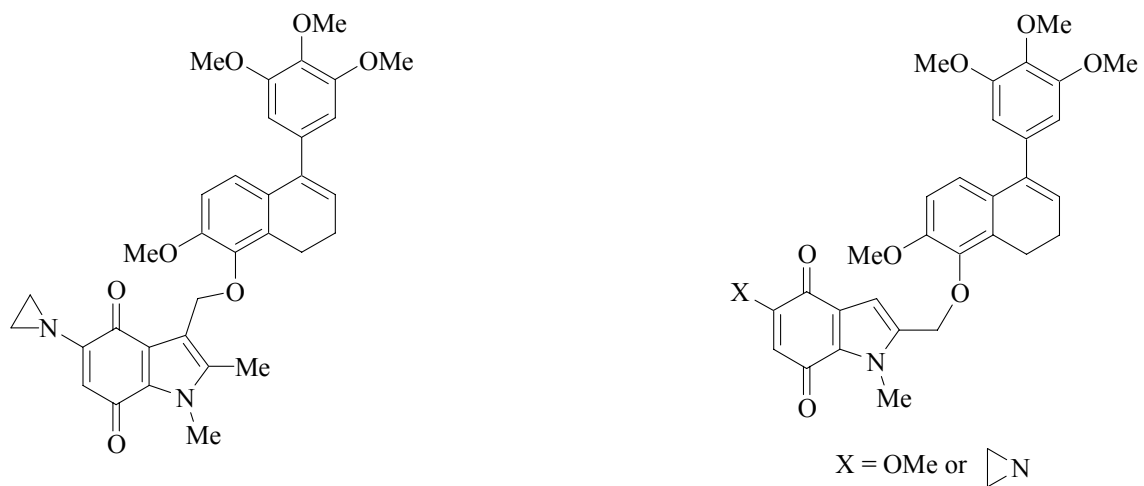


Figure 26. Future compounds based on indolequinones

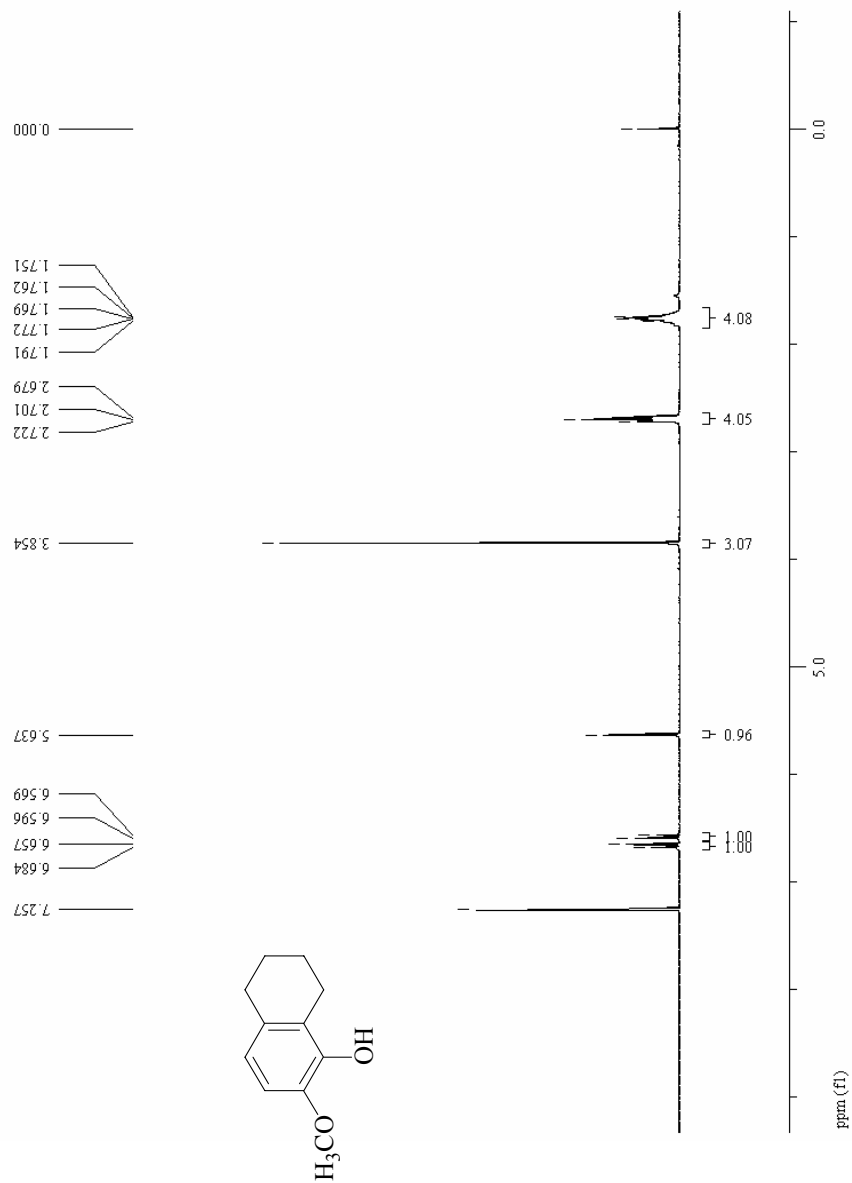
APPENDIX

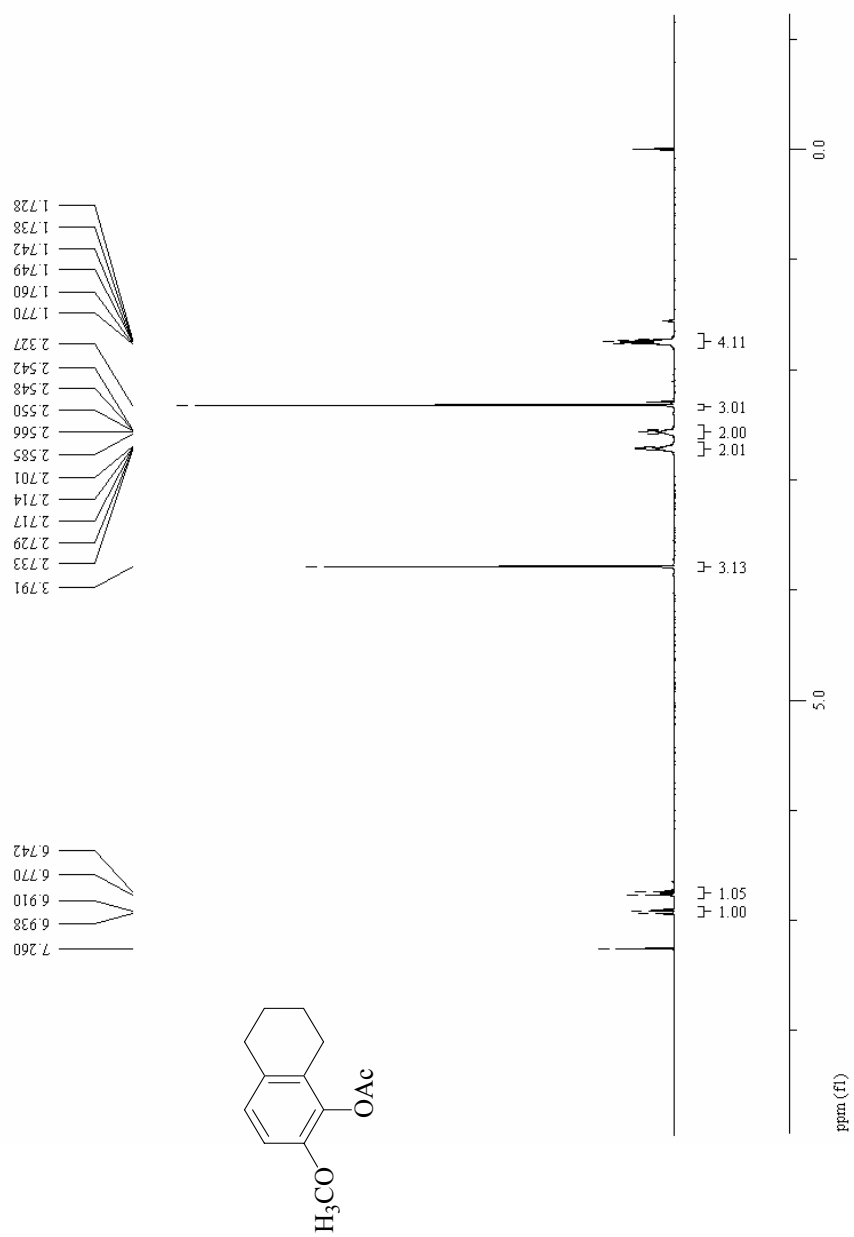
SELECTED NMR SPECTRA

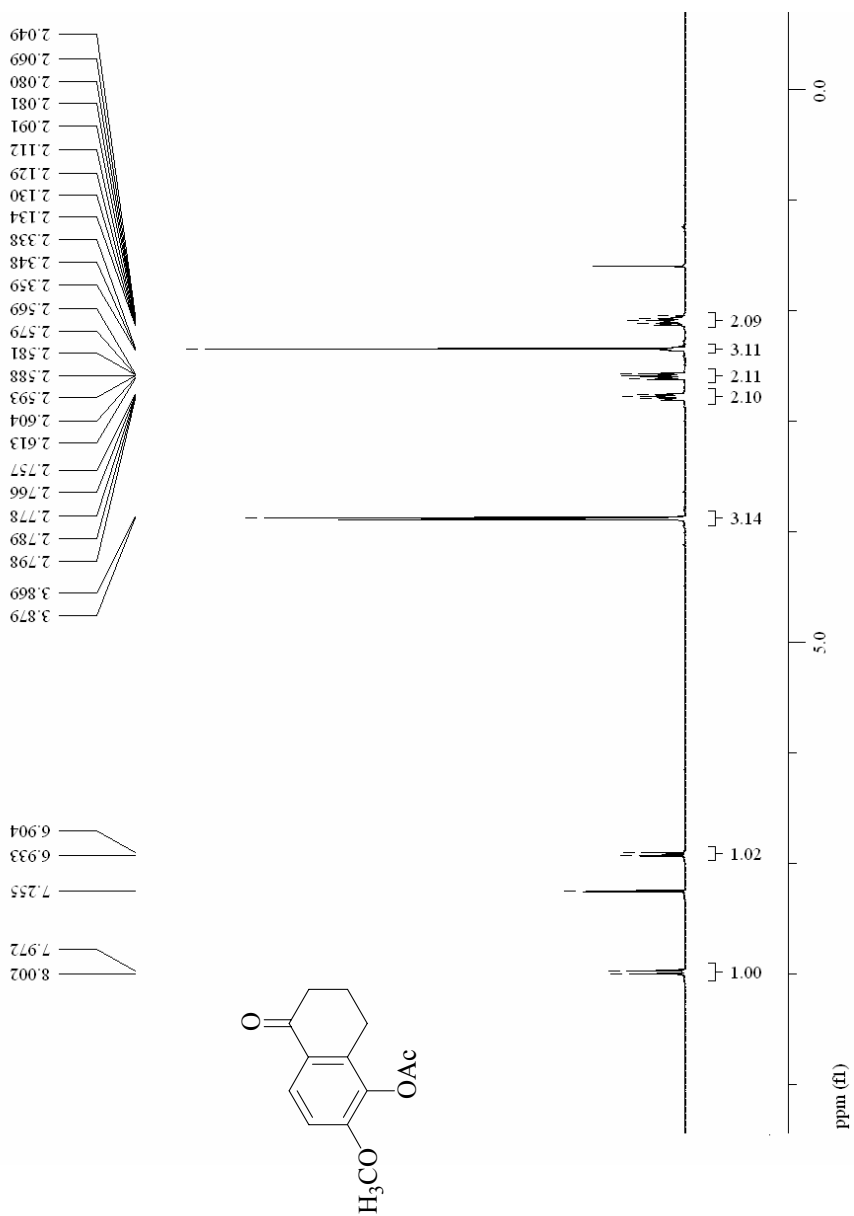
Spectrum

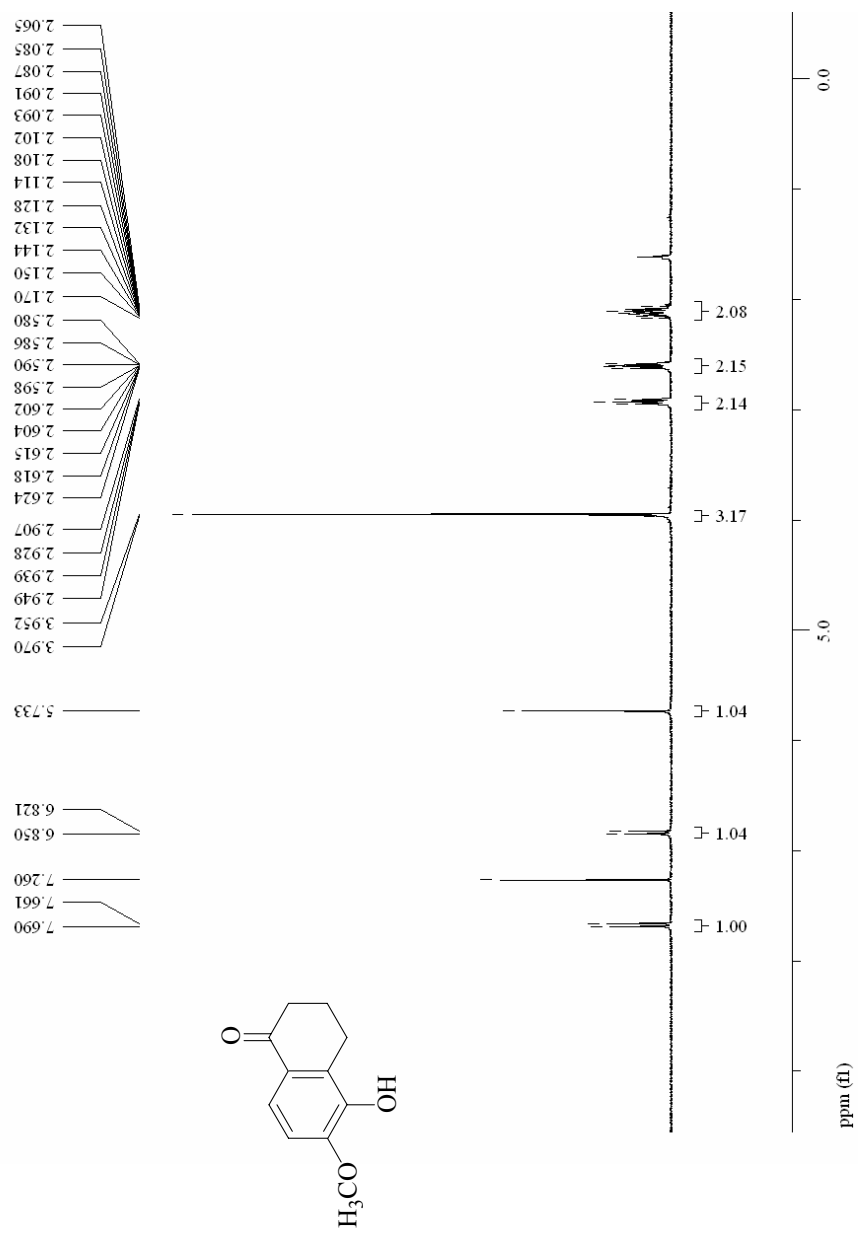
1. ^1H -NMR of Compound 1a	77
2. ^1H -NMR of Compound 2	78
3. ^1H -NMR of Compound 3	79
4. ^1H -NMR of Compound 4	80
5. ^1H -NMR of Compound 5	81
6. ^1H -NMR of Compound 6	82
7. ^1H -NMR of Compound 8	83
8. ^{13}C -NMR of Compound 8	84
9. ^1H -NMR of Compound 9	85
10. ^1H -NMR of Compound 10	86
11. ^1H -NMR of Compound 11	87
12. ^1H -NMR of Compound 12	88
13. ^1H -NMR of Compound 14	89
14. ^1H -NMR of Compound 15	90
15. ^1H -NMR of Compound 16	91
16. ^1H -NMR of Compound 17	92
17. ^1H -NMR of Compound 18	93
18. ^1H -NMR of Compound 19	94
19. ^1H -NMR of Compound 20	95
20. ^{13}C -NMR of Compound 20	96

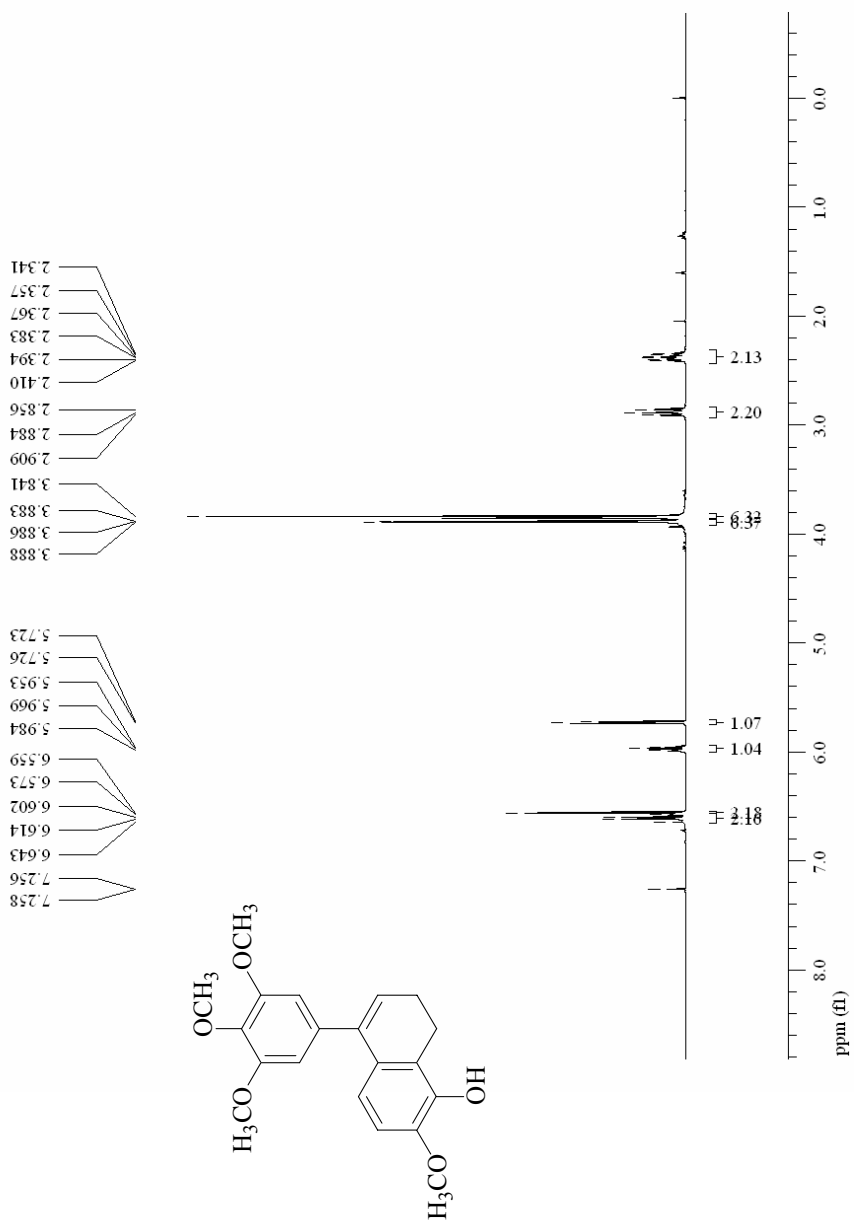
	76
21. ¹ H-NMR of Compound 21	97
22. ¹ H-NMR of Compound 22	98
23. ¹ H-NMR of Compound 23	99
24. ¹ H-NMR of Compound 24	100
25. ¹ H-NMR of Compound 25	101
26. ¹ H-NMR of Compound 26	102
27. ¹ H-NMR of Compound 27	103
28. ¹ H-NMR of Compound 28	104

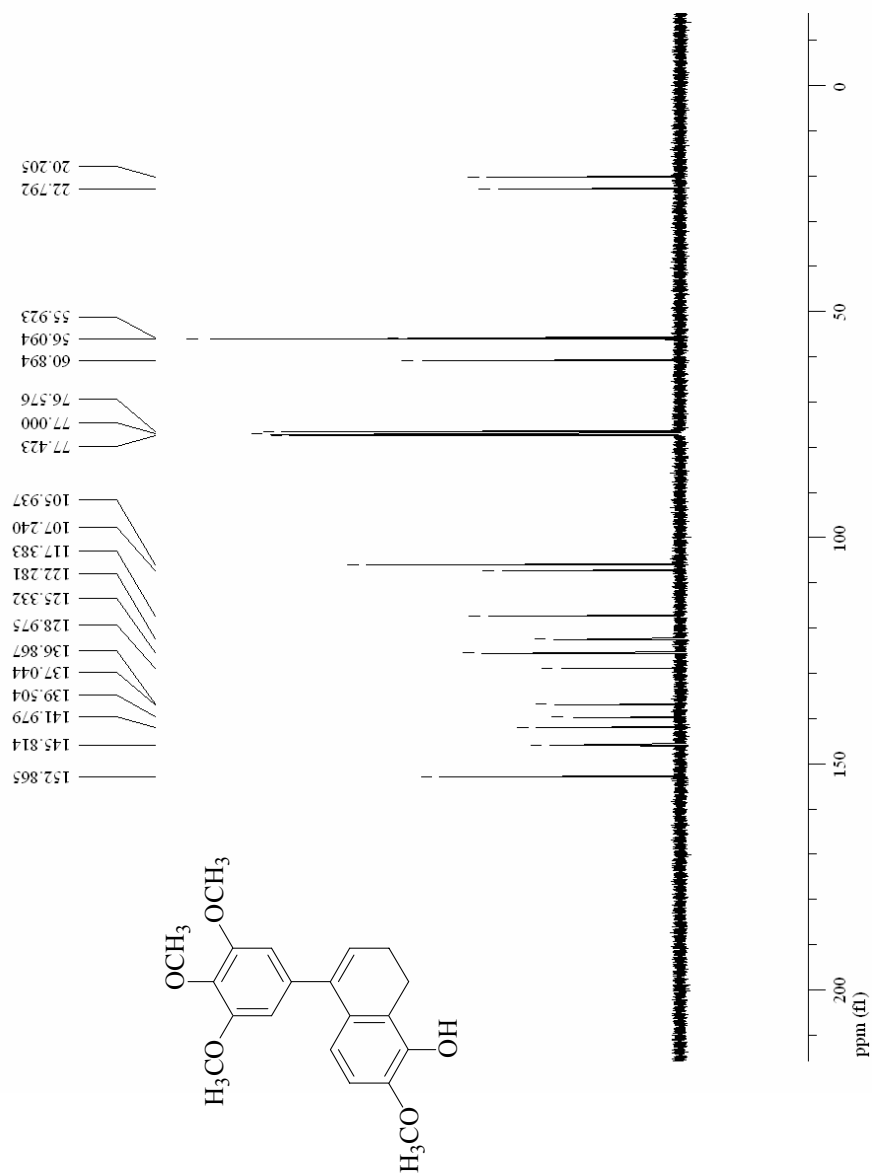
¹H-NMR of Compound **1a**

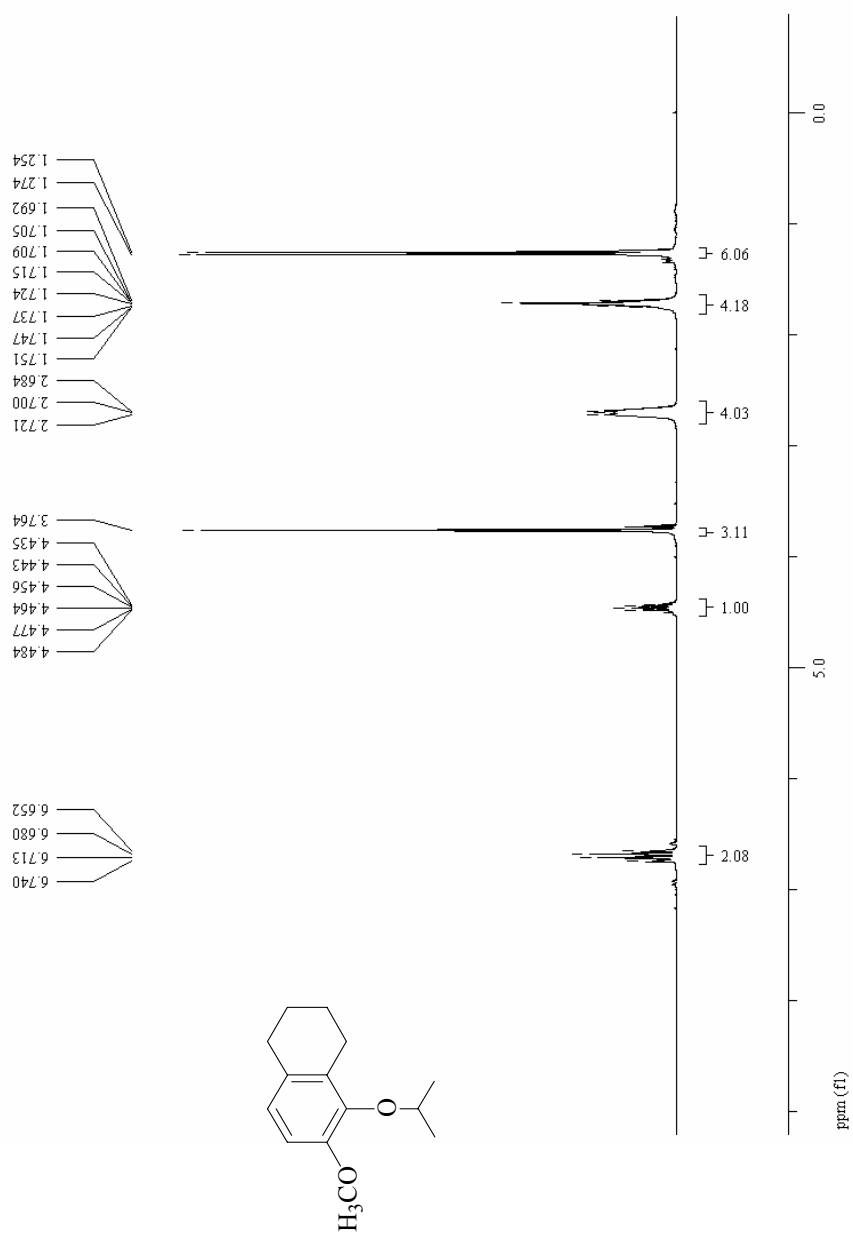
¹H-NMR of Compound 2

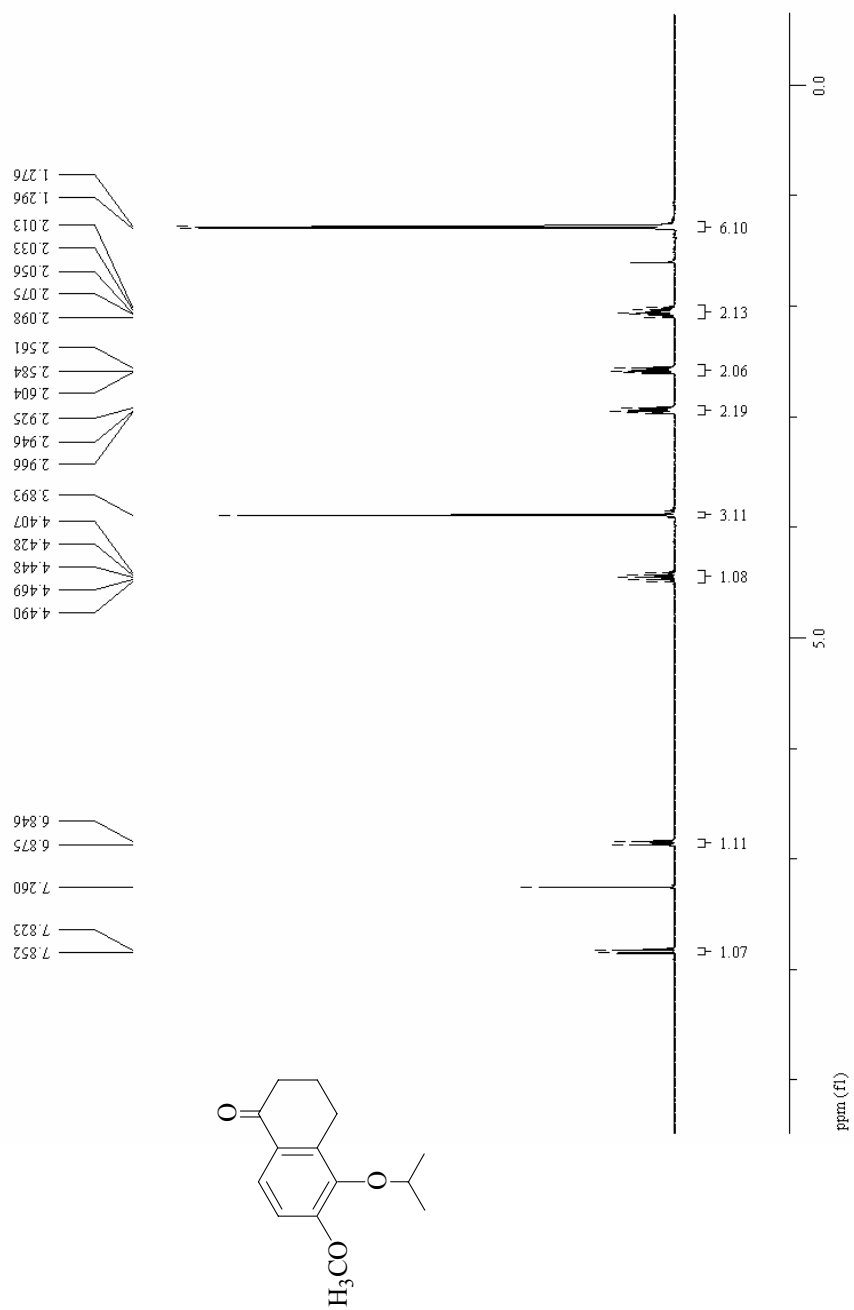
¹H-NMR of Compound 3

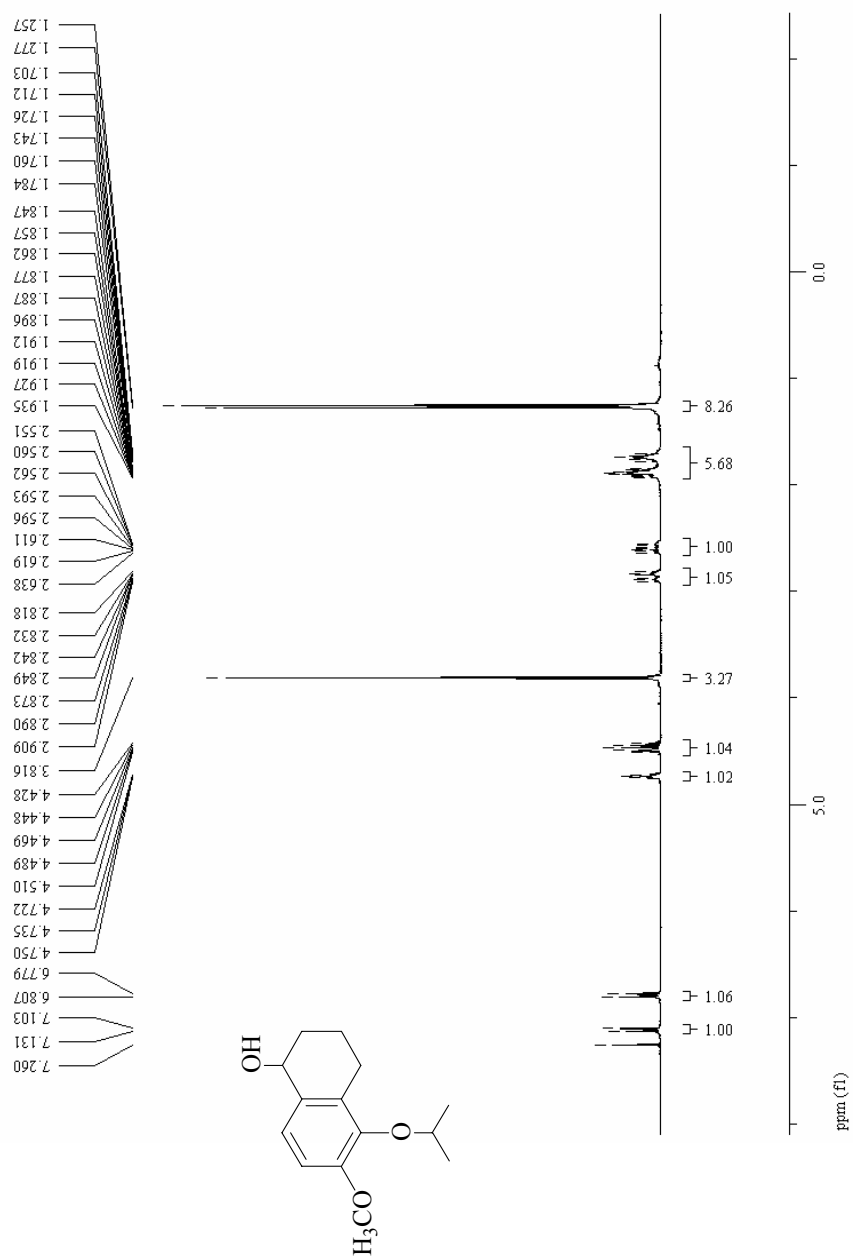
¹H-NMR of Compound 4

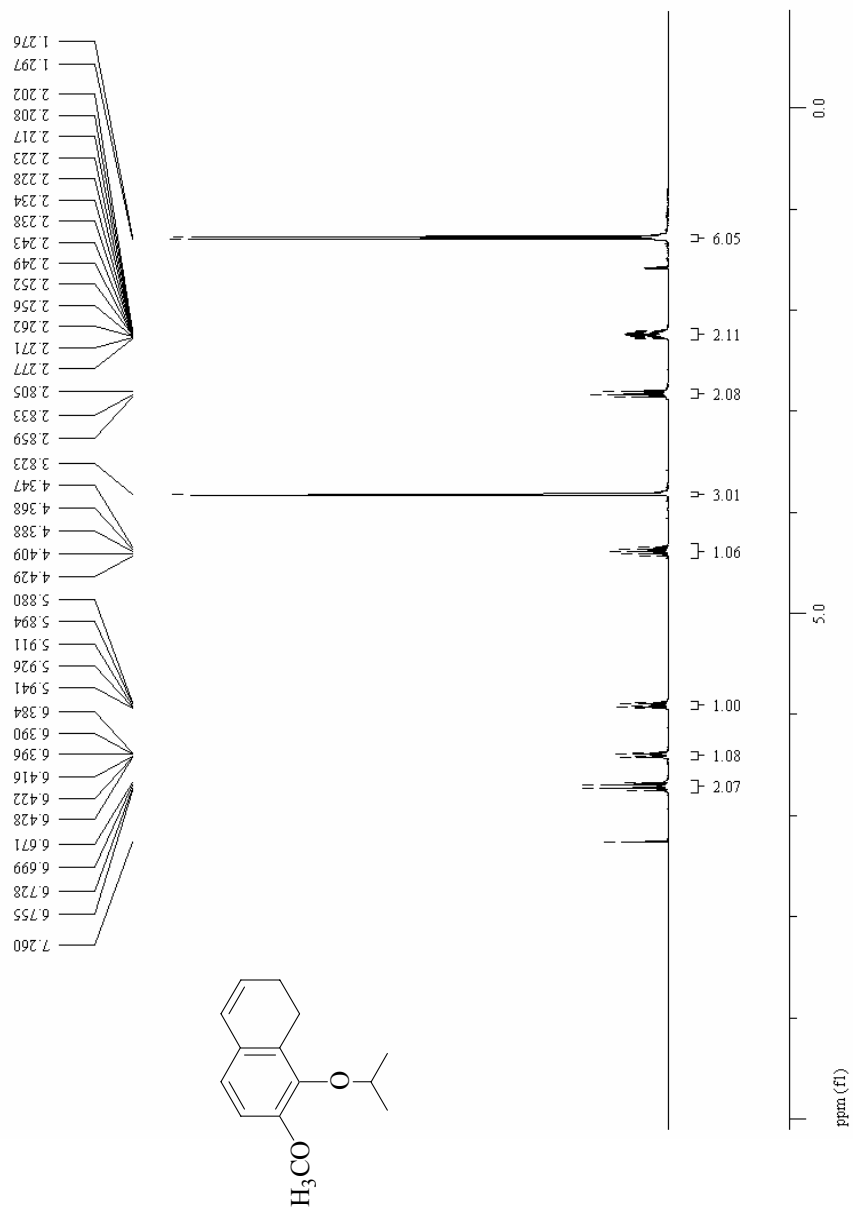
¹H-NMR of Compound **8**

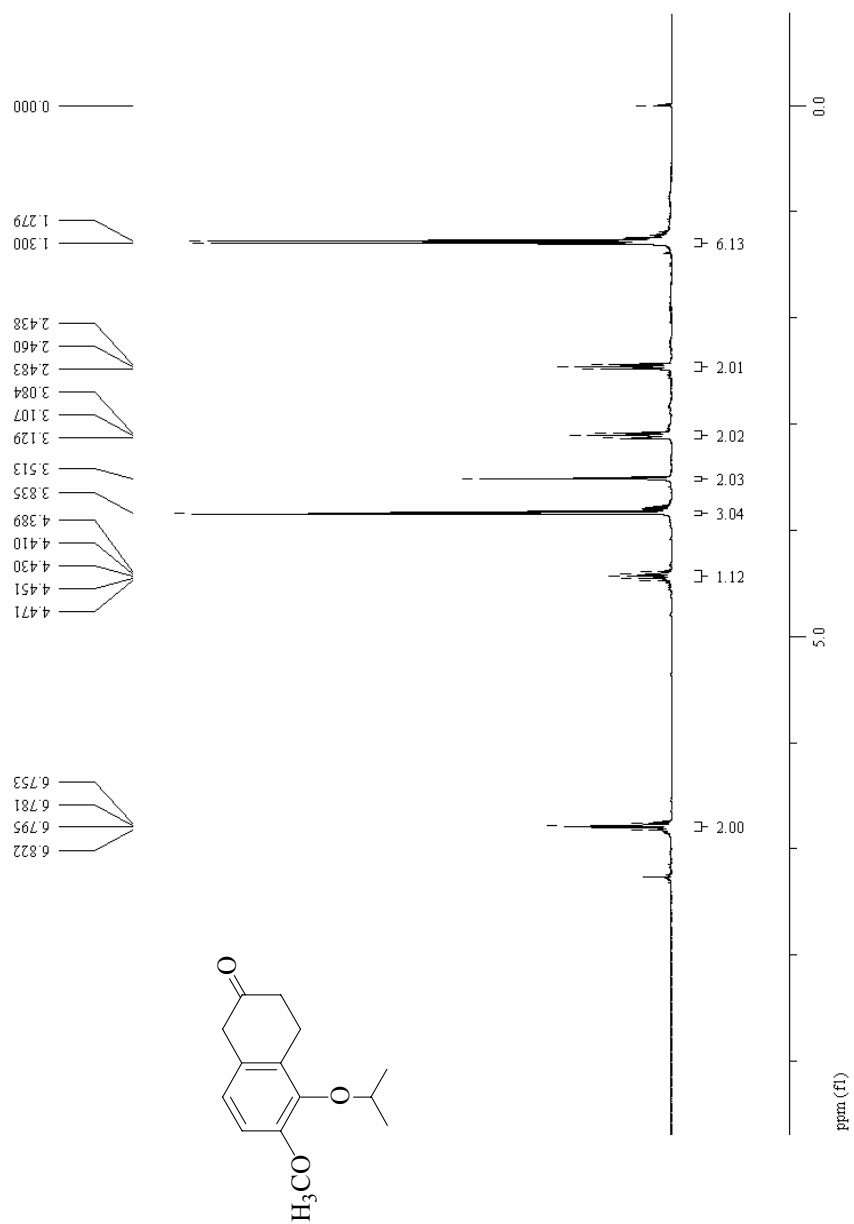
$^{13}\text{C-NMR}$ of Compound **8**

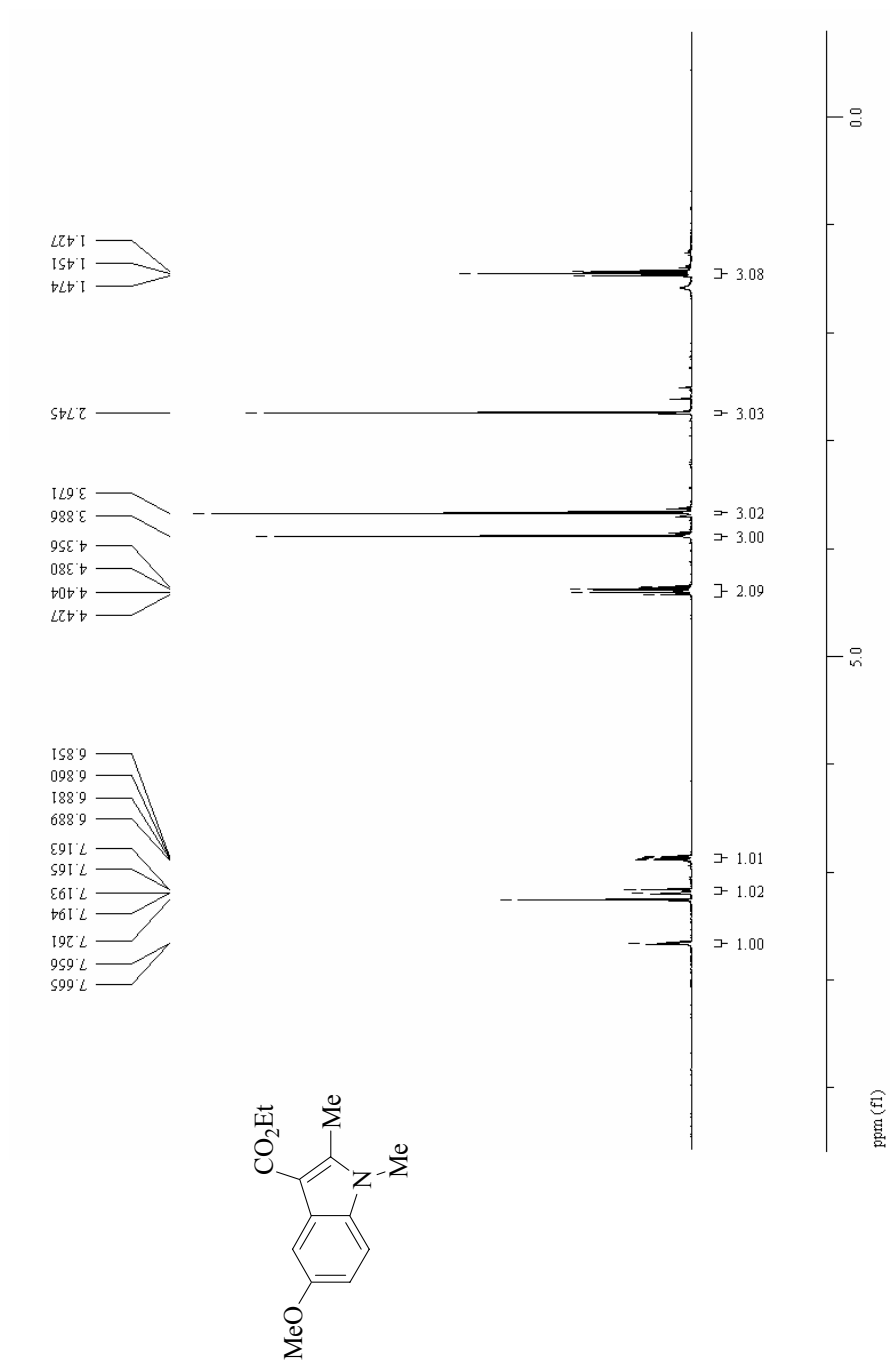
¹H-NMR of Compound 9

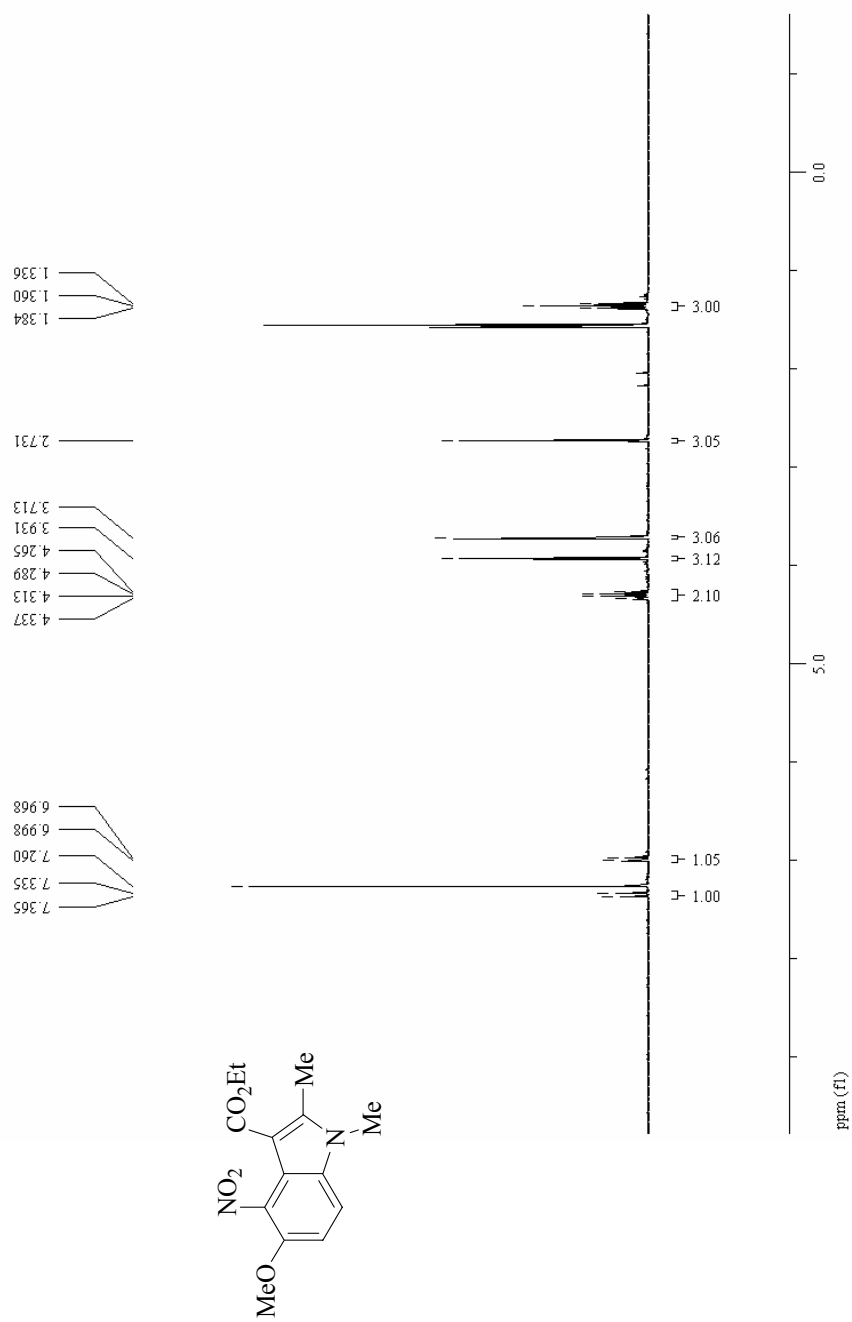
¹H-NMR of Compound 10

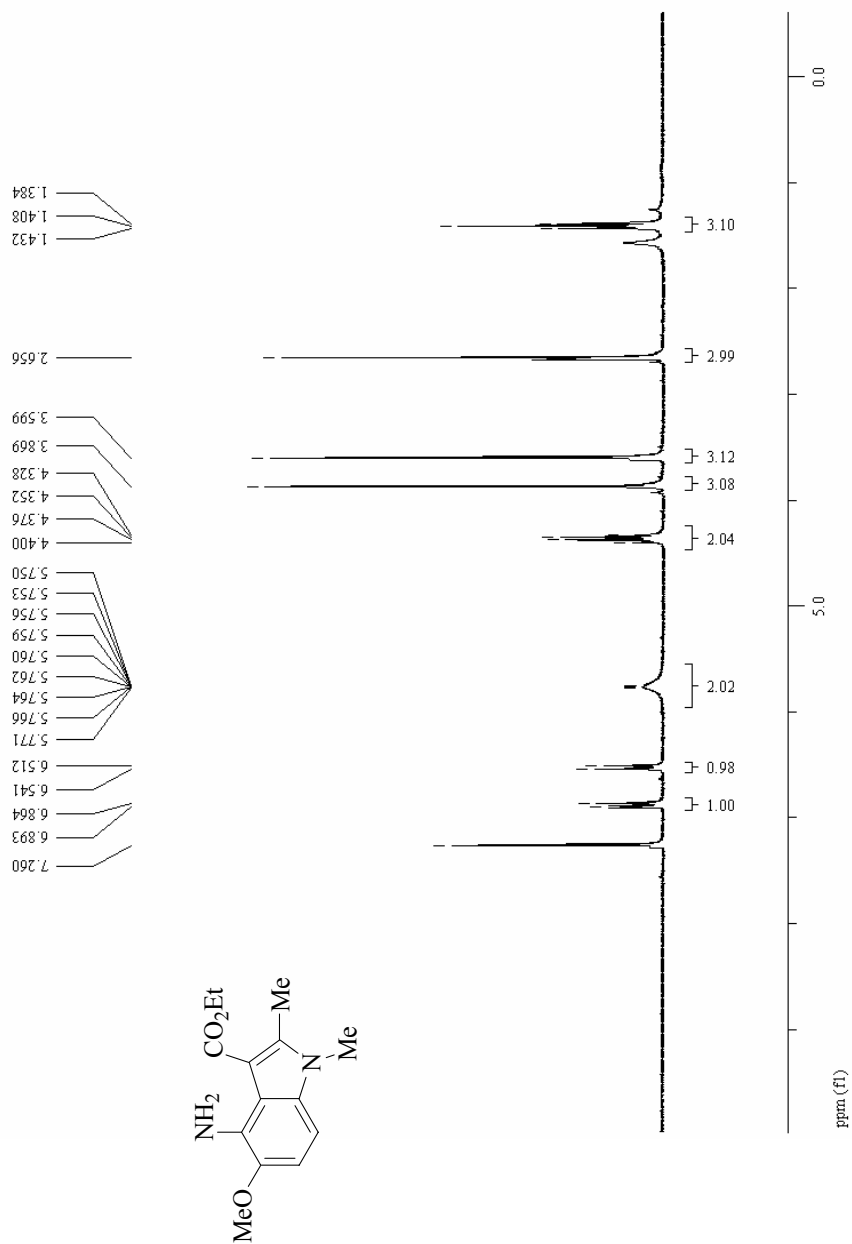
¹H-NMR of Compound 11

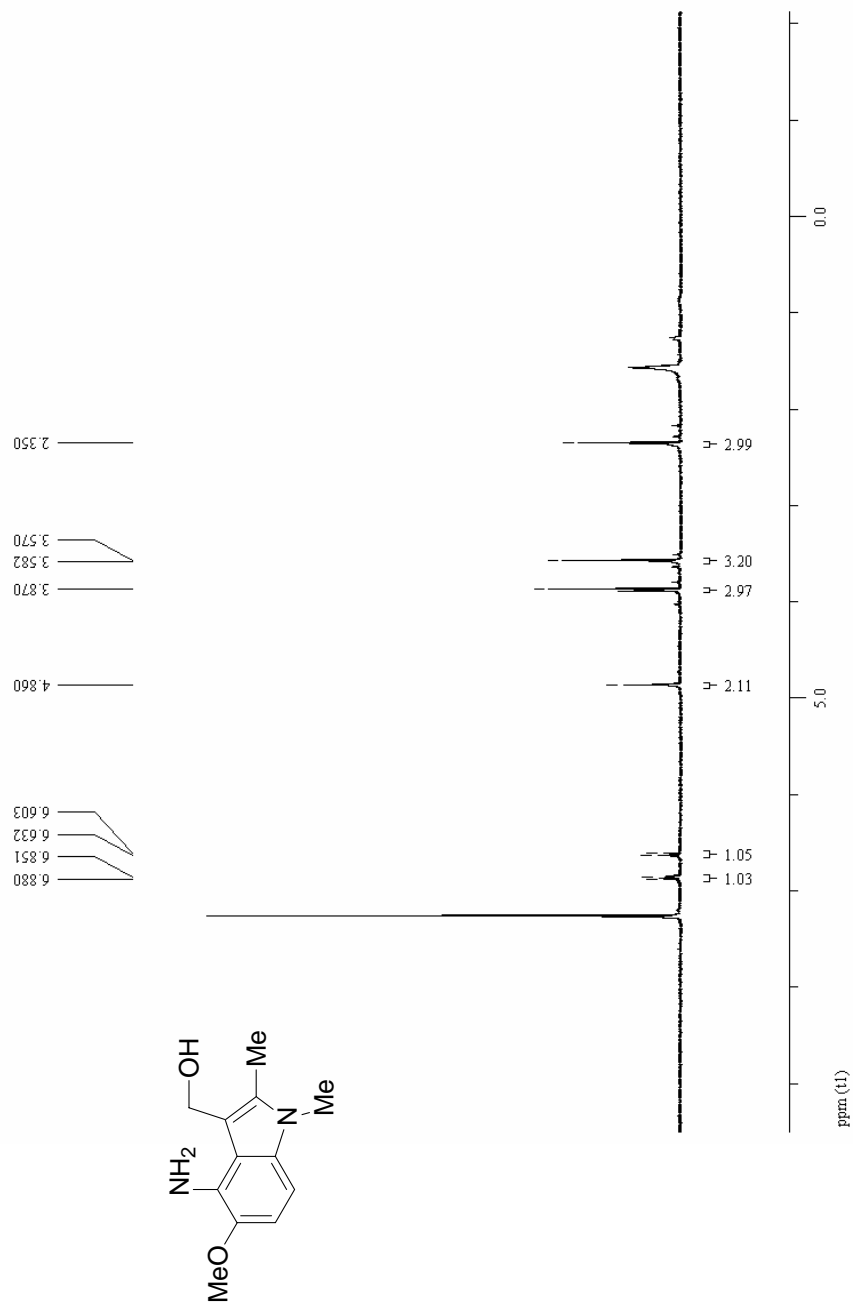
¹H-NMR of Compound 12

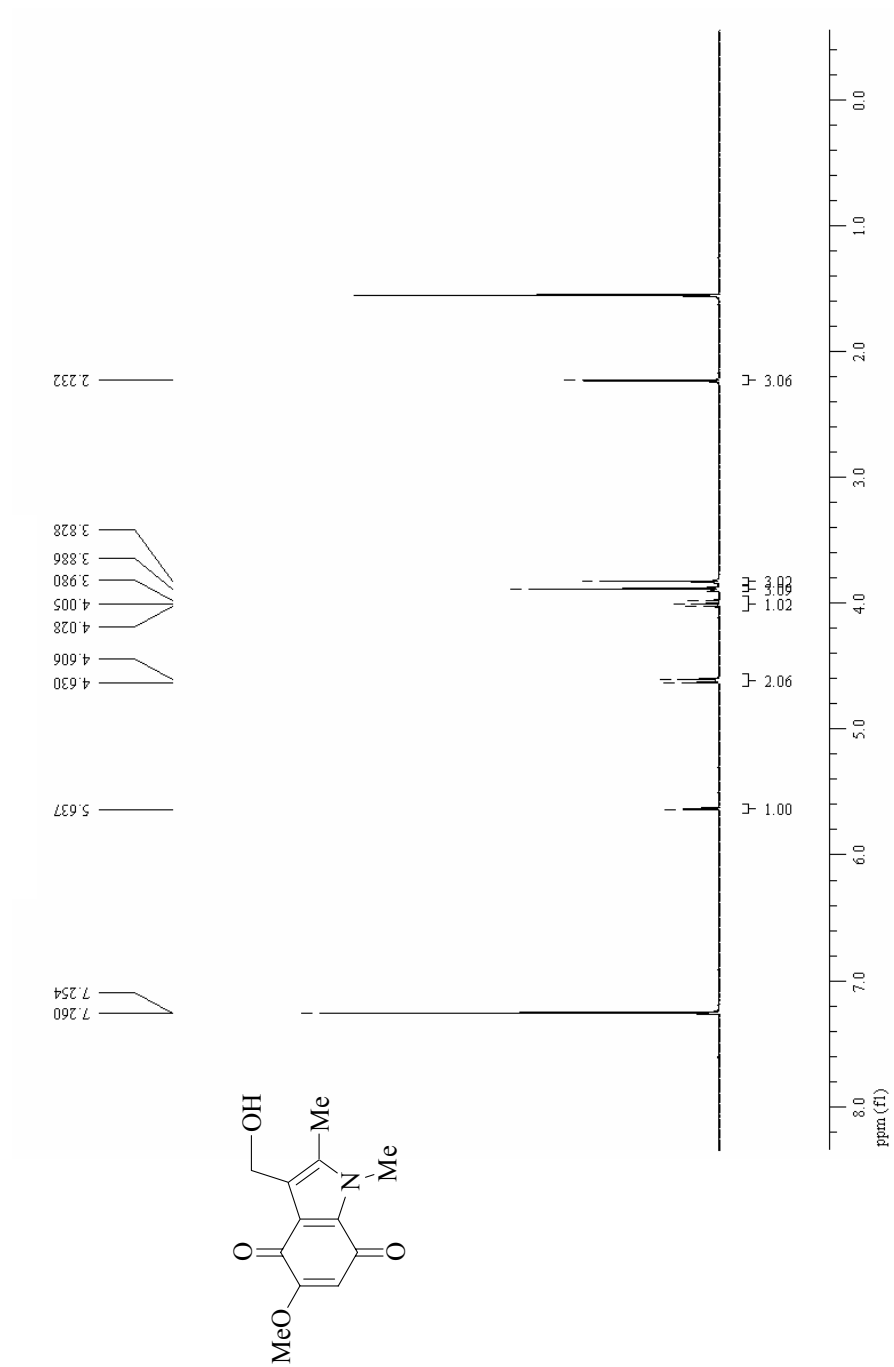
¹H-NMR of Compound 14

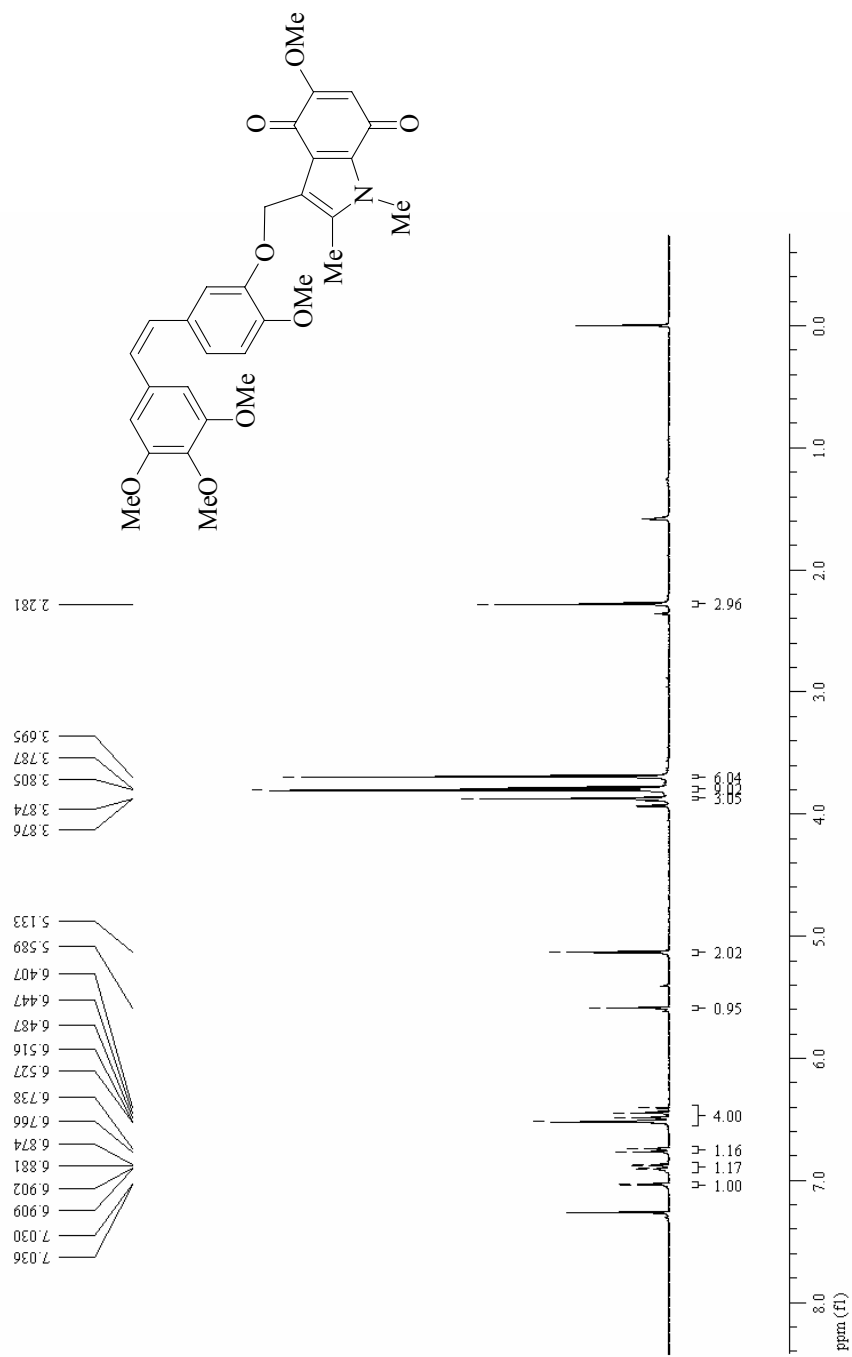
¹H-NMR of Compound 15

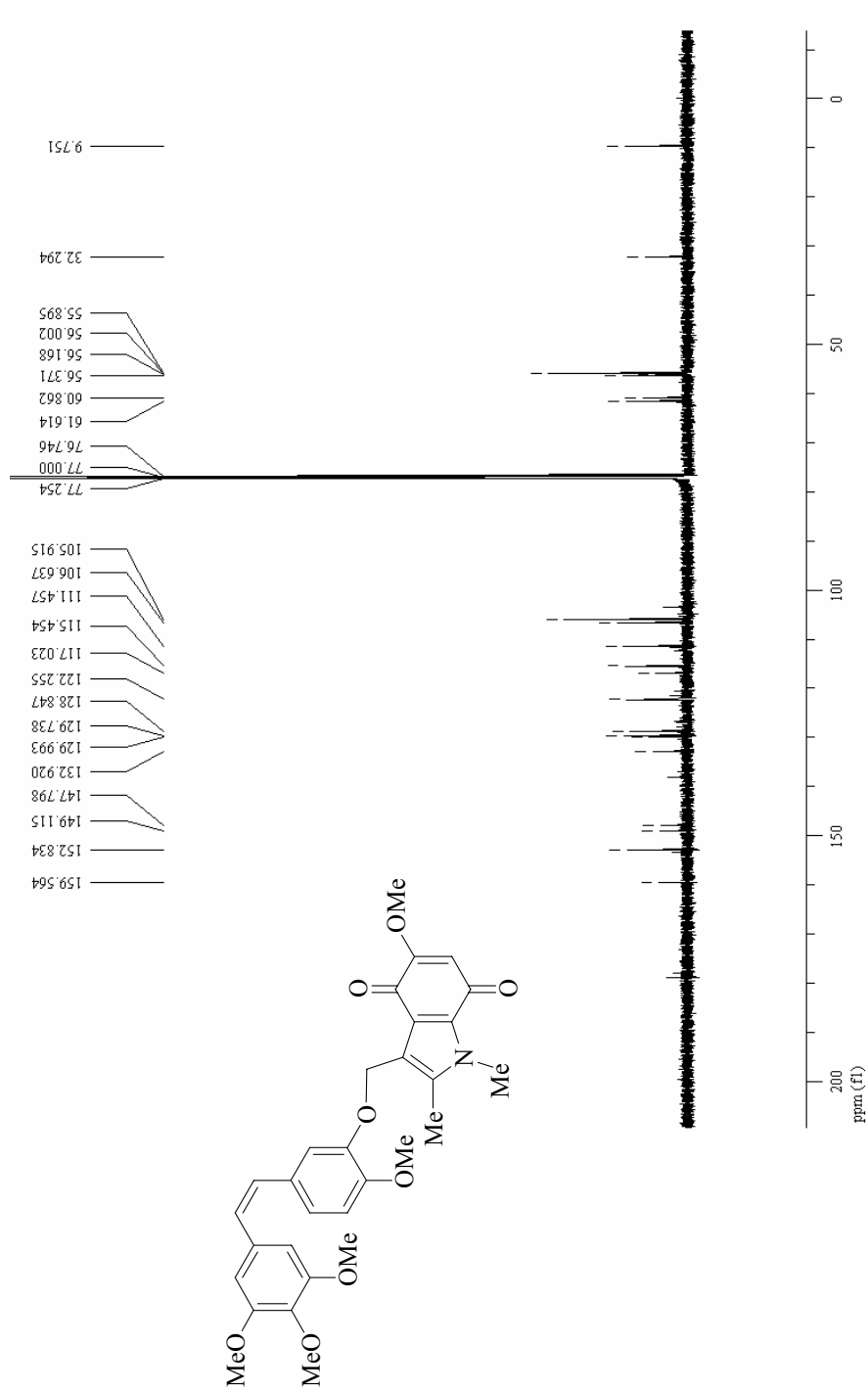
¹H-NMR of Compound 16

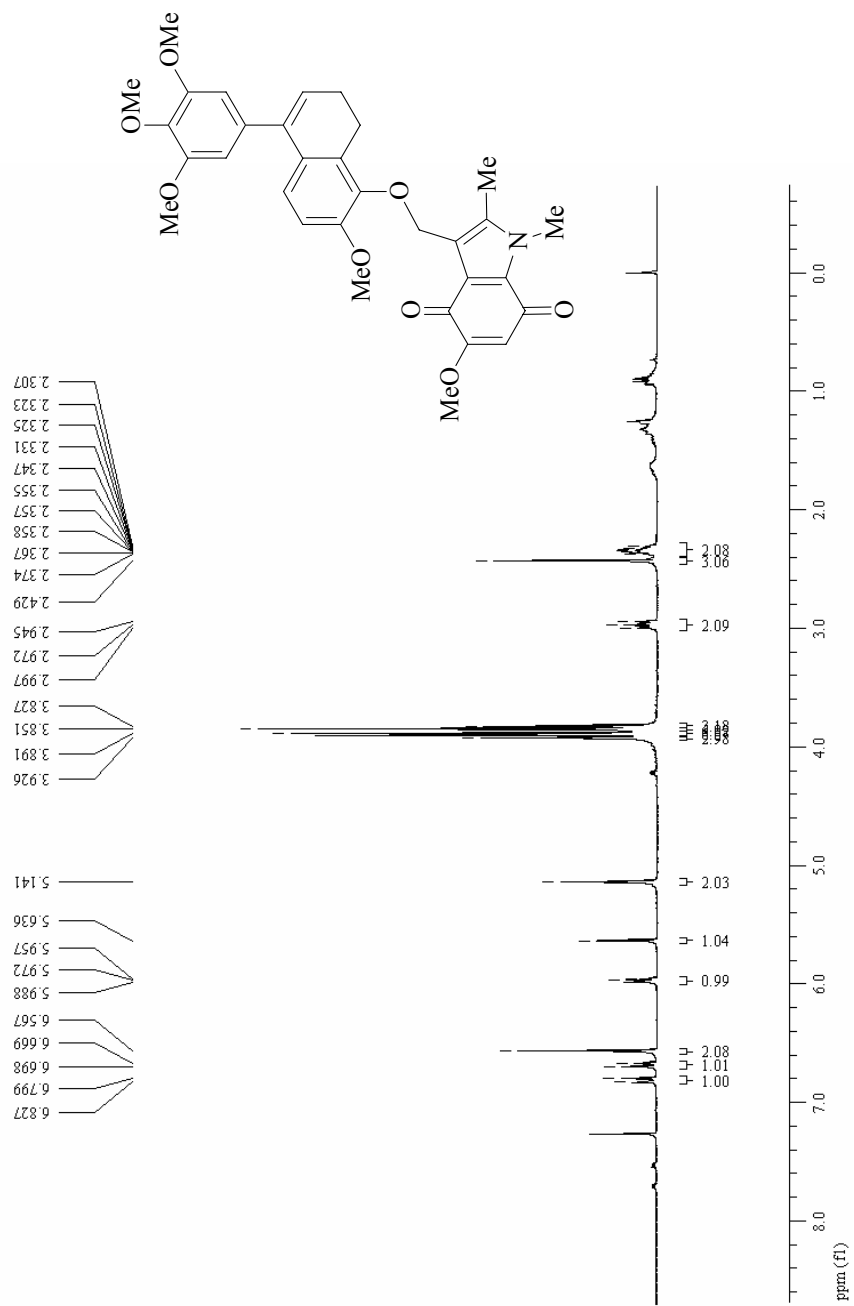
¹H-NMR of Compound 17

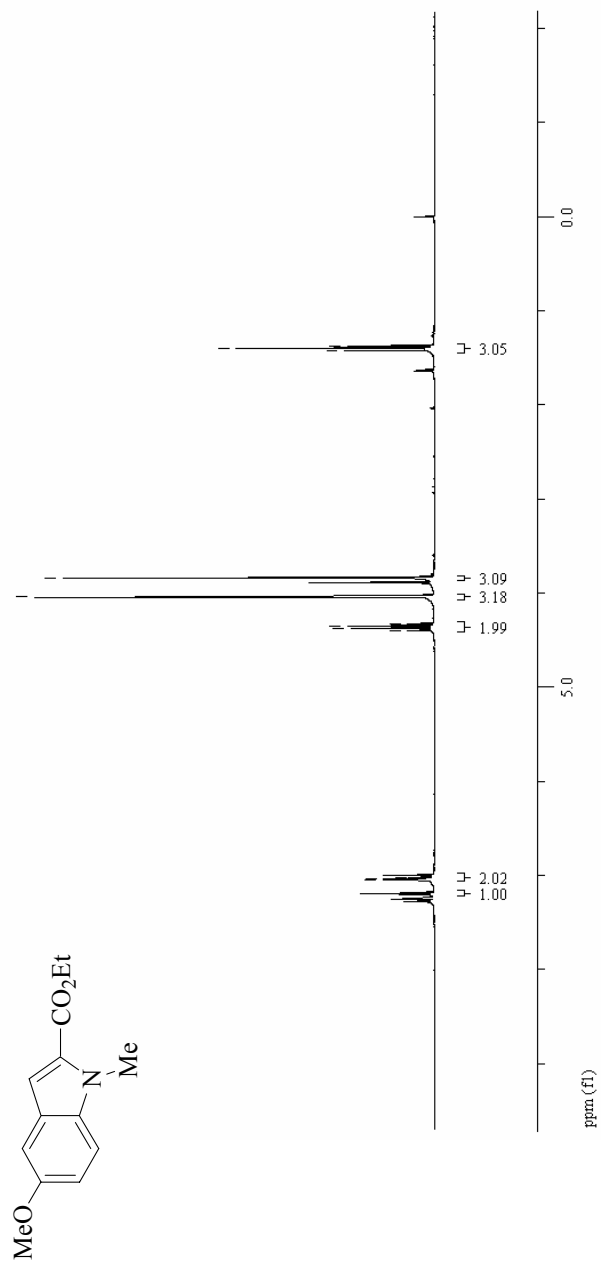
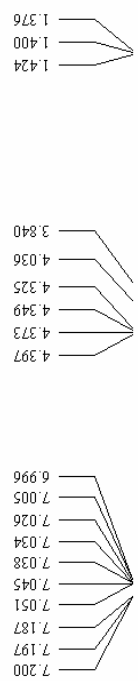
¹H-NMR of Compound **18**

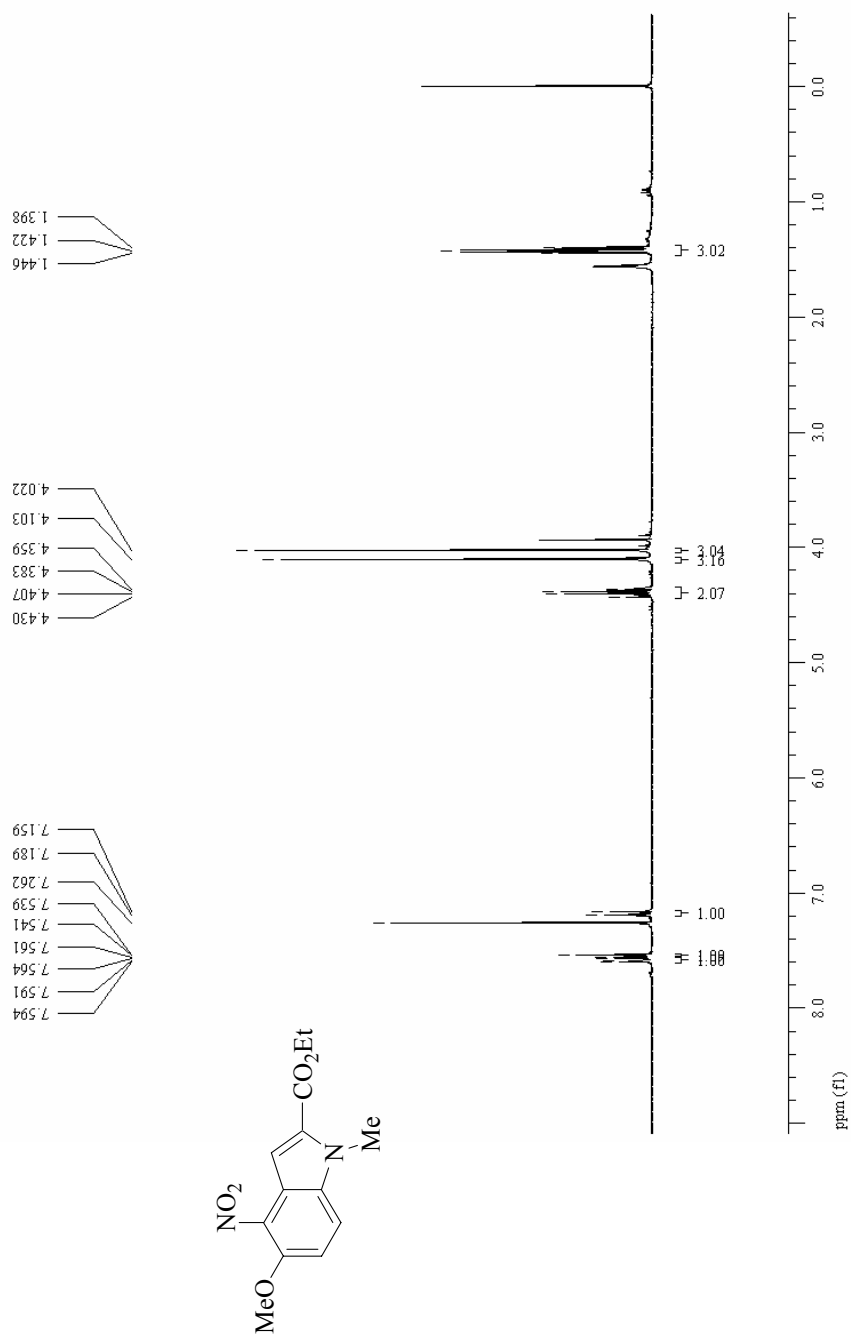
¹H-NMR of Compound **19**

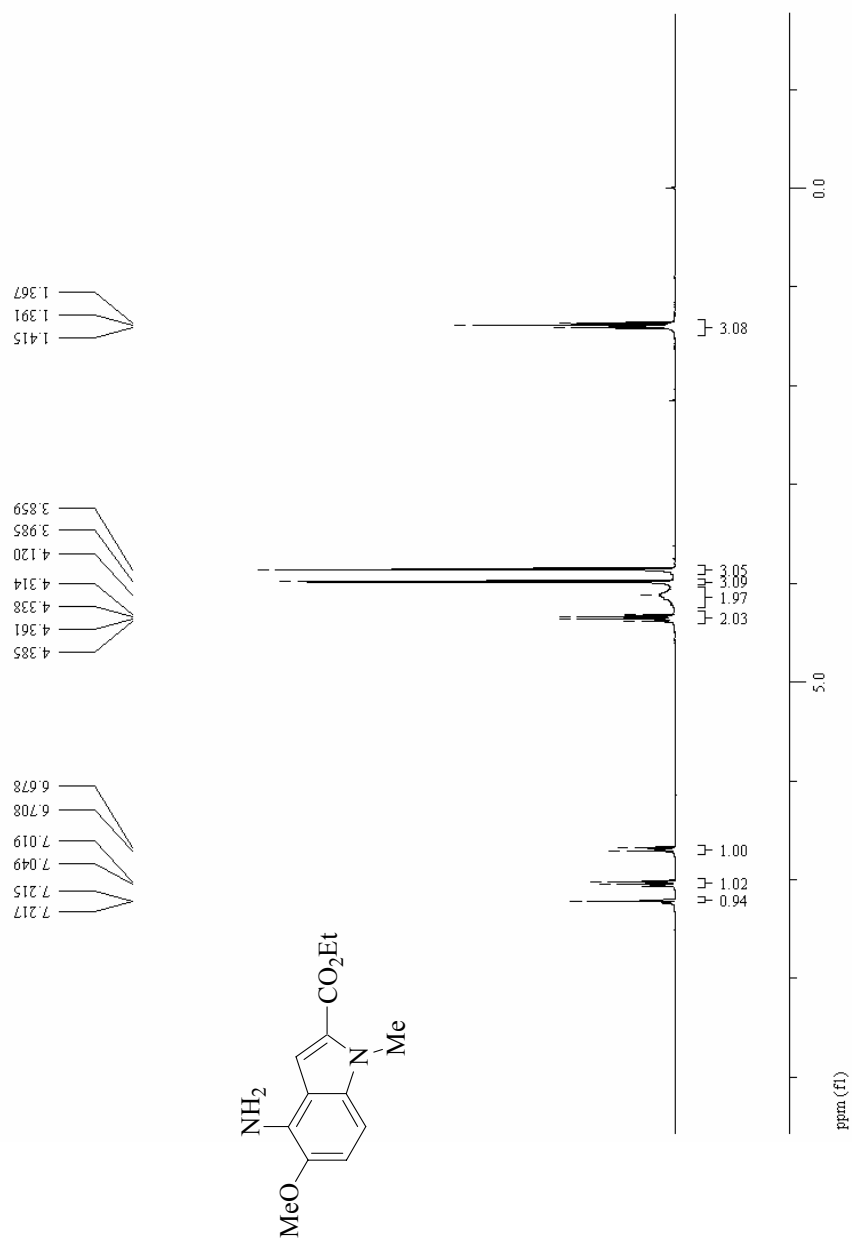
¹H-NMR of Compound 20

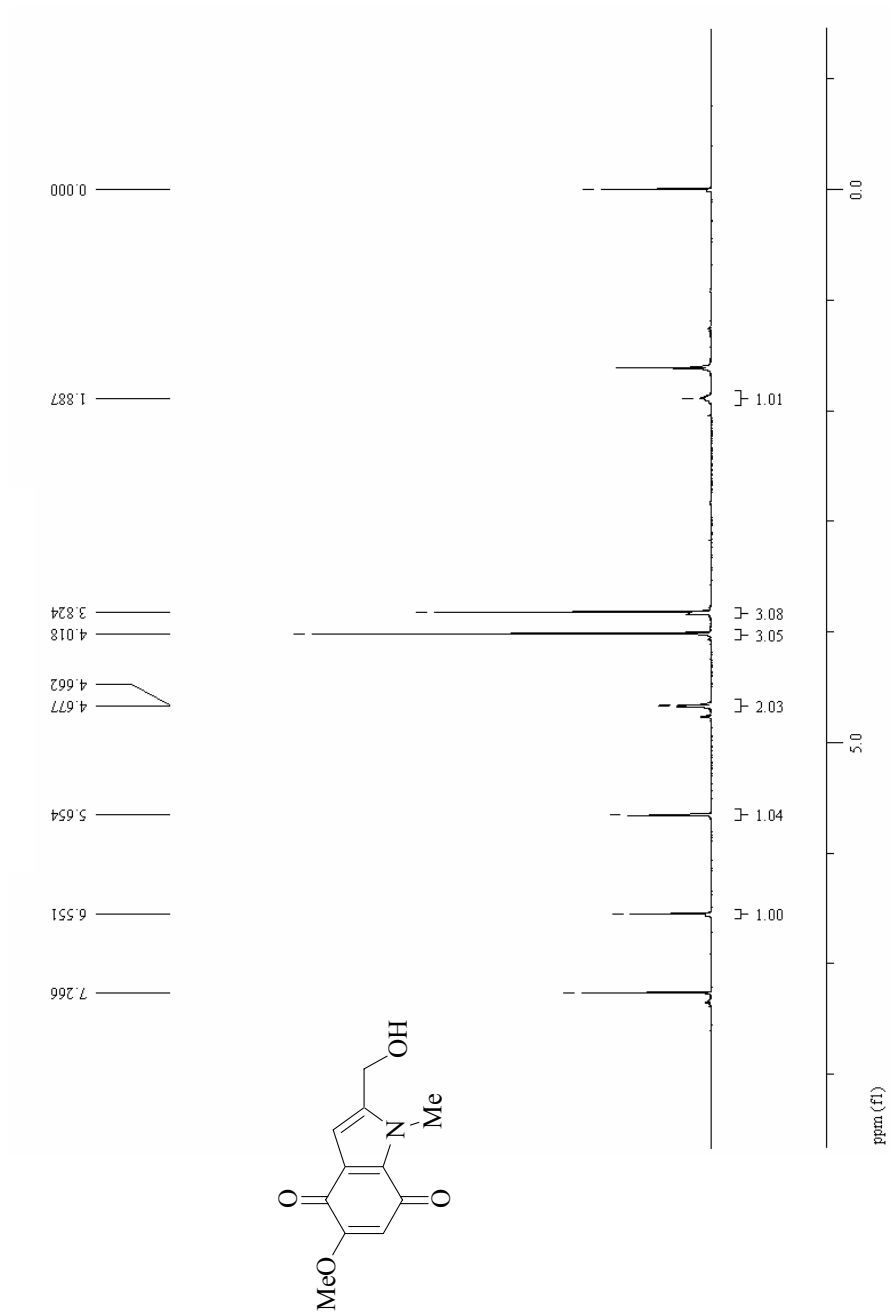
^{13}C NMR of Compound 20

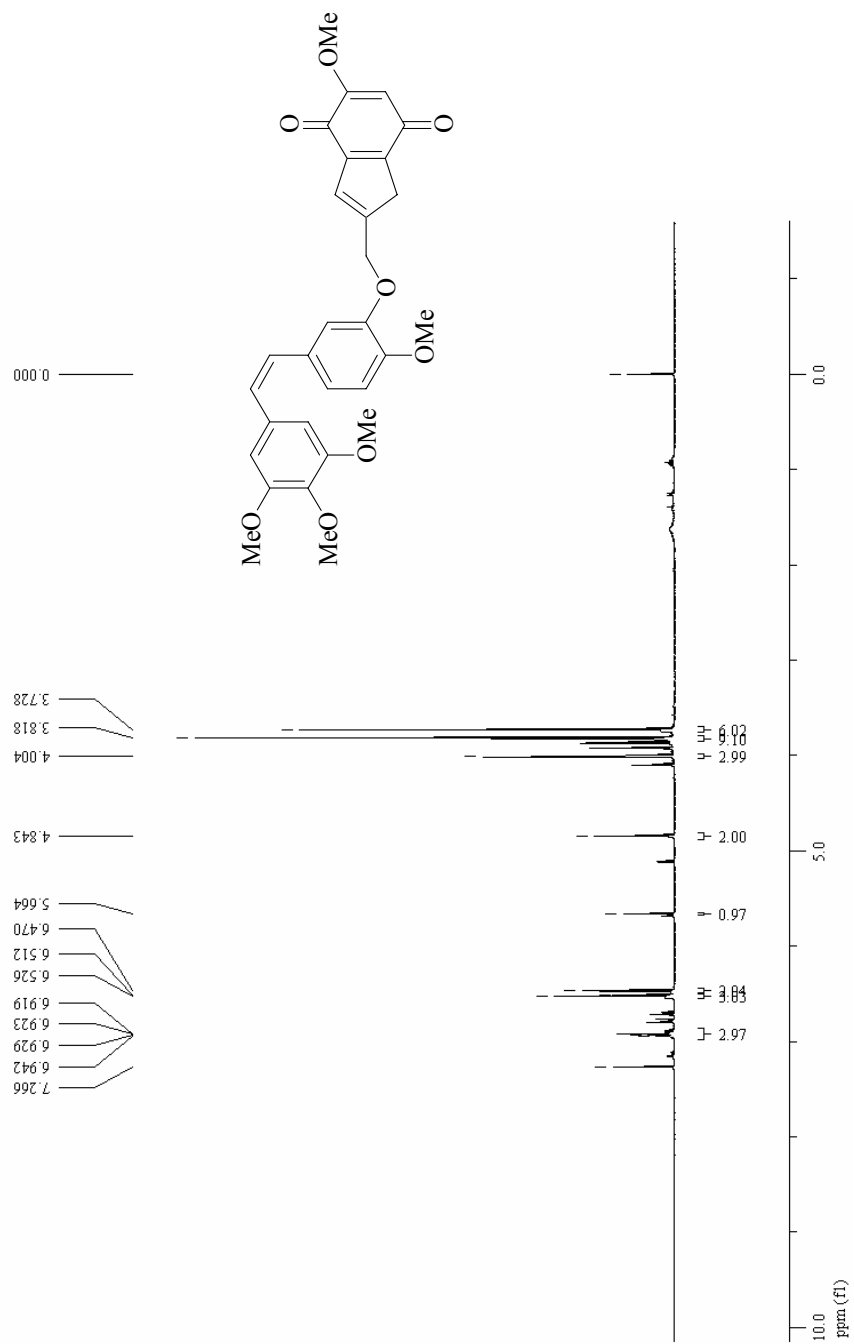
¹H-NMR of Compound 21

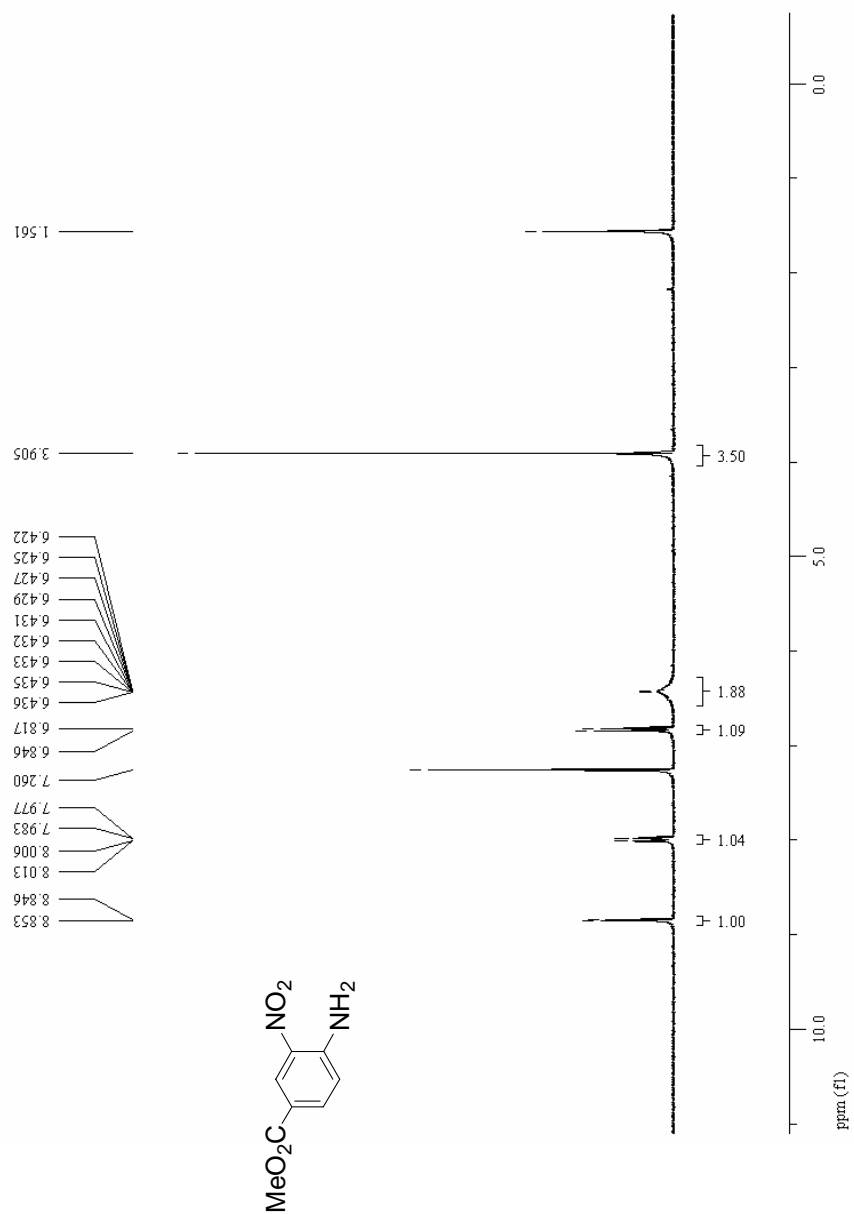
¹H-NMR of Compound 22

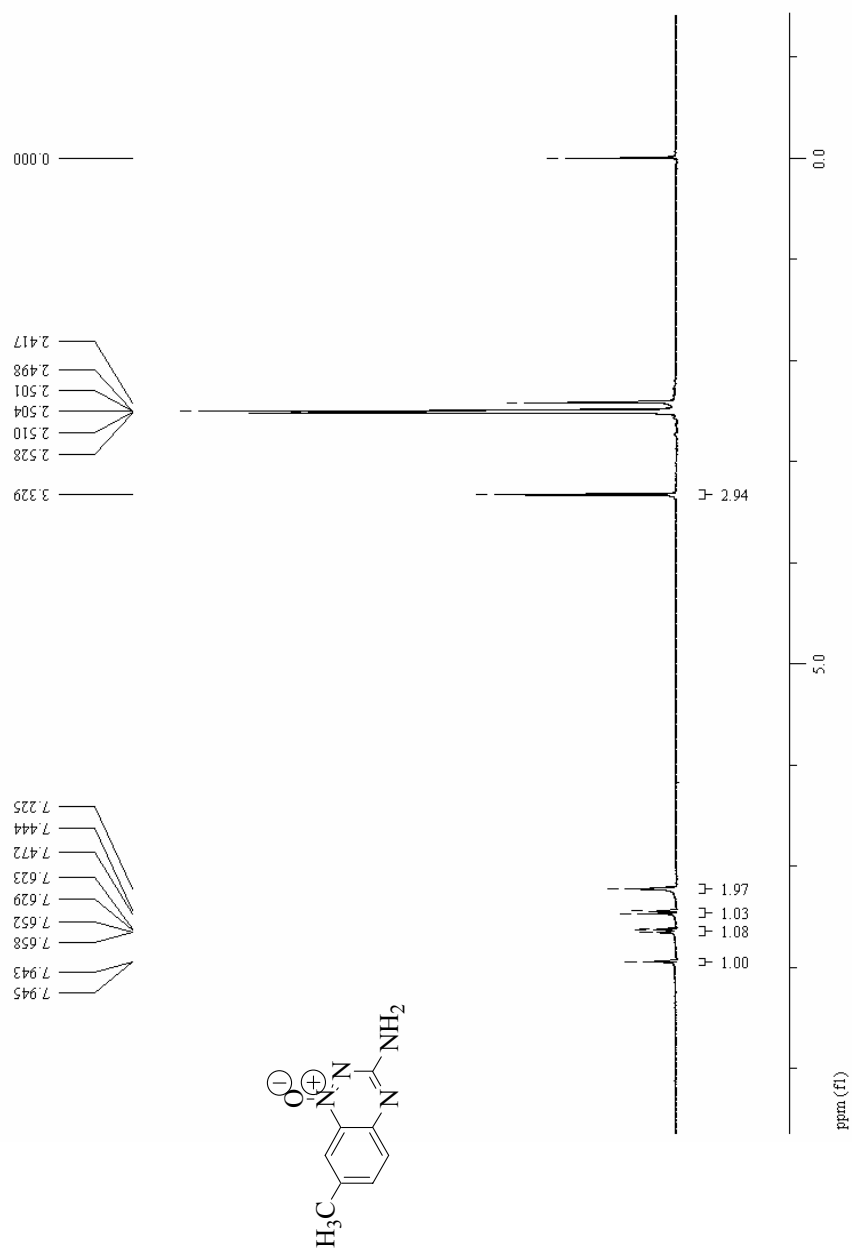
¹H-NMR of Compound 23

¹H-NMR of Compound 24

¹H-NMR of Compound 25

¹H-NMR of Compound 26

¹H-NMR of Compound 27

$^1\text{H-NMR}$ of Compound **28**

REFERENCES

- (1) National Cancer Institute Cancer Trends Progress Report.
http://progressreport.cancer.gov (accessed 07/18, 2005).
- (2) Turkington, C.; LiPera, W. In *The Encyclopedia of Cancer*; New York Facts on File, Inc.: 2005; , pp 448.
- (3) Encyclopaedia Britannica "cancer". *http://www.britannica.com/ebc/article-9359651* (accessed 07/20, 2006).
- (4) Blasco, M. In *Molecular Biology of Cancer*; Khan, M., Pelengaris, S., Eds.; Blackwell Publishing: 2006; , pp 500.
- (5) Eichhorn, M. E.; Strieth, S.; Dellian, M. *Drug Resistance Updates* **2004**, *7*, 125-138.
- (6) Bamias, A.; Dimopoulos, M. A. *Eur. J. Int. Med.* **2003**, *14*, 459-469.
- (7) Hanahan, D.; Weinberg, R. A. *Cell* **2000**, *100*, 57-70.
- (8) Folkman, J.; Kalluri, R. *Nature* **2004**, *427*, 787.
- (9) Bergers, G.; Benjamin, L. E. *Nat. Rev. Cancer* **2003**, *3*, 401-410.
- (10) Brizel, D. M.; Dodge, R. K.; Dewhurst, M. W. *Radiother. Oncol.* **1999**, *53*, 113-117.
- (11) Siemann, D. W.; Horsman, M. R. *Expert Rev. Anticancer Ther.* **2004**, *4*, 321-327.
- (12) Siemann, D. W.; Bibby, M. C.; Dark, G. G.; Dicker, A. P.; Eskens, F.; Horsman, M. R.; Marme, D.; LoRusso, P. M. *Clin. Cancer Res.* **2005**, *11*, 416-420.
- (13) Marme, D. *J. Cancer Res. Clin. Oncol.* **2003**, *129*, 607-620.
- (14) Thorpe, P. E. *Clin. Cancer Res.* **2004**, *10*, 415-427.
- (15) Sorbera, L. A.; Leeson, P. A.; Bayes, M. *Drugs of the Future* **2002**, *27*, 625-632.
- (16) Wedge, S. R.; Ogilvie, D. J.; Dukes, M. *Cancer Res.* **2002**, *62*, 4645-4655.
- (17) Wood, J. M.; Bold, G.; Buchdunger, E. *Cancer Res.* **2000**, *60*, 2178-2189.
- (18) Mross, K. *Drug Resist. Updates* **2000**, *4*, 223-235.
- (19) Scappaticci, F. A. *J. Clin. Oncol.* **2002**, *20*, 3906-3927.
- (20) Denekamp, J. *Acta Radiol. Oncol.* **1984**, *23*, 217-225.

- (21) Denekamp, J. *Eur. J. Clin. Invest.* **1999**, *29*, 733-736.
- (22) Gaya, A. M.; Rustin, G. J. S. *Clin. Oncol.* **2005**, *17*, 277-290.
- (23) Blakey, D. C.; Ashton, S. E.; Westwood, F. R.; Walker, M.; Ryan, A. J. *Int. J. Radiat. Oncol. Biol. Phys.* **2002**, *54*, 1497-1502.
- (24) Chaplin, D. J.; Horsman, M. R.; Siemann, D. W. *Curr. Opin. Invest. Drugs* **2006**, *7*, 522-528.
- (25) Tozer, G. M.; Kanthou, C.; Baguley, B. C. *Nat. Rev. Cancer* **2005**, *5*, 423-435.
- (26) Siemann, D. W.; Shi, W. *Int. J. Radiat. Oncol. Biol. Phys.* **2004**, *60*, 1233-1240.
- (27) Siemann, D. W.; Chaplin, D. J.; Horsman, M. R. *Cancer* **2004**, *100*, 2491-2499.
- (28) Mahadevan, V.; Malik, S. T.; Meager, A.; Fiers, W.; Lewis, G. P.; Hart, I. R. *Cancer Res.* **1990**, *50*, 5537-5542.
- (29) Chaplin, D. J.; Dougherty, G. J. *Br. J. Cancer* **1999**, *80*, 57-64.
- (30) Meurer-Frob, P.; Kasparian, J.; Wade, R. H. *Biochemistry* **2001**, *40*, 8000-8008.
- (31) Nogales, E. *Ann. Rev. Biophys. Biomol. Struct.* **2001**, *30*, 397-420.
- (32) Nogales, E.; Wolf, S. G.; Downing, K. H. *Nature* **1998**, *391*, 199-203.
- (33) Lowe, J.; Li, H.; Downing, K. H.; Nogales, E. *J. Mol. Biol.* **2001**, *313*, 1045-1057.
- (34) Jordan, M. A.; Wilson, L. *Nat. Rev. Cancer* **2004**, *4*, 253-265.
- (35) Nogales, E.; Whittaker, M.; Milligan, R. A.; Downing, K. H. *Curr. Opin. Struct. Biol.* **1998**, *8*, 785-791.
- (36) Rodionov, V. I.; Borisy, G. G. *Science* **1997**, *300*, 215-218.
- (37) Jordan, A.; Hadfield, J. A.; Lawrence, N. J.; McGown, A. T. *Med. Res. Rev.* **1998**, *18*, 259-296.
- (38) Downing, K. H. *Annu. Rev. Cell Dev. Biol.* **2000**, *16*, 89-111.
- (39) Hadfield, J. A.; Duckie, S.; Hirst, N.; McGown, A. T. *Prog. Cell. Cycle Res.* **2003**, *5*, 309-325.
- (40) Shi, Q.; Chen, K.; Morris-Natschke, S. L.; Lee, K. H. *Curr. Pharm. Des.* **1998**, *4*, 219-248.
- (41) Davis, P. D.; Dougherty, G. J.; Blakey, D. C. *Cancer Res.* **2002**, *62*, 7247-7253.

- (42) Damayanthi, Y.; Lown, J. W. *Curr. Med. Chem.* **1998**, *5*, 205-252.
- (43) Petit, G. R.; Toki, B.; Herald, D. L.; Verdier-Pinard, P.; Boyd, M. R.; Hamel, E.; Pettit, R. K. *J. Med. Chem.* **1998**, *41*, 1688-1695.
- (44) Siles, R.; Monk, K. A.; Hadimani, M. B.; Mugabe, B. E.; Ackley, J. F.; Studerus, S. W.; Edvardsen, K.; Trawick, M. L.; Garner, C. M.; Rhodes, M. R.; Pettit, G. R.; Pinney, K. G. *Bioorg. Med. Chem.* **2006**, *14*, 3231-3244.
- (45) Burrige, K.; Wennerberg, K. *Cell* **2004**, *116*, 167-179.
- (46) Pinney, K. G.; Jelinek, C. J.; Edvardsen, K.; Chaplin, D. J.; Petit, G. R. In *The discovery and development of the combretastatins*; Kingston, D., Newman, D. and Cragg, G., Eds.; Antitumor Agents from Natural Products; CRC Press: 2005; pp 23-46.
- (47) Pinney, K. G. In *Molecular Recognition of the Colchicine Binding Site as a Design Paradigm for the Discovery and Development of Vascular Disrupting Agents*; Siemann, D. W., Ed.; Vascular-targeted Therapies in Oncology; John Wiley & Sons: 2006; pp 95-121.
- (48) Petit, G. R.; Temple, C. J.; Narayanan, V. L.; Varma, R.; Simpson, M. J.; Boyd, M. R.; Reiner, G. A.; Bansal, N. *Anti-Cancer Drug Des.* **1995**, *10*, 299-309.
- (49) Petit, G. R.; Lippert, J. W. *Anti-Cancer Drug Des.* **2000**, *15*, 203-216.
- (50) Chaplin, D. J.; Petit, G. R.; Hill, S. A. *Anticancer Res.* **1999**, *19*, 189-195.
- (51) Young, S. L.; Chaplin, D. J. *Expert Opin. Invest. Drugs* **2004**, *13*, 1171-1182.
- (52) Thomlinson, R.; Gray, L. *Br. J. Cancer* **1955**, *9*, 539-549.
- (53) Harris, A. L. *Nat. Rev. Cancer* **2002**, *2*, 38-47.
- (54) Brown, J. M.; Wilson, W. R. *Nat. Rev. Cancer* **2004**, *4*, 437-447.
- (55) McNally, V. A.; Patterson, A. V.; Williams, K. J.; Cowen, R. L.; Stratford, I. J.; Jaffar, M. *Curr. Pharm. Des.* **2002**, *8*, 1319-1333.
- (56) Semenza, G. L. *Nat. Rev. Cancer* **2003**, *3*, 721-732.
- (57) Kung, A. L.; Wang, S.; Kico, J. M.; Kaelin, W. G.; Livingston, D. M. *Nat. Med.* **2000**, *6*, 1335-1340.
- (58) Jaffar, M.; Willims, K. J.; Stratford, I. J. *Adv. Drug. Del. Rev.* **2001**, *53*, 217-228.
- (59) Naylor, M. A.; Thomson, P. *Mini-Rev. Med Chem.* **2001**, *1*, 17-29.

- (60) Cole, S.; Stratford, I. J.; Bowler, J. *Int. J. Radiat. Oncol. Biol. Phys.* **1991**, *21*, 387-395.
- (61) Stratford, I. J.; Walling, J. M.; Silver, A. R. *J. Br. J. Cancer* **1986**, *35*, 105-109.
- (62) Phillips, R. M. *Exp. Opin. Invest. Drugs* **1998**, *7*, 905-928.
- (63) Jaffar, M.; Naylor, M. A.; Robertson, N.; Stratford, I. J. *Anticancer Drug Des.* **1998**, *13*, 593-609.
- (64) Oostveen, E. A.; Speckamp, W. N. *Tetrahedron* **1987**, *43*, 255-262.
- (65) Phillips, R. M.; Naylor, M. A.; Jaffar, M.; Doughty, S. W.; Everett, S. A.; Green, A. G.; Choudry, G. A.; Stratford, I. J. *J. Med. Chem.* **1999**, *42*, 4071-4080.
- (66) Hargreaves, Robert H. J.; Hartley, J. A.; Butler, J. *Front. Biosci.* **2000**, *5*, 172-180.
- (67) Danson, S.; Ward, T. H.; Butler, J.; Ranson, M. *Cancer Treat. Rev.* **2004**, *5*, 437-439.
- (68) Faig, M.; Bianchet, M. A.; Winski, S.; Hargreaves, R.; Moody, C. J.; Hudnott, A. R.; Ross, D.; Amzel, L. M. *Structure* **2001**, *9*, 659-667.
- (69) Jaffar, M.; Everett, S. A.; Naylor, M. A.; Moore, S. G.; Ulhaq, S.; Patel, K. B.; Stratford, M. R. L.; Nolan, J.; Wardman, P.; Stratford, I. J. *Bioorg. Med. Chem. Lett.* **1999**, *9*, 113-118.
- (70) Everett, S. A.; Swann, E.; Naylor, M. A.; Stratford, M. R. L.; Patel, K. B.; Tian, N.; Newman, R. G.; Vojnovic, B.; Moody, C. J.; Wardman, P. *Biochem. Pharmacol.* **2002**, *63*, 1629-1639.
- (71) Jaffar, M.; Phillips, R. M.; Williams, K. J.; Mrema, I.; Cole, C.; Wind, N. S.; Ward, T. H.; Stratford, I. J.; Patterson, A. V. *Biochem. Pharmacol.* **2003**, *66*, 1199-1206.
- (72) Hernick, M.; Borch, R. F. *J. Med. Chem.* **2003**, *46*, 148-154.
- (73) Bai, R.; Pei, X.; Boye, ; Getahun, Z.; Grover, S.; Bekisz, J.; Nguyen, N. Y.; Brossi, A.; Hamel, E. *J. Biol. Chem.* **1996**, *271*, 12639-12645.
- (74) Mocharla, V. P. Design, Synthesis and Biological Evaluation of Diverse Small Molecular Frameworks as Tubulin Binding Ligands, Doctoral Dissertation, Baylor University, Waco, TX, 1999.
- (75) Seegers, J. C.; Aveling, M. L.; van Aswegen, C. H.; Cross, M.; Koch, F.; Joubert, W. S. *J. Steroid Biochem.* **1989**, *32*, 797-809.

- (76) Chen, Z. Synthesis of Tubulin Binding Ligands Incorporating Dihydronaphthalene, Indene and Benzo[b]thiophene Molecular Frameworks and Preparation of their Corresponding Phosphorous Containing Prodrugs as Tumor Specific Vascular Targeting Agents, Master's Thesis, Baylor University, Waco, TX, 2000.
- (77) Cushman, M.; He, H.; Katzenellenbogen, J. A.; Varma, R. K.; Hamel, E.; Chii, M.; Ram, S.; Sachdev, Y. P. *J. Med. Chem.* **1997**, *40*, 2323-2334.
- (78) Ghatak, A.; Dorsey, J. M.; Garner, C. M.; Pinney, K. G. *Tet. Lett.* **2003**, *44*, 4145-4148.
- (79) Pinney, K. G.; Mocharla, V. P.; Chen, Z.; Garner, C. M.; Ghatak, A.; Hadimani, M.; Dorsey, J. U.S. Patent 6,593,374, 2003.
- (80) Beak, P.; Brown, R. A. *J. Org. Chem.* **1982**, *47*, 34-46.
- (81) Ramdayal, F. D.; Kiemle, D. J.; LaLonde, R. T. *J. Org. Chem.* **1999**, *64*, 4607-4609.
- (82) Saito, M.; Yasutaka, K.; Watanabe, T.; Fukushima, H.; Hara, T.; Koyano, K.; Takenaka, A.; Sasada, Y. *J. Med. Chem.* **1980**, *23*, 1364-1372.
- (83) Talekar, D. G.; Rao, A. S. *Synthesis* **1983**, *7*, 595-597.
- (84) Braun, M.; Bernard, C. *Liebigs Ann. Chem.* **1985**, *2*, 435-437.
- (85) Bartlett, P. D. *Rec. Chem. Prog.* **1950**, *11*, 47-51.
- (86) Naylor, M. A.; Swann, E.; Everett, S. A.; Jaffar, M.; Nolan, J.; Robertson, N.; Lockyer, S. D.; Patel, K. B.; Dennis, M. F.; Stratford, M. R. L.; Wardman, P.; Adams, G. E.; Moody, C. J.; Stratford, I. J. *J. Med. Chem.* **1998**, *41*, 2720-2731.
- (87) Giethlen, B.; Schaus, J. M. *Tet. Lett.* **1997**, *38*, 8483-848.
- (88) Takacs, J. M.; Xu, Z.; Jiang, X.; Leonov, A. P.; Theriot, G. C. *Org. Lett.* **2002**, *4*, 3843-3845.
- (89) Miranda, M. G. Design, Synthesis and Biological Evaluation of Novel Serotonin Reuptake Inhibitors and Novel Derivatives of a Nitrogen-Containing Combretastatin Analog, Doctoral Dissertation, Baylor University, Waco, TX, 2006.
- (90) Hernick, M.; Flader, C.; Borch, R. F. *J. Med. Chem.* **2002**, *45*, 3540-3548.
- (91) Hay, M. P.; Gamage, S. A.; Kovacs, M. S.; Pruijn, F. B.; Anderson, R. F.; Patterson, A. V.; Wilson, W. R.; Brown, J. M.; Denny, W. A. *J. Med. Chem.* **2003**, *46*, 169-182.